



Norwegian University of  
Science and Technology

# Feasibility of ground freezing as potential stabilizing measure for tunnelling through soil filled depression at Bergåsen road tunnel

**Ivan Vakulenko**

Cold Climate Engineering

Submission date: June 2018

Supervisor: Bjørn Nilsen, IGP

Norwegian University of Science and Technology  
Department of Geoscience and Petroleum



# Feasibility of ground freezing as potential stabilizing measure for tunnelling through soil filled depression at Bergåsen road tunnel

Ivan Vakulenko

June 2018

Master Thesis

Department of Geoscience and Petroleum  
Norwegian University of Science and Technology



**Feasibility of ground freezing as potential stabilizing measure for tunnelling through soil filled depression at Bergåsen road tunnel**

**Program for MSc-thesis**

**Ivan Vakulenko**

As part of upgrading of Highway E6 at Bergåsen, close to Mosjøen in northern Norway, an approximately 1.3 km long road tunnel is under planning by the Norwegian Public Roads Administration (NPRA). The tunnel will pass mainly through hard rock, to be excavated by conventional drilling and blasting, but has an about 20 m long, soil filled depression in the middle which will require special methods for safe excavation.

Several alternative methods for tunnelling through the soil- (moraine-) filled depression may be relevant. This assignment is to focus particularly on artificial ground freezing as a possible option. The master assignment is a follow up of a project assignment completed by the candidate in the autumn semester 2017, discussing ground freezing technology, conditions and potential limitations for use, and review of relevant case histories. This master assignment is to focus on the feasibility of this method for the Bergåsen tunnel.

As basis for ongoing planning and design work, quite extensive ground investigations have been carried out, focusing on hard rock- as well as soil- and groundwater conditions. NPRA has confirmed interest in cooperating on this masters-assignment and allows use of available material from ground investigations for this assignment. Among factors of particular significance for the study are particularly mentioned:

- Evaluation of ground conditions based on review of reports from ground investigations.
- Sampling of soil from the depression and if possible, testing of soil properties in frozen condition.
- Evaluation of the significance of ground water.
- Numerical analysis (based on Rocscience software available at NTNU/IGP, such as RS2) of stability and requirement for permanent support after freezing.
- Cost and schedule estimation for excavation through the soil filled section.
- Evaluation of potential risk elements and methodology for minimizing risk

The assignment is associated with N5T Joint Master's Programme in Cold Climate Engineering, organized jointly between NTNU with Prof. Bjørn Nilsen as main supervisor and DTU with Prof. Thomas Ingeman-Nielsen as co-supervisor. Contact person at NPRA is Mikael Bergman.

The thesis work starts January 15, 2018 and is to be completed by June 11, 2018.

Norwegian University of Science and Technology (NTNU)  
Department of Geosciences and Petroleum

January 9, 2018

Bjørn Nilsen

Professor of geological engineering, main supervisor

*This sheet is to be inserted as page 1 of the Master thesis*



---

## **Preface**

The master thesis was written as the final 30 ECTS part of Nordic master program "Cold Climate engineering" during spring semester in 2018. The paper was prepared in department of Geoscience and Petroleum at Norwegian University of Science and Technology (NTNU) in collaboration with Technical University of Denmark (DTU).

The intention of the master thesis – to analyze the feasibility of artificial ground freezing as a possible method for soil stabilization during tunnelling project in Norway.

The provisions of the thesis were presented at international conference "AIC 2018 –Transportation Infrastructure Engineering in Cold Regions" in Sisimiut (Greenland) in May 2018.

---

## Acknowledgment

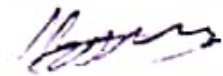
I wish to thank my supervisor, professor Bjørn Nilsen at Norwegian University of Science and Technology for the idea of this master thesis, further guidance and important feedback.

Special thanks to Karlsen Finn Sverre at Statens Vegvesen for useful project information providing and interest in my research.

I would like to thank my co-supervisor Thomas Ingeman-Nielsen from DTU for his assistance and my program coordinator Gunvor Marie Kirkelund for her general, but very helpful guidance.

To my family and friends who supported me through the whole period of my studies.

Trondheim, 2018-06-11

A handwritten signature in dark ink, appearing to read 'Ivan Vakulenko', with a stylized, cursive script.

Ivan Vakulenko

---

## Abstract

The master thesis describes a technique of artificial ground freezing (AGF) using as a potential method of water saturated soil stabilizing during tunnel excavation in North Norway. The research is based on real project of a tunnel planned by Statens vegvesen – Norwegian public roads administration – as a part of European highway E6 reconstruction in Grane kommune of Nordland region.

Based on geotechnical sounding, it was found that the 675 m long tunnel will cross a depression over a section of approximately 20m, which is filled by a mix of water-saturated materials (silt, sand and gravel). To “handle” this section, artificial ground freezing method is taken into consideration.

The tunnel route is based on assumption that even crossing the deepest section of moraine, the tunnel bottom part will still lie on the rock basement. Therefore, the designed ice-wall covers only that part of the tunnel, which will be excavated in soil.

The paper includes an analysis of geological and hydrological conditions of moraine deposit area based on Statens Vegvesen project papers, which is followed by the determination of design parameters for an ice-wall created by AGF method in the water saturated soil section. The ice-wall function is to stabilize soil layer for safe excavation and permanent lining installation. Thus, it is shown, how moraine deposit parameters including seepage velocity, cohesion, Young's modulus and friction angle, affect ice-wall structure.

The stability analysis of the tunnel is carried out in Rocscience RS2 software. Therefore, the model of designed ice-wall is set-up for simulation to get the distribution of displacements on the merge of excavated tunnel and frozen ground layer. Thereafter the stability with permanent lining is analyzed. Results of the simulation show that the designed ice-wall and further permanent lining are sufficient to maintain the tunnel stability. However, due to lack of broad geological and hydrological data, more comprehensive research should be carried out. To show the hazards of incorrect geology data, a case of the tunnel completely excavated in moraine deposit is considered and modeled as well.

---

## Sammendrag

Denne masteroppgaven beskriver grunnfrysing teknikk som potensiell stabiliseringsmetode for vannmettet materialer for driving av tunnel i Nord Norge. Forskningen er basert på Statens Vegvesen prosjektering av tunnel i Grane kommune i forbindelse med bygging av ny E6.

Grunnundersøkelser viser at en 675 m lang tunnel skal utgraves gjennom en svakhetssone på ca. 20 m fylt med vannmettet løsmasser og grunnfrysing teknikk er derfor tatt i betraktning. Tunnelen er planlagt å ligge helt i bunnen av svakhetssone og i overgangen mellom løsmasse og fast fjell. Kun den delen av tunnelen som utgraves i jord skal stabiliseres med grunnfrysing.

Denne masteroppgave inneholder en analyse av geologiske og hydrogeologiske forholdene i området, basert på prosjektoppgaver utarbeidet av Statens Vegvesen, som etterfølges av bestemmelse av prosjekteringsparametere angående dannelse av isveggen rundt delen av tunnelen inneholdt i jorden.

Både jord relaterte parametere inkludert Youngs modul og friksjonsvinkel, og strømningsforhold i området påvirker strukturen av isveggen som dannes for å stabilisere jordlaget, dermed for å sikre trygge utgraving og installasjon av permanent bergsikring i tunnelen.

Stabilitetsberegninger er utført ved hjelp av Rocscience RS2, hvor prosjektert isveggen er modellert med sikte på å få setninger rundt den utgravde tunnelen. Deretter, stabiliteten etter installasjonen av bergsikring er også vurdert.

Resultater viser at prosjektert isvegg og permanent bergsikring er tilstrekkelige for å opprettholde stabiliteten av tunnelen. Mer omfattende forskning burde imidlertid utføres på grunn av mangel på flere geologiske og hydrogeologiske data. For å vise farene knyttet til feil geologiske data, en kasusstudie hvor tunnelen er helt utgravd i moreneavsetninger er også modellert.

# Contents

Preface . . . . .	ii
Acknowledgment . . . . .	iii
Abstract . . . . .	iv
Sammendrag . . . . .	v
List of Figures . . . . .	ix
List of Tables . . . . .	xii
Notations . . . . .	xiii
<b>1 Introduction</b>	<b>15</b>
1.1 Background . . . . .	15
1.2 Objectives . . . . .	16
1.3 Approach . . . . .	16
1.4 Limitations . . . . .	16
1.5 Project data sources . . . . .	17
<b>2 Geology and ground conditions at the project zone</b>	<b>18</b>
2.1 Geology of the project area . . . . .	18
2.1.1 Grain size distribution in moraine . . . . .	21
2.2 Groundwater conditions . . . . .	22
2.2.1 Seepage velocity . . . . .	22
<b>3 Artificial ground freezing for tunnel stabilizing</b>	<b>24</b>
3.1 Artificial ground freezing description . . . . .	24
3.1.1 Comparisson of induced methods with artificial ground freezing . . . . .	28
3.2 Artificial ground freezing practice in Scandinavian countries . . . . .	29
3.2.1 Norway . . . . .	29
3.2.2 Sweden . . . . .	32
3.2.3 Finland . . . . .	34
3.2.4 Comparison of the projects . . . . .	35

<b>4</b>	<b>Artificial freezing and grounds interference</b>	<b>36</b>
4.1	Freezing process . . . . .	36
4.2	Soils testing and measuring . . . . .	37
4.2.1	Mechanical properties of unfrozen and frozen soils . . . . .	37
4.2.2	Thermal properties of soils . . . . .	39
4.2.3	Seepage flow velocity . . . . .	41
4.2.4	Salinity . . . . .	42
4.3	Affects of freezing . . . . .	42
4.3.1	Frost heave . . . . .	42
4.3.2	Ground settlements . . . . .	44
4.3.3	Ground creep . . . . .	45
<b>5</b>	<b>Design of Bergåsen tunnel</b>	<b>46</b>
5.1	Tunnel profile . . . . .	46
5.2	Tunnel excavation . . . . .	47
<b>6</b>	<b>Design of artificial ground freezing</b>	<b>50</b>
6.1	Theory of ice-wall design . . . . .	50
6.1.1	Positioning . . . . .	50
6.1.2	Ice wall thickness . . . . .	51
6.1.3	Time evaluation methods . . . . .	52
6.1.4	Costs . . . . .	54
6.1.5	Freezing process completion . . . . .	55
6.1.6	Risks . . . . .	56
6.2	Ice-wall design for Bergåsen tunnel . . . . .	59
6.2.1	Ice-wall thickness . . . . .	59
6.2.2	Temperature of freezing . . . . .	61
6.2.3	Time of freezing . . . . .	61
6.2.4	Approximate costs evaluation . . . . .	63
6.2.5	Risk assessment . . . . .	64
<b>7</b>	<b>Modelling of the tunnel stability</b>	<b>65</b>
7.1	Rocscience modelling . . . . .	65
7.1.1	Principles of modelling . . . . .	65
7.1.2	Field stress parameters . . . . .	67
7.1.3	Strength parameters . . . . .	68
7.1.4	Ground material parameters . . . . .	69
7.1.5	Ice-wall modelling in Rocscience . . . . .	71
7.1.6	Groundwater flow modelling . . . . .	72

7.1.7	Support modelling . . . . .	73
7.2	Tunnel displacements . . . . .	74
7.2.1	Unlined tunnel . . . . .	74
7.2.2	Lined tunnel . . . . .	75
7.2.3	Ice-wall protection . . . . .	76
7.3	Tunnel excavation in soil . . . . .	77
7.3.1	Displacements . . . . .	77
7.3.2	Groundwater conditions . . . . .	79
7.4	Moraine parameters effects . . . . .	80
<b>8</b>	<b>Discussion</b>	<b>82</b>
8.1	Geology and hydrology . . . . .	82
8.2	Tunnel design . . . . .	82
8.3	Design of ice-wall parameters . . . . .	83
8.4	Modeling of the tunnel stability . . . . .	83
<b>9</b>	<b>Conclusions</b>	<b>85</b>
9.1	Further work recommendations . . . . .	85
	<b>References</b>	<b>86</b>
<b>A</b>	<b>Drawings of the project</b>	<b>92</b>
<b>B</b>	<b>Time evaluation (Sangers&amp;Sayles)</b>	<b>95</b>
<b>C</b>	<b>Risk assessment table</b>	<b>97</b>
<b>D</b>	<b>Road tunnels standards</b>	<b>98</b>
<b>E</b>	<b>Hoek-Brown criteria</b>	<b>99</b>
<b>F</b>	<b>Model with natural ground level set-up</b>	<b>103</b>
<b>G</b>	<b>K-value estimation</b>	<b>104</b>
<b>H</b>	<b>Safety factor of reinforced concrete lining</b>	<b>105</b>

# List of Figures

1.1	Tunnel location . . . . .	15
2.1	Placement of wells . . . . .	18
2.2	Bedrock map (after Ngi.no (2018)) . . . . .	19
2.3	Soils map (after Ngi.no (2018)) . . . . .	20
2.4	Longitudinal cross-section of tunnel route . . . . .	21
2.5	Grain size distribution (after Selmer-Olsen (1976)) . . . . .	21
2.6	Groundwater flow direction . . . . .	22
3.1	Brine freezing scheme . . . . .	25
3.2	Liquid nitrogen freezing scheme . . . . .	26
3.3	Thermosyphon scheme and an example of their application in West Siberia . .	27
3.4	Section through the Hurum weakness zone along the tunnel centre line ( from Backer and Blindheim (1999)) . . . . .	30
3.5	Site plan and cross-section of the weakness zone (from Jøsang (1980)) . . . . .	30
3.6	Cross section of tunnel systems (from Jøsang (1980)) . . . . .	31
3.7	Ice-wall for Moss centre tunnel design (from Berggren (2007)) . . . . .	32
3.8	Time schedule of AGF applying at Moss centre tunnel (from Berggren (2007)) . .	32
3.9	Schematic view of the MBZ freezing area (from Schubert (2013)) . . . . .	33
3.10	Longitudinal profile of the ground freezing area at the Bothnia Line (from Jo- hansson (2009)) . . . . .	33
3.11	Tunnel section with a circular arc, showing various installation depths of freeze- tubes (from Johansson (2009)) . . . . .	34
3.12	Longitudinal section of Heslinki metro tunnel (from Vuorela and Eronen (1982))	35
4.1	Temperature influence on uniaxial compression strength for sand, clay and silt (from Andersland and Ladanyi (2004)) . . . . .	37
4.2	Young's modulus variation (from Harris (1995)) . . . . .	38
4.3	Frozen grounds testing, carried out for a tunnel construction in Hong Kong (from Hu et al. (2013)) . . . . .	38
4.4	Stress-strain curves for sand and clay (from Andersland and Ladanyi (2013)) . .	39
4.5	Thermal conductivity variance due to temperature (from Harris (1995)) . . . . .	40
4.6	Specific heat capacity variance due to temperature (from Harris (1995)) . . . . .	40



4.7	Frozen ground support system: a) in soils with steady groundwater; b) in soils with seepage flow . . . . .	41
4.8	Frost susceptibility criteria in Norway (from Hoppe (2000)) . . . . .	43
4.9	Artificially frozen ground thawing around tunnel . . . . .	44
4.10	Ground settlements (from Hill and Stärk (2015)) . . . . .	45
4.11	Creep performance in frozen soils (from Lackner et al. (2008)) . . . . .	45
5.1	Tunnel profile dimensions (after Vegvesen (2010)) . . . . .	47
5.2	Open length of ice-wall, (after Berggren (2000)) . . . . .	48
5.3	Drill and blast rounds, (after Berggren (2000)) . . . . .	48
6.1	Freeze-tubes positioning in tunnels . . . . .	51
6.2	Risk assessment (after Einarson (2014)) . . . . .	57
6.3	Ice-wall scheme . . . . .	60
7.1	Steps of simulation in RS2 . . . . .	65
7.2	Tunnel model . . . . .	66
7.3	Mesh fitting for the tunnel model . . . . .	67
7.4	Field stress dialog . . . . .	68
7.5	Strength criteria (after Saiang et al. (2014)) . . . . .	68
7.6	Ice-wall model in RS2 . . . . .	71
7.7	Natural groundwater level . . . . .	72
7.8	Groundwater level variation in case of ice-wall applying . . . . .	72
7.9	Lining properties . . . . .	73
7.10	Deformations occurred in the unlined tunnel . . . . .	74
7.11	Deformations occurred in the tunnel with lining . . . . .	75
7.12	Deformations occurred in the tunnel with artificial frozen ground layer . . . . .	76
7.13	Location of shifted tunnel . . . . .	77
7.14	Deformations occurred in the shifted tunnel with ice-wall layer . . . . .	78
7.15	Deformations occurred in the shifted tunnel with lining . . . . .	78
7.16	Groundwater level variation, when ice-wall is applied for the shifted tunnel . . . . .	79
7.17	Points indication for displacements analysis . . . . .	80
7.18	Displacements due to parameters variation . . . . .	81
A.1	Bedrock geology (from Vegvesen (2013b)) . . . . .	92
A.2	Soil section (from Vegvesen (2018)) . . . . .	93
A.3	Bedrock geology (from Vegvesen (2013b)) . . . . .	94
B.1	2 stages of ice-wall freezing; ( $\delta = 0,393S$ ) (from Sanger and Sayles (1979)) . . . . .	96
D.1	Tunnel categories classification (from Vegvesen (2010)) . . . . .	98
D.2	Tunnel cross-section elements (from Vegvesen (2016)) . . . . .	98

E.1	Quantification of GSI (from Hoek et al. (2013) . . . . .	99
E.2	Values of the constant $m_i$ for intact rock (from Hoek et al. (2013) . . . . .	100
E.3	Field estimates of uniaxial compressive strength (from Hoek (2007) . . . . .	101
E.4	Disturbance factor D (from Hoek (2007) . . . . .	102
F.1	Displacements distribution in soil layer before tunnel excavation . . . . .	103
G.1	K values impact on displacement distribution . . . . .	104
H.1	Safety factor for 0,3 m thick concrete layer . . . . .	105
H.2	Safety factor for reinforcement framework . . . . .	105

# List of Tables

2.1	Hydraulic conductivity $k$ and porosity $n$ . . . . .	23
2.2	Ground water flow calculation . . . . .	23
3.1	Freezing methods comparison . . . . .	27
3.2	Ground stabilizing methods (from Harris (1995)) . . . . .	28
3.3	Comparison of projects with AGF method using . . . . .	35
4.1	Frost susceptibility classification of soils (after Barry et al. (2005)) . . . . .	36
4.2	Frost-susceptibility of soils (from Slunga and Saarelainen (1989)) . . . . .	43
5.1	Geometrical specification for T9,5 profile tunnel . . . . .	46
6.1	Probability of hazards occurrence (after Shahriar et al. (2008)) . . . . .	56
6.2	Consequence of hazards (after Shahriar et al. (2008)) . . . . .	56
6.3	Risk level evaluation (after Shahriar et al. (2008)) . . . . .	56
6.4	Risk assessment range (after (Harris, 1995)) . . . . .	58
6.5	Variation of wells number by spacing . . . . .	60
6.6	Freezing temperature fluctuation due to seepage velocity and spacing variation	61
6.7	Input data for freezing time calculation . . . . .	62
6.8	Risk assessment for Bergåsen tunnel ice-wall creation . . . . .	64
7.1	Marble strength properties . . . . .	70
7.2	Moraine properties . . . . .	70
7.3	Artificially frozen ground parameters . . . . .	71
7.4	Moraine parameters variation . . . . .	80
C.1	Risks mitigation for artificial groud freezing method (from Harris (1995)) . . . .	97

# Notations

## Greek symbols

Symbol	Represents	Unit
$\nu$	Poisson ratio	[-]
$\rho$	Density	kg/m <sup>3</sup>
$\sigma'_1$	Maximum effective principal stress	MPa
$\sigma'_3$	Minimum effective principal stress	MPa
$\sigma_H$	Horizontal field stress	MPa
$\sigma_V$	Vertical field stress	MPa
$\sigma_c$	Uniaxial compressive strength	MPa
$\sigma_n$	Normal stress	MPa
$\sigma_t$	Tensile strength	MPa
$\tau$	Shear strength	MPa
$\tau_f$	Critical shear stress	MPa
$\phi$	Angle of internal friction	deg

## Roman Symbols

Symbol	Represents	Unit
C	Specific heat capacity	kJ/kg°C
D	Diameter of tunnel	m
E	Young's modulus	GPa
$E_{iw}$	Thickness of ice-wall	m
F	Freeze-tubes surface	m <sup>2</sup>
$F_s$	Safety factor	[-]
$H_{gw}$	Height of water column above the tunnel	m
L	Length of freeze-tubes	m
$L_p$	Distance between two piezometers	m
$L_u$	Unsupported length of ice-wall	m
N	Number of a single row of freeze-tubes	[-]
P	Water saturated soils pressure on the ice-wall	MPa
Q	Latent heat of ice formation	kJ/kg
$Q_{25}$	25th percentile of grain size distribution	[-]
$Q_{50}$	50th percentile of grain size distribution	[-]
$Q_{75}$	75th percentile of grain size distribution	[-]
$Q_c$	Refrigeration required to cool soil to the designed temperature of freezing	kJ/h
$Q_f$	Refrigeration required to freeze designed volume of soil	kJ
$Q_t$	Heat absorption capability of freeze-tubes	kJ/h
$Q_{rp}$	Cooling capacity of refrigeration plant	kJ

$R_{ex}$	External radius of ice-wall	m
$R_{in}$	Internal radius of ice-wall	m
$R_t$	Radius of tunnel	m
$S$	Spacing between nearby freeze-tubes	m
$S_n$	Salinity	g/l
$T_0$	Difference between ambient ground temperature and groundwater freezing point	°C
$\Delta T$	Temperature of freezing difference	°C
$T_f$	Designed temperature of freezing (coolant)	°C
$T_k$	Reference temperature	°C
$T_s$	Difference between freeze-tube surface temperature and water freezing point	°C
$V_s$	Volume of soil to be frozen	m <sup>3</sup>
$V_{gw}$	Groundwater volume in 1 m <sup>3</sup> of soil	m <sup>3</sup> /m <sup>3</sup>
$V_{ds}$	Dry soil volume in 1 m <sup>3</sup> of water saturated soil	m <sup>3</sup> /m <sup>3</sup>
$c$	Cohesive strength	MPa
$h$	Depth of tunnel	m
$i$	Hydraulic gradient	-
$k$	Soil hydraulic conductivity	m/day
$k_f$	Thermal conductivity of frozen soil	W/m°C
$n$	Porosity	[-]
$p_0$	Overbudden pressure	MPa
$p_h$	Hydraustatic pressure	MPa
$q_1$	Refrigeration for 1 m <sup>3</sup> of groundwater cooling	kJ/m <sup>3</sup>
$q_2$	Refrigeration for ice forming	kJ/m <sup>3</sup>
$q_3$	Refrigeration to cool ice to the average temperature in the ice-wall zone	kJ/m <sup>3</sup>
$q_4$	Refrigeration for dry soil cooling to the designed freezing temperature	kJ/m <sup>3</sup>
$q_c$	Heat infiltration to the 1 m <sup>2</sup> of ice-wall structure	kJ/m <sup>2</sup> h
$q_f$	Required refrigeration for freezing of 1 m <sup>3</sup> of soil	kJ/m <sup>3</sup>
$q_t$	Specific heat flow rate	kJ/m <sup>2</sup> h
$r_0$	Freeze-tube radius	m
$t$	Time of active freezing	days
$t_0$	Groundwater freezing point temperature	°C
$t_f$	Average temperature in the ice-wall zone	°C
$t_s$	Natural temperature of groundwater	°C
$u_c$	Critical groundwater velocity	m/day
$v$	Unit weight	[-]
$v_d$	Discharge velocity	m/day
$v_s$	Seepage velocity	m/day

### Other

Symbol	Represents
AGF	Artificial ground freezing
NPRA	Norwegian Public Roads Administration
gw	groundwater
m	marble
i	ice
iw	ice-wall
s	soil

# Chapter 1: Introduction

## 1.1 Background

The project of E-6 national road reconstruction includes the extension of the existing road system with the construction of new road sections along with bridges and tunnels. Bergåsen tunnel will be the part of new E-6 highway in Helgeland district in Northern Norway (Figure 1.1). This project is included in the complex plan of the existing road reorganisation, which is designed by Statens Vegvesen (Norwegian Public Roads Administration). The project of the new highway was implemented to meet the demands of raised traffic at E-6 national pass, operating from 1970. Thus, the design and construction of the new 15,2 km long free-way, connecting Brattåsen to Lien, was planned to complete from 2014 to 2023. The new E-6 will cover distance 2,5 km shorter then the old road and will be located next to the existing railway (Vegvesen, 2013a).

675 m long Bergåsen tunnel will be constructed near Trofors in Grane municipality. Mostly excavated in rock, it will cross a depression, filled by moraine deposit with high groundwater saturation which demands special methods of soils stabilisation.



Figure 1.1: Tunnel location

## 1.2 Objectives

The analysis of underground constructions stability is critically important in the design of geotechnical projects. When an artificial ground freezing method is applied, created ice-wall should provide sufficient stability for an excavation through the whole time period before permanent lining will be installed. The existing methods allow to determine AGF parameters for diverse underground constructions, such as mine shafts or tunnels.

The tunnel stability is investigated for two principal construction stages:

- Unlined tunnel under the protection of designed ice-wall;
- Tunnel with permanent lining after the ice-wall thawing.

Thus, the main aim of the master thesis is to design an ice-wall, which will be sufficient to stabilize the section of water saturated moraine soils. The research of groundwater and moraine deposit strength parameters impact on the ice-wall creation will be carried out in the thesis. Furthermore, risk analysis and costs evaluation will be researched.

## 1.3 Approach

The master thesis includes an estimation of ice-wall parameters, which is formed by artificial ground freezing method applying for the project. This approach is based on Eurocode 7 design method by calculation (Bond and Harris, 2008).

In order to estimate AGF parameters, the methods described in technical literature, were used.

The analysis of the tunnel stability is simulated in Rocscience Phase<sup>2</sup> (RS2) software for an ice-wall stage as well as for a stage with permanent reinforced concrete lining.

## 1.4 Limitations

Considering that there was no possibility to get samples of moraine sediments (because of harsh winter condition in the project area), the research, applied in the master thesis, is based only on the analysis of technical papers for the project, which are limited by incomplete data regarding the site geological and groundwater conditions.

Moraine natural and frozen strength and thermal properties are determined by the analysis of research papers, applied for materials with similar properties. Therefore, all design estimations of the ice-wall are theoretical and can vary from the real conditions. Such AGF hazards as frost heave, ground creep and settlements are discussed, but are not evaluated because of absence of laboratory analysis of frozen moraine sediments for the project.

Thus, the following stability analysis is similarly theoretical. Furthermore, the results obtained during modelling, are affected by model simplification and are not deprived of Rocscience phase<sup>2</sup> software errors.

## 1.5 Project data sources

The research, applied in the master thesis is based on the analysis of following technical papers, published for the Bergåsen tunnel project:

- Reguleringsplan E6 Bråttasen-Lien – General outlook on the region of the project, future road mapping (Vegvesen, 2013a)
- Geotechnical report (Geoteknikk E6-01/02) – Mapping of the future road including the tunnel section and data from total sounding wells (Vegvesen, 2013c)
- Geological report (Geologi E6 TUNNEL VED TROFORS I GRANE KOMMUNE) – Geology of the tunnel area and mapping of the tunnel route (Vegvesen, 2013b)
- Hydrological report (Hydrologi Ev. 06 Bergåstunnelen, Svenningdal - Valryggen) – Ground-water conditions in the area of tunnel construction (Vegvesen, 2018)

Following NPRA standards were used in the master thesis:

- Håndbok N500 Vegtunneler – Tunnel cross-section elements (Vegvesen, 2016);
- Håndbok 021: Vegtunneler – The categories of tunnels, its profile dimensions and natural temperature of soil (Vegvesen, 2010);
- Prosseskode 1. Standard beskrivelse for vegkontrakter – Standard for lining of tunnels (Vegvesen, 2015)

Background information about AGF projects in Scandinavia, theory of frozen ground behaviour and design considerations were generally studied during autumn semester 2017 within specialization project course "Ground freezing as stabilizing measure during tunnelling" (Vakulenko, 2017).



## Chapter 2: Geology and ground conditions at the project zone

Comprehensive information about geology in the area of the tunnel construction was obtained by total sounding wells test included in NPRA geotechnical report (Vegvesen, 2013c). However, the most detailed information about soil section was obtained from pump wells drilled in summer 2017 and then described in (Vegvesen, 2018). In general, data from 5 wells was analyzed (Figure 2.1). Wells BR 6, BR 1 and BR 7 are located on the line of tunnel route, while BR 1 is situated presumably in the middle of the moraine deposit section.

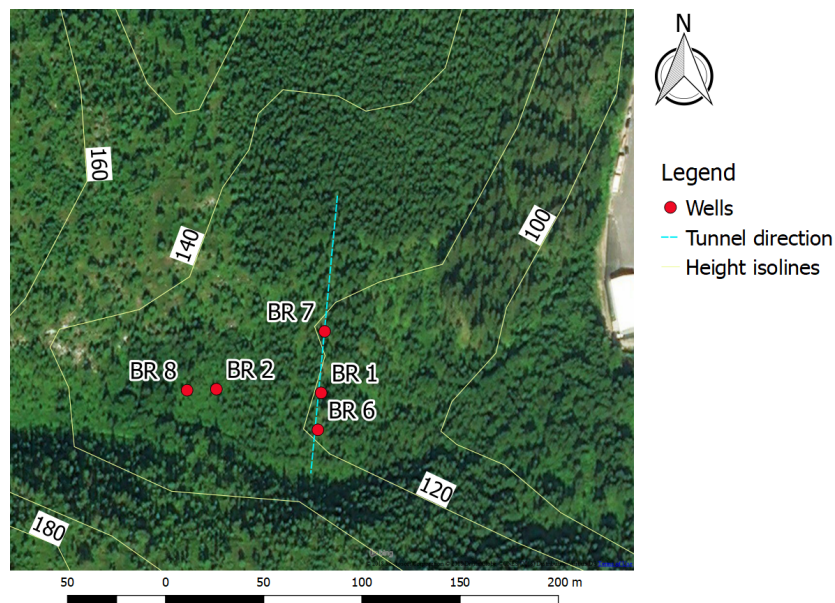


Figure 2.1: Placement of wells

### 2.1 Geology of the project area

The area of the planned tunnel is located in the intersection of sedimentary and igneous rocks. That presumably represent the case, when precambrian originally "sedimented" rocks were intruded by Caledonian rocks formed during Silurian and Devonian periods.

The bedrock map of Geological survey of Norway shows that the tunnel will lie in the intersection of granite and limestone (Figure 2.2). However, further geological research of

the area has discovered that the bedrock in the area of the tunnel route is presented mainly by marble which overlays by granite and thin layer of mica schist (Vegvesen, 2013b).

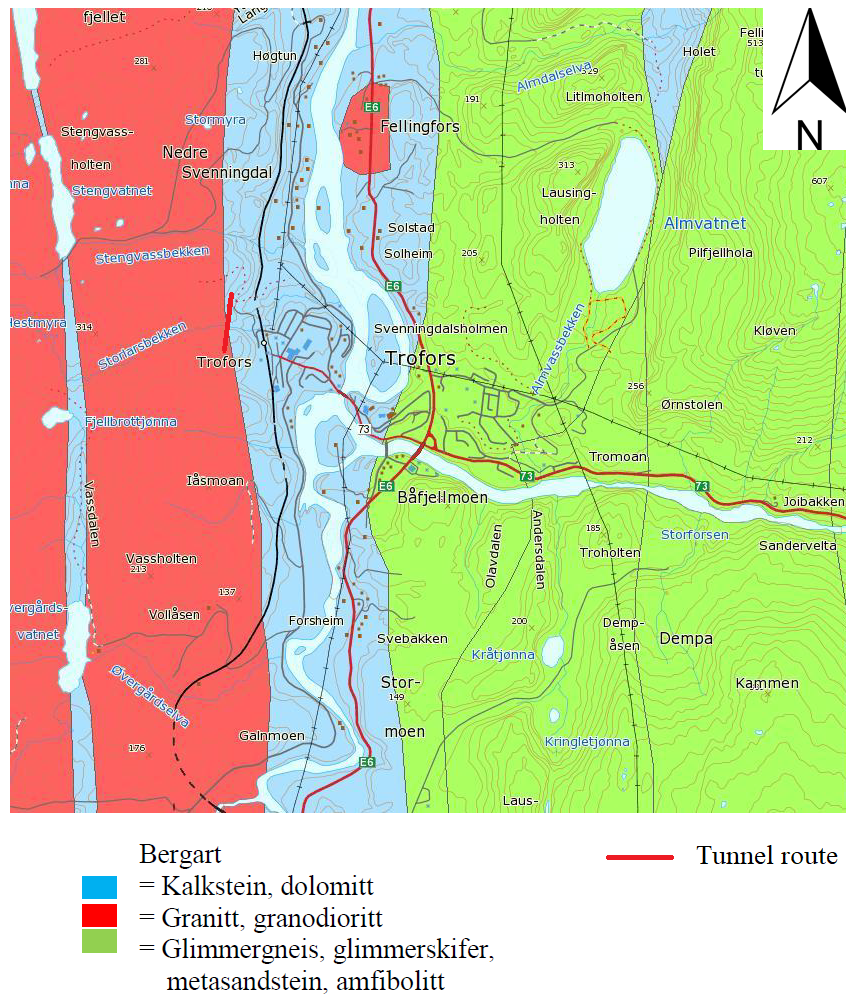


Figure 2.2: Bedrock map (after Ngi.no (2018))

Soils map (Figure 2.3) is widely characterized by bartonite layer in the tunnel route area. While alluvium deposits are common for the river and Trofors area to the east from the tunnel route and wide moraine deposits are to the west.

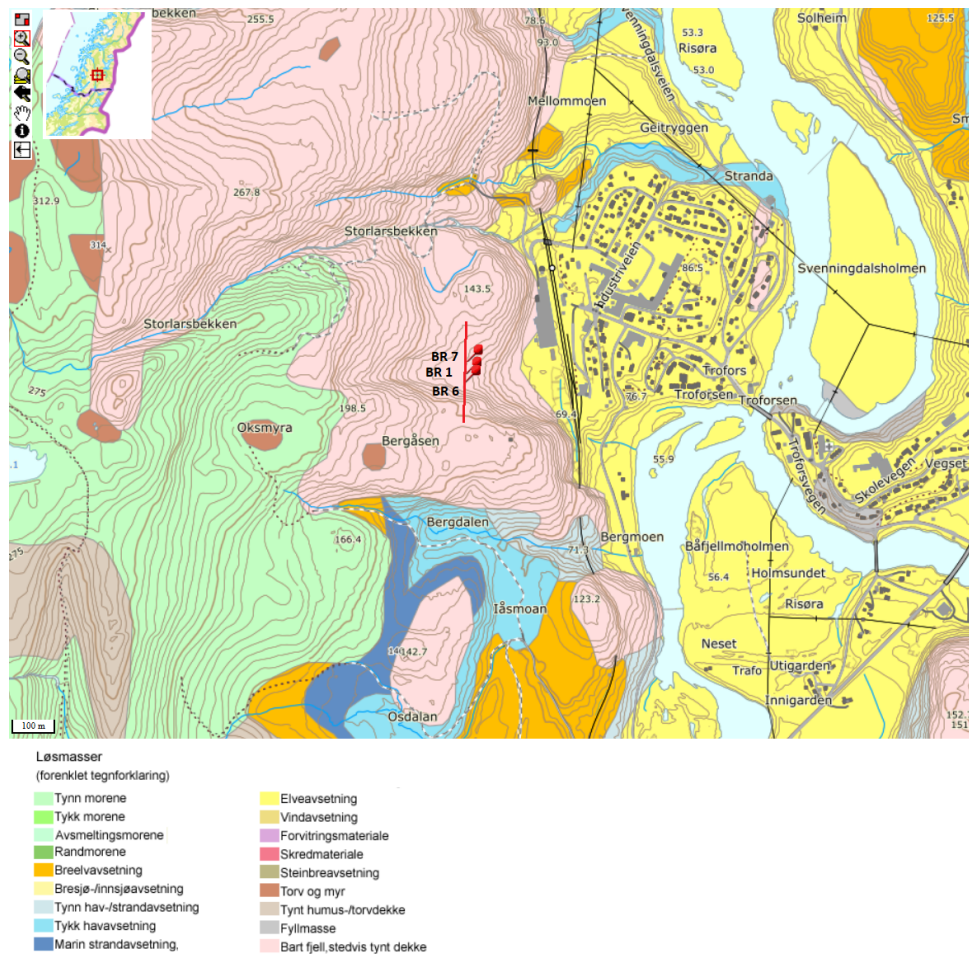


Figure 2.3: Soils map (after Ngi.no (2018))

Generally, the area of moraine deposit is situated below a flat plateau with relatively steep slopes to the south, west and east, and some lower slopes to the north (Figure 2.4).

The tunnel will cross a depression in marble, which is filled by moraine sediments. The main part of moraine deposit is filled by mix of clay, sand and gravel. The lower part, which strains to the tunnel bottom is presumably consisted of crushed rock with high water content (Vegvesen, 2018). However, geological surveys of this site allow to presume, that if the tunnel construction will follow the designed route, even in the point of maximal moraine appearance, its bottom will lay on the blocky marble layer. Figure 2.4 is a simplified drawing of the soil section at the designed tunnel route depicted in detail in Figure A.2.



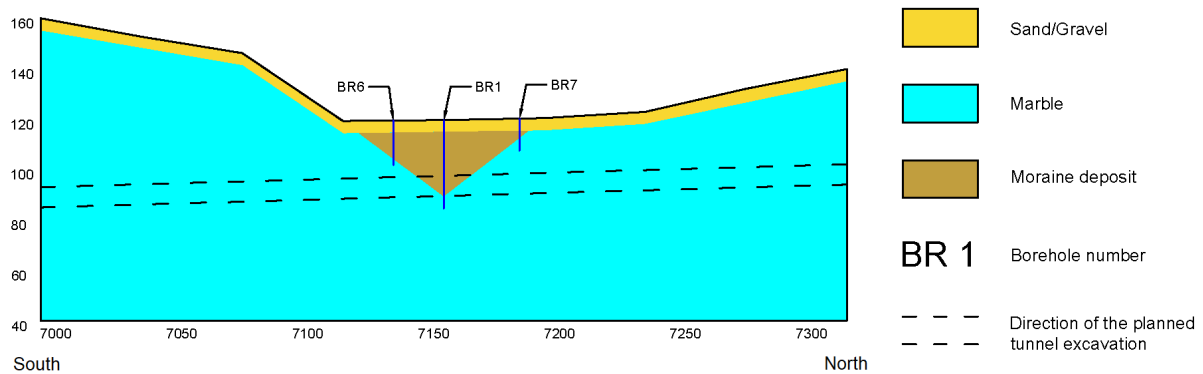


Figure 2.4: Longitudinal cross-section of tunnel route

### 2.1.1 Grain size distribution in moraine

The analysis of the collected samples grain size distribution from boreholes BR 1, BR 2, BR 6, BR 7 can give information about moraine content (Figure 2.5). Parameter  $M_d = Q_{50}$  represents the average grain size with 50% passage in the grain distribution curve. Parameter  $S_o = \log Q_{75} - \log Q_{25}$  measures the steepness of the grain distribution curve.

Therefore, moraine deposit mainly consists of mixed gravel and clay. However, it should be noted, because of limited data, moraine content could be analyzed only from the grain size distribution of samples from 5-10 m depth.

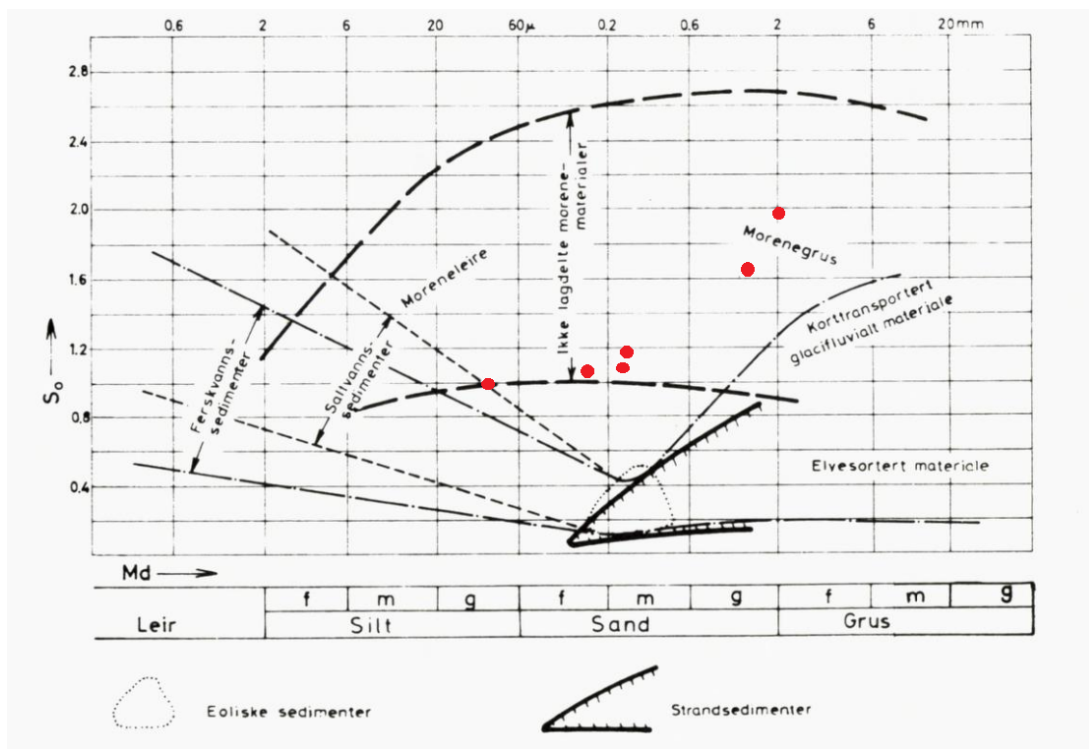


Figure 2.5: Grain size distribution (after Selmer-Olsen (1976))

## 2.2 Groundwater conditions

### 2.2.1 Seepage velocity

The existing data gives information about average groundwater level, hydraulic conductivity and porosity . Therefore, the calculation of seepage velocity in moraine layer is theoretical and gives relatively low results.

Seepage velocity was calculated between wells BR2–BR1;BR2-BR6 and BR2–BR7 ( Figure 2.6).

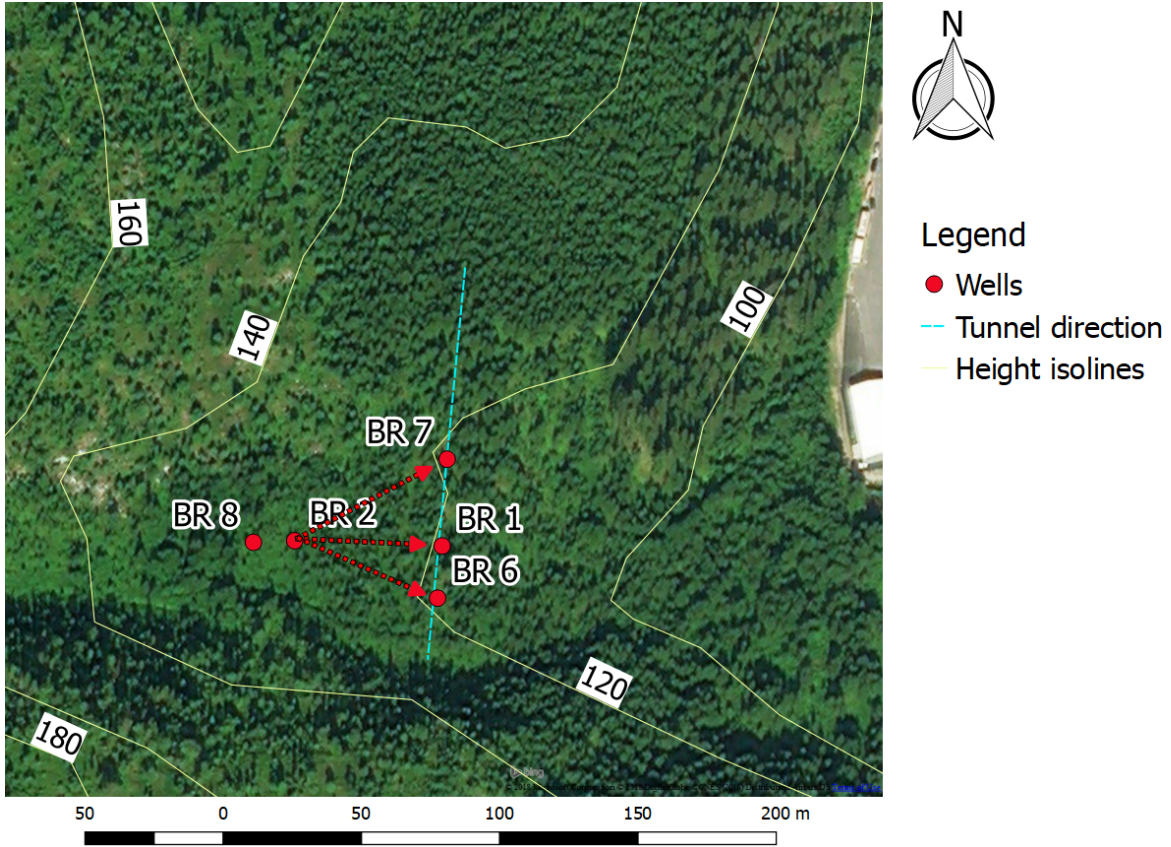


Figure 2.6: Groundwater flow direction

To calculate seepage velocity, following parameters should be determined:

1. Distance between points  $L_p$
2. Head loss between points  $\Delta h$
3. Hydraulic gradient  $i$
4. Discharge velocity  $v$

$L_p$  and  $\Delta h$  are found from the data. Then, it is possible to find hydraulic gradient.

$$i = \frac{\Delta h}{L_p} \quad (2.1)$$

Discharge velocity is found by Darcy's law:

$$v_d = ki \quad (2.2)$$

Eventually, seepage velocity is defined by discharge velocity divided by soil porosity.

$$v_s = \frac{v_d}{n} \quad (2.3)$$

$k$  and  $n$  are soil hydraulic conductivity and porosity from the project data. The  $k$  and  $n$  values for boreholes at the tunnel route are shown in Table 2.1.

Table 2.1: Hydraulic conductivity  $k$  and porosity  $n$

		BR1	BR6	BR7
$k$	m/day	4,59	29,16	22,71
$n$	[-]	0,29	0,25	0,25

Obtained discharge velocity and seepage velocity are shown in Table 2.2.

Table 2.2: Ground water flow calculation

		BR2 - BR6	BR2 - BR1	BR2 - BR 7
$L_p$	m	55,8	53,5	62,7
$\Delta h$	m	5,905	7,335	6,64
$i$	[-]	0,106	0,137	0,106
$v_d$	m/day	0,351	0,629	0,705
$v_s$	m/day	12,1	2,2	9,4

Thus, the highest seepage velocity values are related to boreholes BR-7 and BR-6, while BR-1 shows quite low influx speed.

The chemical composition of groundwater was investigated as well. The determined chloride content does not exceed 20 mg/l for all boreholes (Vegvesen, 2018) and can be used along with estimated seepage velocity at AGF design calculations in chapter 6.

# Chapter 3: Artificial ground freezing for tunnel stabilizing

## 3.1 Artificial ground freezing description

Artificial ground freezing technology is a design method, widely accepted in geotechnical projects. It is used for the construction of all kind of underground facilities excavated in weak water saturated soils and rocks. The principle of the method is the construction of a temporary cofferdam consisted of frozen ground, which prevents water flow to underground constructions and stabilizes weak grounds around excavation.

Artificial ground freezing method is based on naturally freezing technology, which was used in Siberia in the 19th century (*procede sibirienne*). Understanding of heat transfer physics allowed engineers to excavate mineral resources under river bottom (Vakulenko and Nikolaev, 2015).

The first mention about artificial freezing in mining refers to 1862, when series of freeze-tubes with circulated brine were used to freeze ground massive around a mineshaft in Swansea, South Wales. The same principle of freezing was patented by German engineer Poetsch in 1883. The method was consisted of freezing by the circulation of negative temperature salt brine in tubes buried in water saturated soil (Harris, 1995).

Nowadays, artificial ground freezing technique is widely applicable in different underground constructions projects. The method is used for mining shafts, tunnels, deep excavations, contamination sites with different geometry and positioning constructed as in soils as in rocks. The practice of the method use includes excavations up to 45 m diameter and to the depth of 900 m from the surface (Vakulenko and Nikolaev, 2015).

Artificial ground freezing technology is divided on brine and brine-less methods which include nitrogen, solid reagents and others. Furthermore, there is another classification on direct (nitrogen, solid reagents) and indirect (brine freezing) methods (Johansson, 2012).

### Brine freezing

Usage of brine refrigerant is the most common option of ground freezing. Brine circulates through a refrigeration plant, where it is cooled by a compressor, containing ammonia or freon (Figure 3.1). The average temperature of brine coolant is around -20 °C, although

it can reach  $-50\text{ }^{\circ}\text{C}$ . Calcium chloride solution is commonly used for brine coolant, however propylene glycol, ethylene glycol and other solutions are applied as well. Refrigeration plants can be stationary or transportable.

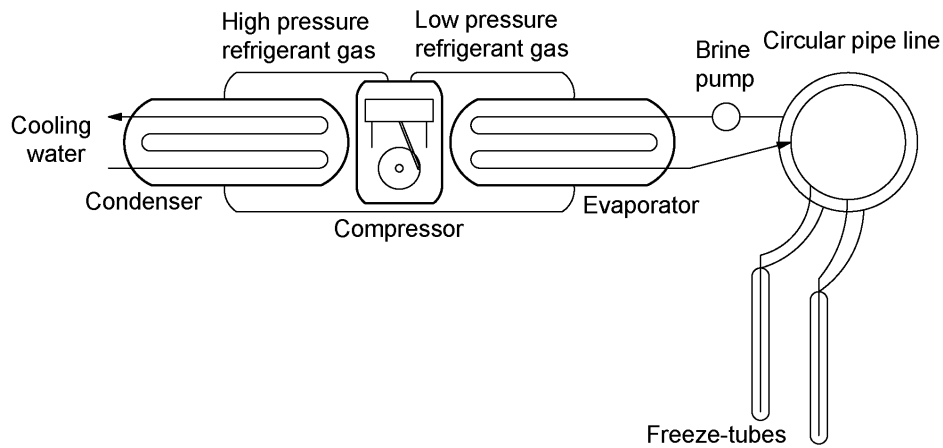


Figure 3.1: Brine freezing scheme

Despite this technique is the oldest of existing and is successfully used nowadays, there are some significant disadvantages. Preliminary work takes long time, also as the process of freezing, considering practical experience. Soil freezing speed can plunge lower  $0.1\text{ m/day}$  due to insufficient temperature of freezing. Moreover, circulated through freezing-columns brine has high reactivity and destroys frozen soils massive in the case of their destruction.

### Brine-less freezing

Besides brine option there is kind of coolants evaporating directly in freeze-columns. In this case propane, ammonia, freon 12, nitrogen, carbon dioxide and others can be used as coolants.

Liquid nitrogen ( $LN_2$ ) is the most often applied coolant for brine-less freezing. The first practical experience of direct  $LN_2$  injection into freeze-tubes was in France in 1962 (Chamberlain, 1979). The temperature of  $LN_2$  evaporation at atmospheric pressure (760 mm Hg) is  $-195,8\text{ }^{\circ}\text{C}$ . Other known coolants, considering the same pressure, evaporate at temperatures: Propane ( $-42,2\text{ }^{\circ}\text{C}$ ); ammonia ( $-34\text{ }^{\circ}\text{C}$ ); freon 12 ( $-29,8\text{ }^{\circ}\text{C}$ ).  $LN_2$  is the most often used for accident elimination at underground constructions caused by groundwater flooding

The technological scheme of Liquid Nitrogen freezing considers its injection in freeze-tubes with the same construction as for brine freezing.  $LN_2$  is filled from the vacuum reservoir to freeze-tubes, where it evaporates and afterwards is vented to the atmosphere (Figure 3.2).



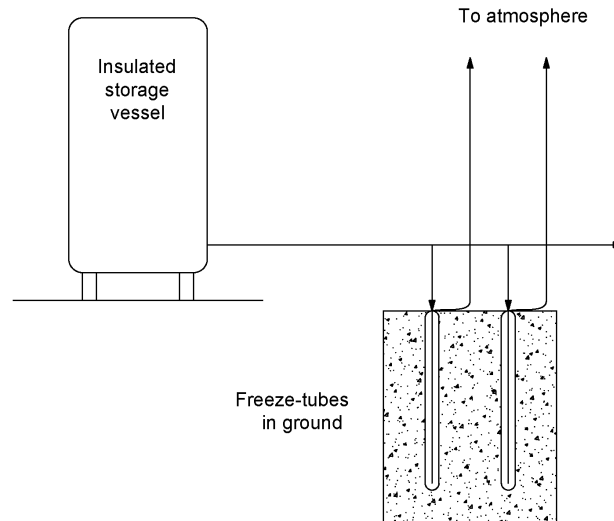


Figure 3.2: Liquid nitrogen freezing scheme

In comparison with brine freezing,  $LN_2$  usage has a number of advantages:

1. Due to low temperatures of evaporating,  $LN_2$  initiates intensive ground freezing around columns, therefore minimal time required for ice-wall closure is 4-6 times less than with brine freezing;
2. There is no demand in refrigeration plant, as  $LN_2$  is supplied in special vacuum tanks;
3. Preparation works are simplified;
4. Freezing is applied without brine, and, therefore, there is no need in brine pump, where freeze losses occur;
5.  $LN_2$  is inactive to frozen grounds and, in case of leakages, does not affect them in contrast to brine;
6. Liquid nitrogen is non-toxic, blast and fire-proof coolant.

However, despite significant advantages, this option is not wide accepted in artificial ground freezing. There are several reasons: high cost and consumption for freezing carrying out, there is no developed practice of the option realization.

The scheme, when solid carbon dioxide (cardice) is applied, is similar to liquid nitrogen option. In this case freeze-columns are filled by cardice, which sublimates at temperature - 78,9 °C. Also solid carbon dioxide can be used as refrigerant for brine cooling at refrigeration plant. This option reduces energy costs and temperature of brine, which, in total, is more cost effective in comparison with simple brine freezing (Table 3.1 ).

Table 3.1: Freezing methods comparison

	Quality	Brine	Brine-less	
			$NO_2$	Solid Carbon dioxide
Site installation	Electric power	+	-	-
	Refrigeration plant	+	-	-
	Circulation pumps	+	-	-
	Pipe system for distribution of coolant	Supply and return	Supply only	Supply only
Execution of freezing	Physical condition of coolant	Liquid	Liquid/Vapour	Solid/Vapour
	Minimum temperature achievable (theoretic)	$-34^{\circ}C$ $MgCl_2$ , $-55^{\circ}C$ $CaCl_2$	$-196^{\circ}C$	$-78,9^{\circ}C$
	Reuse of coolant	+	-	-
	Control of system	+	Labour-intensive	+
	Support of freeze wall shape	Designed	Complicated to design	Designed
	Frost penetration	Slow	Fast	Moderate
	Impact on freeze wall in case of damage to freeze-tubes	Thawing effect	-	-

### Other artificial ground freezing methods

For Arctic region, where average temperature is below  $0^{\circ}C$ , season cooling systems are wide accepted, which are called thermosyphons. They are made as sealed freeze-columns filled by non-freezing coolant with one part buried in soil, while the other part is on surface (Figure 3.3 ). Thus, a coolant cooled by air, sinks to the bottom part of thermosyphons, where it, because of heat transfer with surrounding soils, warms and rises again to the top part.

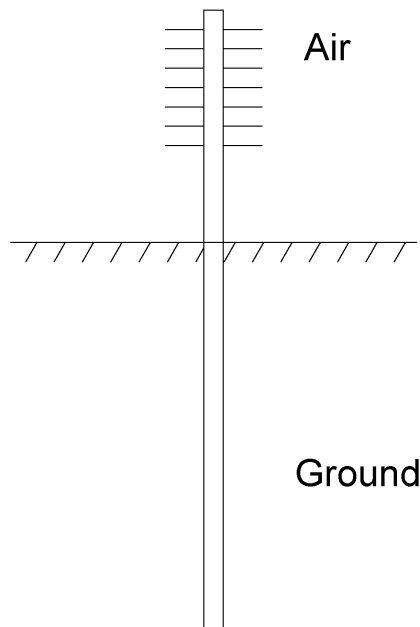


Figure 3.3: Thermosyphon scheme and an example of their application in West Siberia

Although these freezing systems can be as vertical as horizontal and can be buried up to 100 m in ground, they have quite low efficiency and mostly are used for foundations stabilization in permafrost.

### 3.1.1 Comparisson of induced methods with artificial ground freezing

The comparison of AGF technique with other most common methods of soils stabilization can be summarized by Table 3.2, which describes difference between methods during underground construction design. As it is seen from Table 3.2, the most of techniques are applicable for limited ground conditions in contrast to AGF, which has the highest versatility. Moreover, most of other methods are more complicated in realization and environmentally dangerous than AGF (Vakulenko, 2017).

Table 3.2: Ground stabilizing methods (from Harris (1995))

Particle size		mm											
		0.01		0.1		1		10					
Osmosis													
Dewatering													
Grouting	Cement												
	Bentonite												
	Chemical												
Ground freezing													
Compressed air													
Soil type		f		m		c		f		m		c	
		Clay		Silt		Sand		Gravel		cobbles			

## 3.2 Artificial ground freezing practice in Scandinavian countries

Artificial ground freezing is a common method around the world. At all there are more than 1000 objects constructed under the protection of frozen grounds (Vakulenko and Nikolaev, 2015). However, due to geological characteristics the method performing can vary from region to region. Therefore, the section will describe construction projects, carrying out in Norway and other Scandinavian countries, where geological conditions were similar to Norwegian.

### 3.2.1 Norway

Norway, due to its landscape, actively develops tunnels system. Thus, by 2017 year there has been constructed almost 3000 km of railway, road and subsea tunnels in total, while the length of hydropower tunnels exceeded 4000 km (Hansen et al., 2017).

Despite the good quality of rock, there are local discontinuities summoned by joints and weakness zones which are presented by crushed rocks or moraine sediments. Stability problems of these zones have to be handled, while not all the special methods of grounds stabilization are equally effective in areas of intersected rocks and sedimentary (moraine) deposits.

The projects, successfully performed by artificial ground freezing in similar geological conditions, are discussed below.

#### Oslofjord tunnel

7,2 km long tunnel is the part of a highway, connecting communities on both sides of Oslofjord 50 km south of Oslo. During investigation of geological conditions it was found that the tunnel will cross the weakness zone formed at the end of glaciation period and filled in with loose materials. The weakness zone consisted of upper soil materials part containing gravel, sand and clay under water pressure of 120 m and lower part with heavily jointed to crushed, clay filled rock (Figure 3.4).

There were considered two methods of stabilization – by grouting and by freezing.

Initially grouting was performed, and trial 11 m<sup>3</sup> of concrete was pumped in the weakness zone. However, due to drilling problems and projected large volumes of grout material required for sufficient stabilization forced to reject grouting as the main stabilization method.

Artificial ground freezing was performed by two rows of horizontal freeze-tubes with brine coolant at temperature of -28 °C for the thickness of 2–3 m. The area of theoretical blasting profile was equal to 130 m<sup>2</sup> (Andreassen, 1999). Drilling of 105 holes for both freeze and temperature control tubes took about one year. Further excavation through the frozen zone was performed by drilling and blasting in full cross section in rounds of 3 m. It took 12

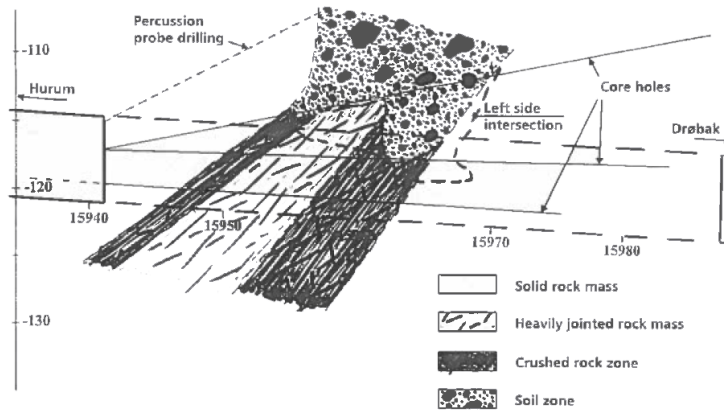
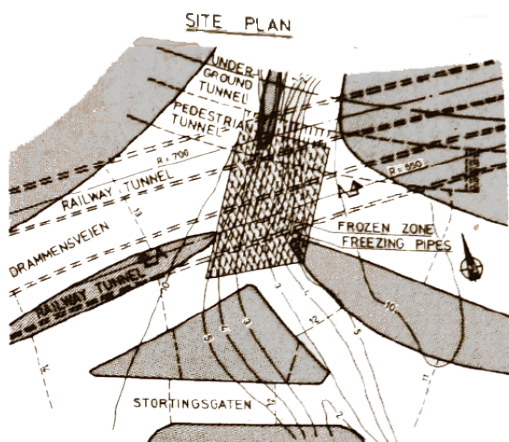


Figure 3.4: Section through the Hurum weakness zone along the tunnel centre line ( from Backer and Blindheim (1999)

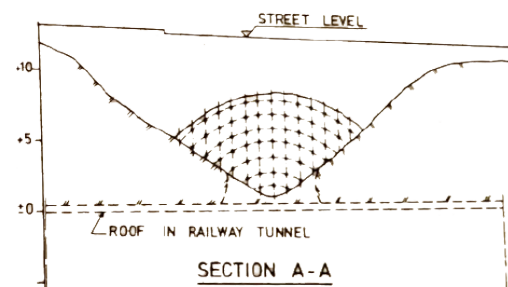
weeks to freeze the required soil massive. Then a layer of 30-40 cm fibre reinforced sprayed concrete with alkali-free additives was applied as immediate support on the exposed frozen ground. As a permanent support, the lining of concrete with 1-1,2 m thickness was used. Tunnel was opened in 2000 after 15 weeks of excavation and support operations.

### Oslo city centre tunnel

3,6 km long railway tunnel passing Oslo centre was opened in 1980. The weakness zone was found below Drammensvein street where was a depression going down to the roof of the tunnel. Moreover, at the same location, just above the railway tunnel, an underground tunnel of functioning subway line and pedestrian tunnel were already constructed (Figure 3.5 a). Therefore, the main demand for the new tunnel construction was in the prevention of settlements in the tunnels and the above lying street. To meet this challenge it was decided to perform artificial freezing of depression filed by sandy gravel and crushed stones (Figure 3.5 b).



a) Site plan



b) Section A-A

Figure 3.5: Site plan and cross-section of the weakness zone (from Jøsang (1980)

It was agreed to drill holes for freeze-tubes from subway tunnel which ran parallel the new tunnel, few meters to the side and above the new tunnel profile (Figure 3.6), as it was a single alternative allow to continue transport operations during the drilling. However that significantly affected the working time, as drilling could be performed only 3-4 hours at night time.

In total, 56 holes were drilled with 26 m length and the distance of 1 – 1,2 m between them. The projected thickness of frozen soil massive was equal to 5 m. That was reached by freon coolant circulation with temperature  $-15^{\circ}\text{C}$  in 8 weeks.

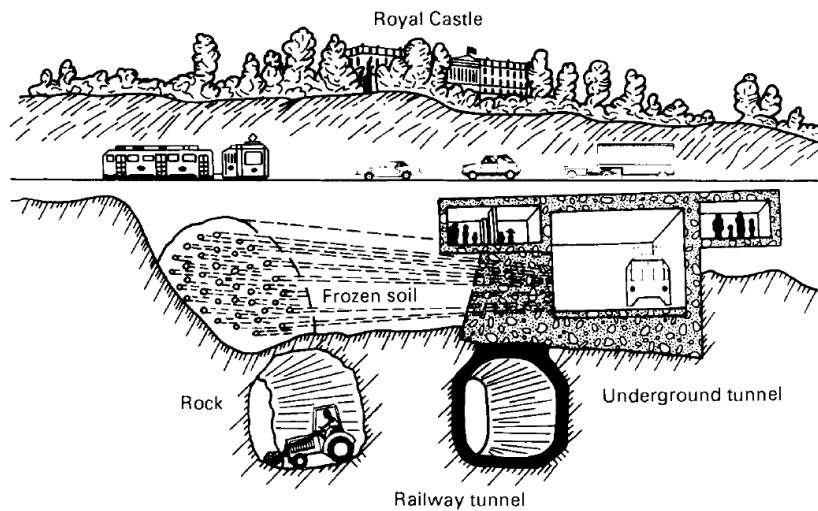


Figure 3.6: Cross section of tunnel systems (from Jøsang (1980))

Further excavation was performed by blasting and permanent lining was made by cast-in place concrete. Generally, the volume of  $1100\text{ m}^3$  was frozen. The total price for the freezing operation was equal to USD 720.000 in 1980, which constitutes more than USD 2,3 m in 2018.

### **Moss town centre tunnel**

The tunnel was designed as a part of new railroad line from Sadbukta to Såstad. 200 m long tunnel crossed groundwater saturated moraine sediments through the whole length. The measured coefficient of permeability  $k$  at the designed 22 m depth of the tunnel was equal to  $1 \cdot 10^6\text{ cm/s}$ . Therefore, it was planned to apply AGF method for soils stabilizing. The projected average temperature in the frozen zone was  $-10^{\circ}\text{C}$ , while the ice-wall thickness was estimated as 3-4 m thick (Figure 3.7).

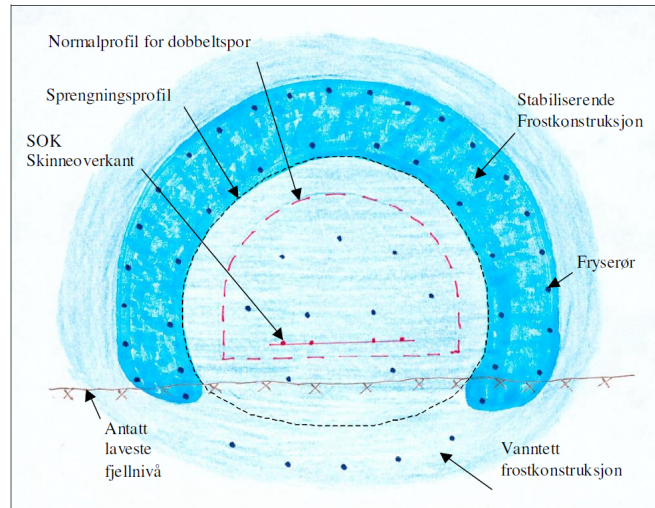


Figure 3.7: Ice-wall for Moss centre tunnel design (from Berggren (2007))

Considering that AGF method was planned for a long section, the freezing process was restricted by the maximum freeze-tubes length which could not exceed 40 m. Thus, it was divided into 7 stages with 10 m overlap (Figure 3.8).

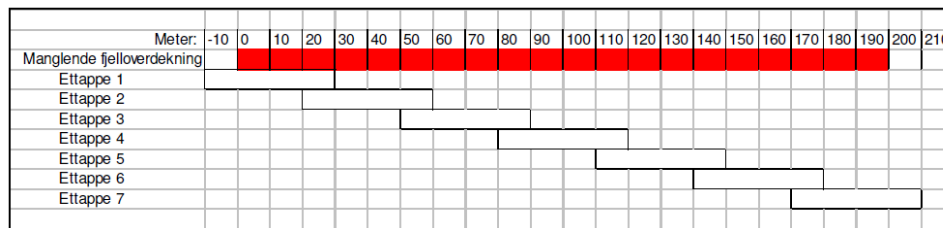


Figure 3.8: Time schedule of AGF applying at Moss centre tunnel (from Berggren (2007))

In total, the project of AGF applying at Moss town centre tunnel was designed for 3 years, with 5 months for each stage.

### 3.2.2 Sweden

#### Hallandsås project

The Hallandsås tunnel is located between Förslöv and Båstard in the north-west part of Sweden and it is part of west coast railway line between Gothenburg and Malmö. The project had two parallel tunnels 8,7 km long. Furthermore, it crosses several weakness zones, the most complex is Mölleback zone filled by extremely weathered gneiss and silty clayey materials with high water pressure. Works at the project began in 1993, however, due to financial difficulties, preparation for Mölleback zone excavation started in 2011.

Ground freezing was designed as the most effective method for this zone. It has been decided to perform horizontal freezing at the tunnel level to create a frozen ring with  $-2\text{ }^{\circ}\text{C}$  isotherm located 2m outside the tunnel with diameter 8m. The designed temperature of

coolant was  $-40\text{ }^{\circ}\text{C}$ , and the freezing of weak zone was performed by 3 sequential sections with 16 freeze-tubes each (Sturk and Stille, 2008). The freezing of 233 m in Mölleback zone was performed in 2 stages (Figure 3.9). The total time of freezing constituted around 180 days and further TBM excavation of the west tunnel was done within 3 weeks. The rings of prefabricated concrete segments were used for permanent lining designed to bear full hydrostatic load and load from heavily weathered poor rock.

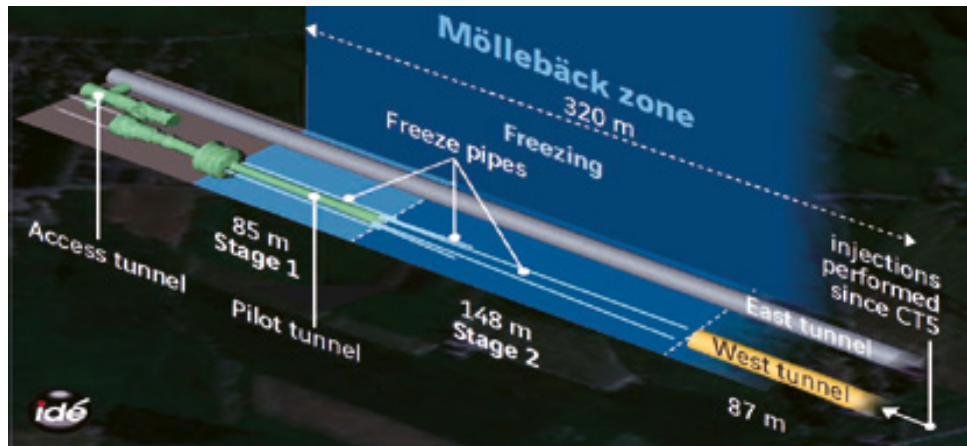


Figure 3.9: Schematic view of the MBZ freezing area (from Schubert (2013))

### Bothnia line tunnel

This tunnel was constructed for railway line in the middle of Sweden between Örnköldsvik and Umeå. The tunnel mostly passes through good conditions Precambrian bedrock, however, there are 95 m of moraine clayey soil deposit where was performed artificial ground freezing (Figure 3.10).

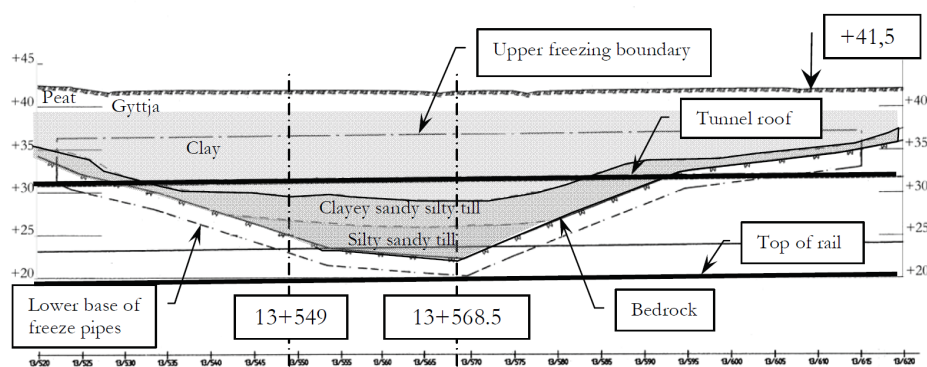


Figure 3.10: Longitudinal profile of the ground freezing area at the Bothnia Line (from Johansson (2009))

The ground was frozen by 350 freeze-tubes drilled vertically from the surface (Figure 3.11). The drilling of holes for freeze tubes was performed in 5 months – from December 2001 to April 2002. The freezing with designed coolant temperature  $-15\text{ }^{\circ}\text{C}$  ran for 90 days, which



created a frozen zone of 3m out of the tunnel contour. Then, during the excavation of the tunnel temporary shotcrete lining was made and permanent lining consisted of in situ concrete casting, which was finished in May 2003. After all, in September 2003, refrigeration plant was shut off with the abandonment of freeze-tubes.

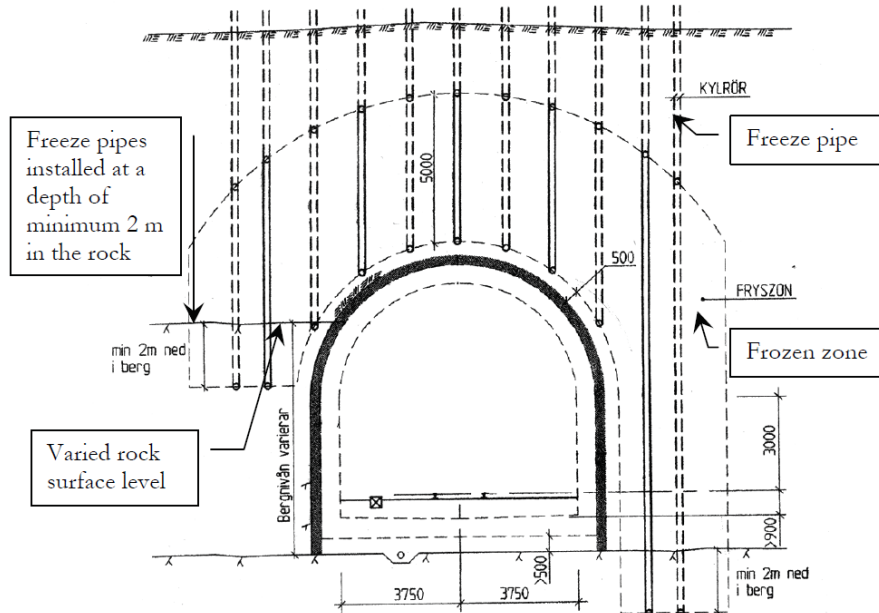


Figure 3.11: Tunnel section with a circular arc, showing various installation depths of freeze-tubes (from Johansson (2009))

### 3.2.3 Finland

#### Helsinki metro tunnels

During Helsinki metro construction the method was applied for 25 m deep tunnels with horizontal freeze-tubes placing (Figure 3.12). Twin tunnels were excavated in bedrock consisted of hard granite and gneiss. However there was a depression formed by a continental glacier and filled up with moraine sediments including sand, silt and clay layers. The depression was called the Kluuvi cleft. The length of soil section crossed by the tunnel was equal 30 m.

It should be noted that Grouting was rejected for that case since it was considered irrational to use it for fine grained and heterogeneous soil of the depression.

The drilling of freeze-tubes holes was performed from both sides of the depression and freeze-tubes overlapped in the middle by 2,5 m. The ice-wall had a thickness of 2,5 m and was created by two concentric freeze-tube rings. The spacing between freeze-tubes was equal to 1,9 m in the outer and 1,6 m in the inner ring with the 750 mm distance between the rings. The freezing plant was located at street level and had three compressors with a total output 280 kW.

To create a 30 m long ice-wall around 6,5 m high tunnels, the freezing plant worked for 55 days. Then, after an excavation process, a permanent lining of cast iron segments was set up. The space between the rings and frozen soil was filled with shotcrete and Portland cement grout.

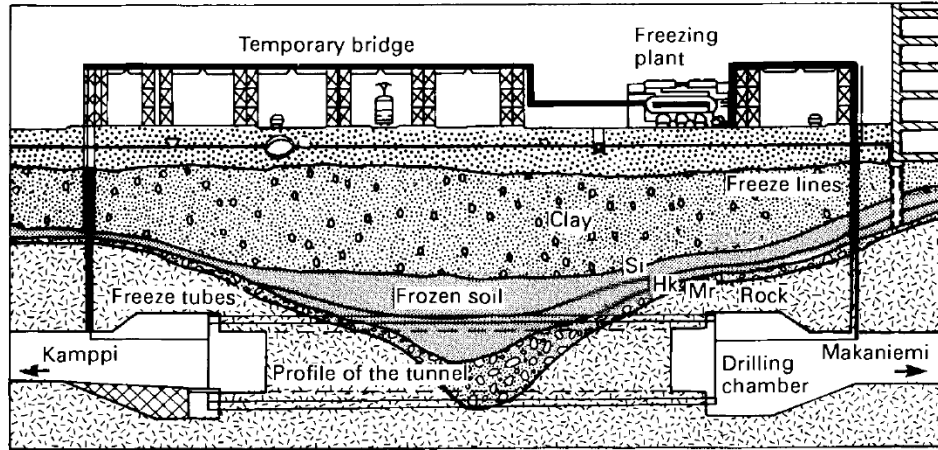


Figure 3.12: Longitudinal section of Helsinki metro tunnel (from Vuorela and Eronen (1982))

### 3.2.4 Comparison of the projects

The main characteristics of projects described above, can be summarized by Table 3.3.

Table 3.3: Comparison of projects with AGF method using

Project	Soil material	Freeze-tubes placing	Tunnel depth	Length of frozen zone	Number of freeze-tubes	Thickness	Coolant temperature	Time of freezing
-	-	-	[m]	[m]	-	[m]	[°C]	[weeks]
Oslo city centre tunnel (1980, Norway)	Sandy gravel and crushed stones	Horizontal	15	26	56	5	-15	8
Oslofjord Tunnel (1999, Norway)	On the top: moraine (gravel, sand, clay) On the bottom: crushed rock	Horizontal	120	30	28	2,5	-28	12
Moss centre railroad tunnel (2007, Norway)	Moraine clayey soil	Horizontal	22	200	35x7	3-4	-40	144
Halandsås tunnel (2011, Sweden)	Weathered gneiss and silty clayey materials	Horizontal	150	233	16x3	2,1-5,4	-40	26
Bothnia line tunnel (2002, Sweden)	Moraine clayey soil	Vertical	25	95	350	3	-15	13
Helsinki metro tunnels (1980, Finland)	Moraine sediments (sand, silt, clay and boulders)	Horizontal	25	30	34	2,5	-26	8

# Chapter 4: Artificial freezing and grounds interference

## 4.1 Freezing process

Generally, soils can be classified as frost susceptible or non-frost susceptible, depending on their resistance to frost-heaving and thaw-weakening properties, which can lead to the damage of geotechnical constructions (Andersland and Ladanyi, 2004).

Thus, soils are divided by several categories in the relation to freezing.

Table 4.1: Frost susceptibility classification of soils (after Barry et al. (2005))

<b>Frost Group</b>	<b>Degree of Frost Susceptibility</b>	<b>Type of Soil</b>	<b>Percentage Finer than 0.075 mm (# 200) by wt.</b>
TI	Negligible to low	Gravelly soils	3-10
T2	Low to medium	Gravelly soils	10-20
		Sands	3-15
T3	High	Gravelly Soils	Greater than 20
		Sands, except very-fine silty sands	Greater than 15
		Clays PI>12	—
T4	Very high	All Silts	—
		Very Fine Silty Sands	Greater than 15
		Clays PI<12	—
		Varied clays and other fine grained, banded sediments	—

In general, frozen soils are useful for geotechnical projects because of their improved properties compared with unfrozen material. However, in order to get an accurate understanding of frozen soils behaviour, it is primary important to make sufficient analysis of

strength and thermal properties of frozen soils. The freezing process of soils includes void water freezing. The volume of frozen soil is increased by water expansion due to ice forming. In general, voids increase depends on the speed of freezing and, therefore, may be different from known 9% standard expansion. Furthermore, the freezing process can be affected by natural soils salinity and infiltration rate (Andersland and Ladanyi, 2004).

Thus, the description of specificities of frozen soils behaviour provided in technical and research literature, is given further in the chapter.

## 4.2 Soils testing and measuring

### 4.2.1 Mechanical properties of unfrozen and frozen soils

Mechanical properties define soils behaviour under loading conditions, which has significant importance for lining stresses calculation. Due to cementing effect of ice containing in pores, frozen grounds cohesion and stress-strain properties respectively are significantly higher than properties of melted. Thus, uniaxial compression tests show that strength of frozen soils can increase more than 10 times for clay and slightly less for sand (Figure 4.1). However thermal micro-cracking during cooling can decrease the growth of compression strength, as it is shown in the case of Le Sueur sand loading.

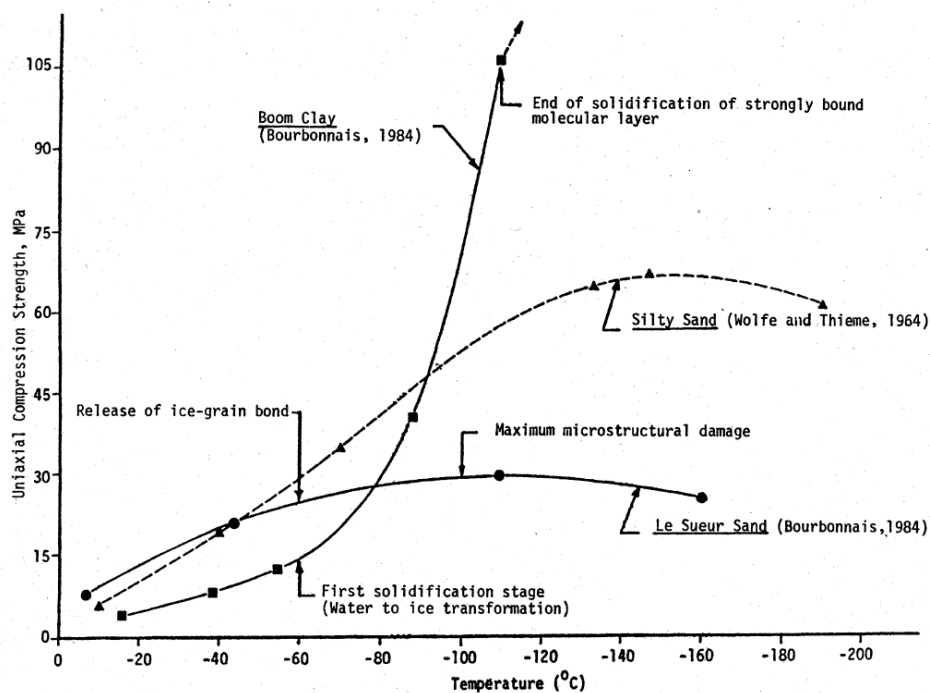


Figure 4.1: Temperature influence on uniaxial compression strength for sand, clay and silt (from Andersland and Ladanyi (2004))

Figure 4.2 shows Young's modulus variation for the same types of soils .

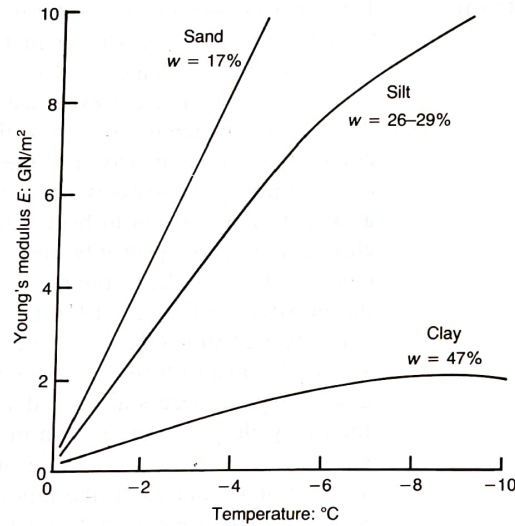


Figure 4.2: Young's modulus variation (from Harris (1995))

Consequently, tests carried out for soils similar to widely observed in Norway, including marine deposits (MD), alluvium and extremely weak granite (EWG) (Figure 4.3). Similarly to the previous testing they show linear relation to temperature. Thus, uniaxial compressive strength and elasticity modulus increase, while Poisson's ratio decreases as long as temperature becomes lower.

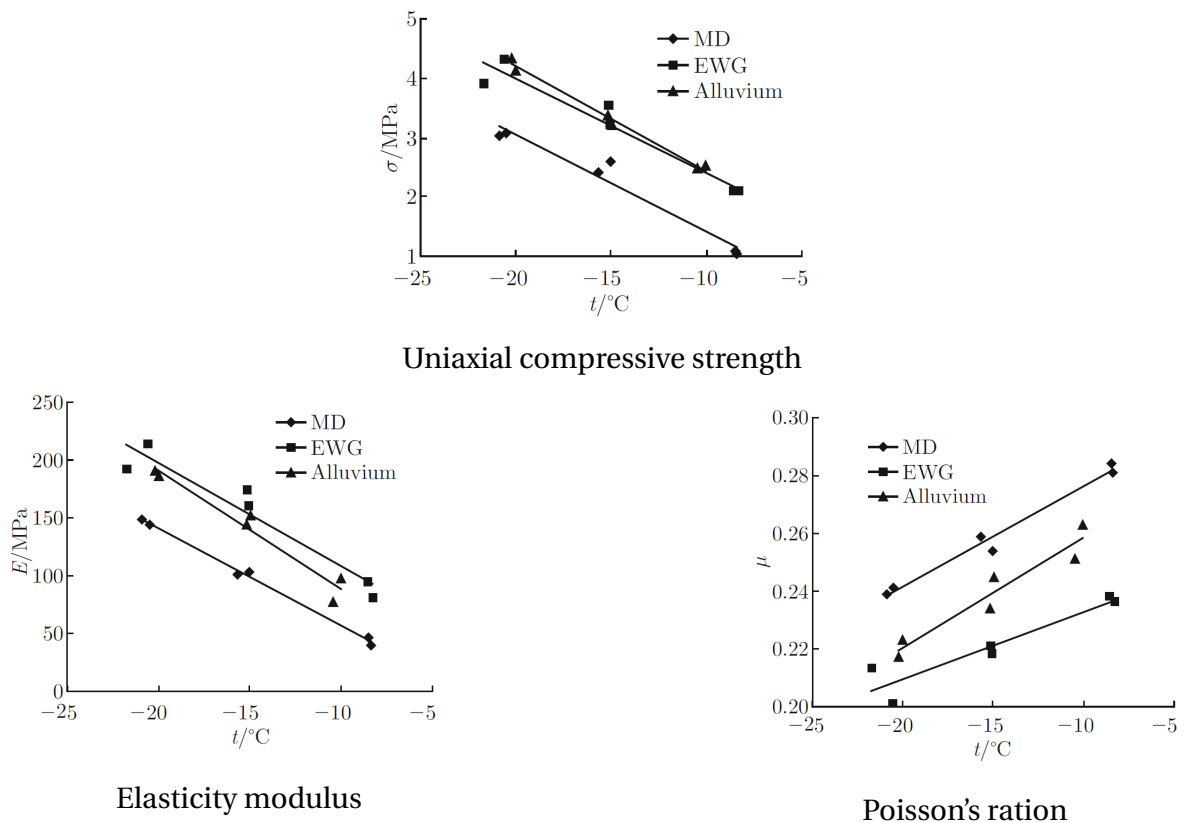


Figure 4.3: Frozen grounds testing, carried out for a tunnel construction in Hong Kong (from Hu et al. (2013))

The comparison of frozen sand and clay stress-strain behaviour made by Bourbonnais and Ladanyi and presented in (Andersland and Ladanyi, 2013) shows that frozen sand strength increases drastically with temperature drop. Furthermore, in general, it is more brittle than clay. By contrast, frozen clay, even at low temperature remains its plastic behaviour (Figure 4.4).

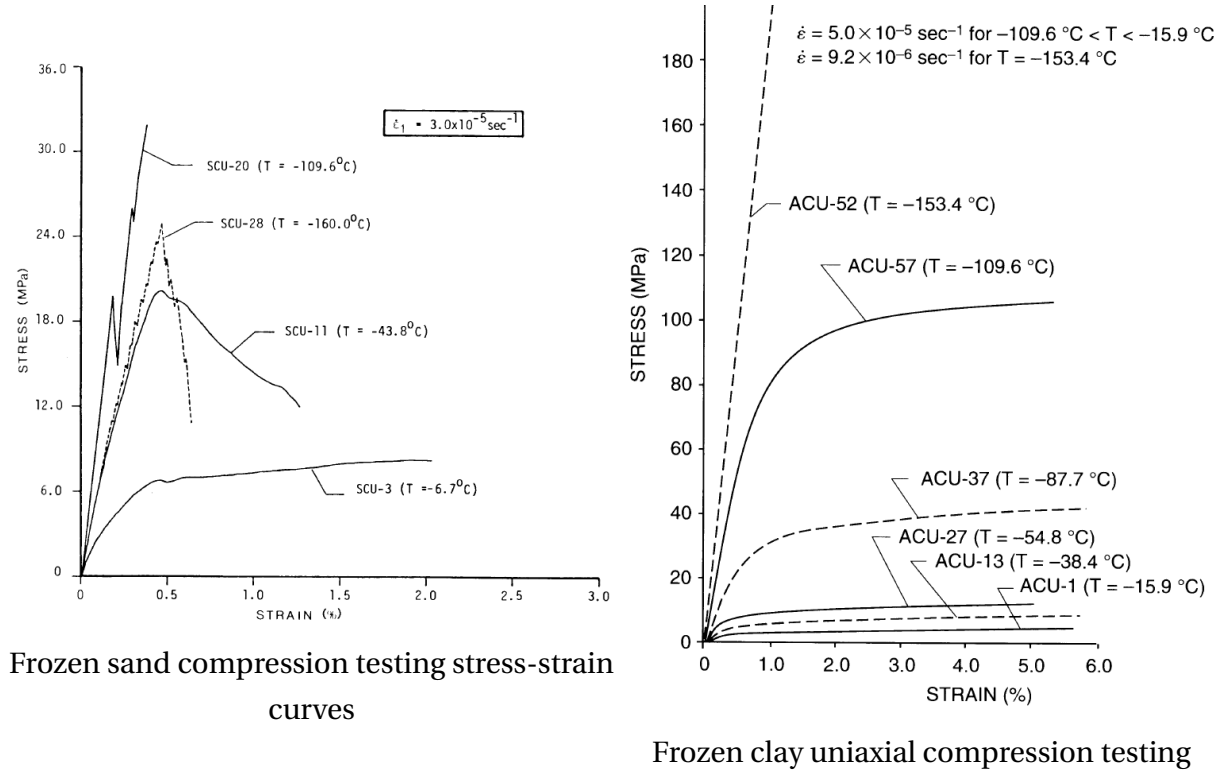


Figure 4.4: Stress-strain curves for sand and clay (from Andersland and Ladanyi (2013))

## 4.2.2 Thermal properties of soils

Thermal properties define soil response to thermal changes. Generally, they describe characteristics of heat transfer in soils. Heat transfer is the process responsible for the forming of artificial frozen cofferdam. All kind of calculations concerning freeze-wall depth, time of freezing and required quantity of heat for the process of freezing are based on equations including soils thermal properties. The main parameters defining thermal properties are thermal conduction, heat capacity, thermal diffusion and expansion and latent heat. These parameters can be measured as in the laboratory as by empirical equations based on the previous measurements.

Thermal conductivity is the transfer of the amount of kinetic energy through a unit area in a unit time under a unit temperature gradient, in other words it represents the transfer of heat from warm part to a cooler part in the soil massive. Thermal conductivity-temperature graph for some types of rocks is shown in Figure 4.5.

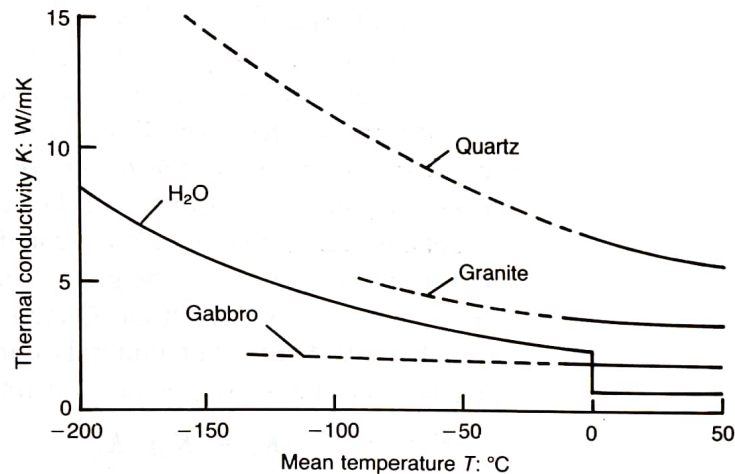


Figure 4.5: Thermal conductivity variance due to temperature (from Harris (1995))

Heat capacity is the amount of heat required to raise the temperature of a unit volume of soil by 1 K, while specific heat capacity is heat raising unit mass temperature by 1 K.

Figure 4.6 shows specific heat capacity distribution for rocks and ice due to temperature fluctuation.

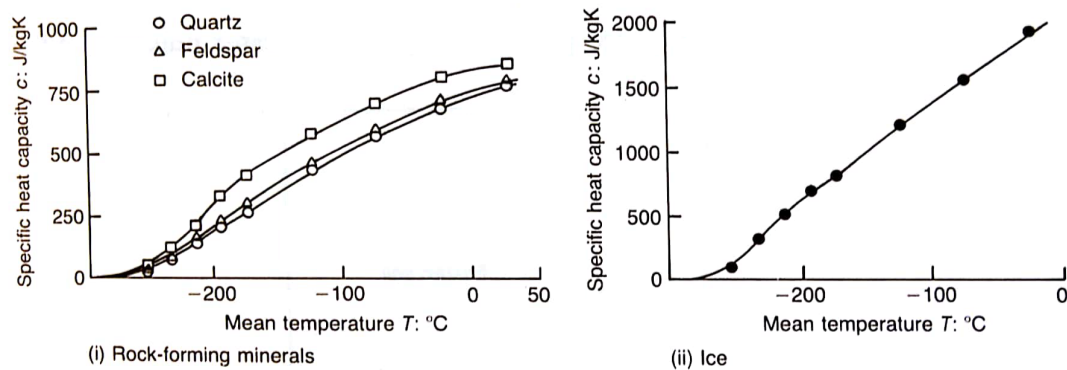


Figure 4.6: Specific heat capacity variance due to temperature (from Harris (1995))

It should be noted that heat capacity and thermal conductivity for all soils are affected by the water content and the porosity of soils. High water content increases thermal conductivity of soils, while high porosity causes lower thermal conductivity and a higher heat capacity. As it can be noticed by figure 4.5, mineral composition of rocks can have significant influence on thermal conductivity, therefore, with higher quartz appearance – the higher thermal conductivity of material containing it. However, with the growth of porosity the influence of material composition decreases (Johansson, 2012).

Relationship between thermal conductivity ( $\lambda$ ), heat capacity ( $c$ ) and bulk density ( $\rho$ ) is

expressed by a ratio called thermal diffusivity (Eq. 4.1).

$$\alpha = \frac{\lambda}{c * \rho} \quad (4.1)$$

### 4.2.3 Seepage flow velocity

Groundwater flow speed often has the crucial importance for artificial ground freezing application. During freezing under stable groundwater aquifer the external heat infiltration from surrounding grounds decreases gradually and it is distributed uniformly. In case of ground freezing with unsteady heat infiltration the power of freeze-tubes is partly absorbed by cooling of seepage flow (Figure 4.7).

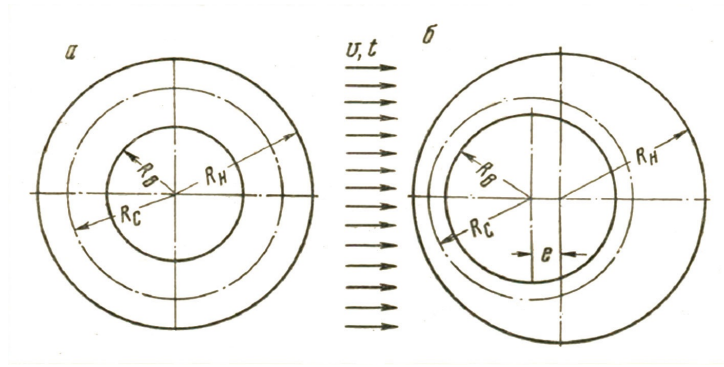


Figure 4.7: Frozen ground support system: a) in soils with steady groundwater; b) in soils with seepage flow

Thus, there is a limit of critical groundwater velocity, when freezing soil columns will merge. Practical experience has shown that for brine freezing the maximum velocity is approximately 1 – 2 m/day, while for liquid-nitrogen systems there were attempts to apply freezing for seepage flow up to 50 m/day.

The critical groundwater velocity  $u_c$ , (m/day) is defined by Eq. 4.2 from (Andersland and Ladanyi, 2004).

$$u_c = \frac{k_f}{4S * \ln\left(\frac{S}{4r_0}\right)} \frac{T_s}{T_0} \quad (4.2)$$

Where  $r_0$ —freeze-tube radius, m;  $k_f$ —frozen soil thermal conductivity, (W/m°C);  $S$ —spacing between adjacent freeze-tubes, m;  $T_s$ —the difference between the freeze tubes surface temperature and the freezing point of water, °C and  $T_0$  is the difference between the ambient ground temperature and the freezing point of water.

The issue of high seepage flow velocity can be solved by additional ground stabilizing methods as dewatering or by increasing of refrigeration plant power. However, in that case the relative costs will rise significantly.



#### 4.2.4 Salinity

Grounds salinity is a huge issue for artificial ground freezing. In this type of soils mechanical properties are significantly affected causing the strength decrease and the increasing of deformation. Salt presence in pore solution cause unfrozen water increase and accordingly, grounds freezing temperature decrease. It was found that mechanical properties of soils are affected not only by salt amount but also by its chemical content (Svintickaya, 1997).

Soils salinity can be classified by sea deposition environment and continental environment. If the first type is common for sea coast mainly in Arctic region with high chloride content, when the second is observed in areas, where salt accumulation happened because of high temperature and negative moisture balance difference. Continental salinity is consisted mainly of sulphates (Ignatova and Svertilov, 2013).

An expression for the calculation of temperature shift  $\Delta T$  due to salinity is shown in Eq. 4.3 by (Andersland and Ladanyi, 2004).

$$\Delta T = T_k \left[ \frac{S_n}{1000 + S_n} \right] \quad (4.3)$$

Where  $S_n$  – salinity in g/l;  $T_k$  – reference temperature equal to 57 °C for sea salt; 62 °C for NaCl and 32,5 °C for  $CaCl_2$ .

### 4.3 Affects of freezing

The main hazards following the process of grounds freezing are frost heave and thaw weakening, which can cause settlements of ground and even a tunnel fault.

#### 4.3.1 Frost heave

Soil volume increase because of freezing is called frost heave. Due to wide practical experience there are studied conditions inducing frost heave. The most significant influence on soils in artificial ground freezing area is exerted by prolonged freezing temperatures; appearance of frost susceptible material in the area; a supply of water from unfrozen region. Frost heave process occurs when freezing front moves so slow that water transport is possible in soil massive in contrast to fast freezing when water freezes in situ. Frozen water forms lenses in soil, which expand these formations. It can reach 10...15% and in some cases up to 40% (Bronfenbrener and Bronfenbrener, 2010).

Frost susceptibility of soil can be defined by in situ testing or on the basis of laboratory investigated parameters. Frost susceptibility can be observed by various types of soils from silt to gravel.

Figure 4.8 shows frost susceptibility propagation depending on grain size distribution. There are 4 groups of soils from no visible frost susceptibility (T1) to high frost susceptibility (T4).

Therefore, most of soils acceptable for artificial ground freezing, are related to frost susceptible category and can be affected by frost heave.

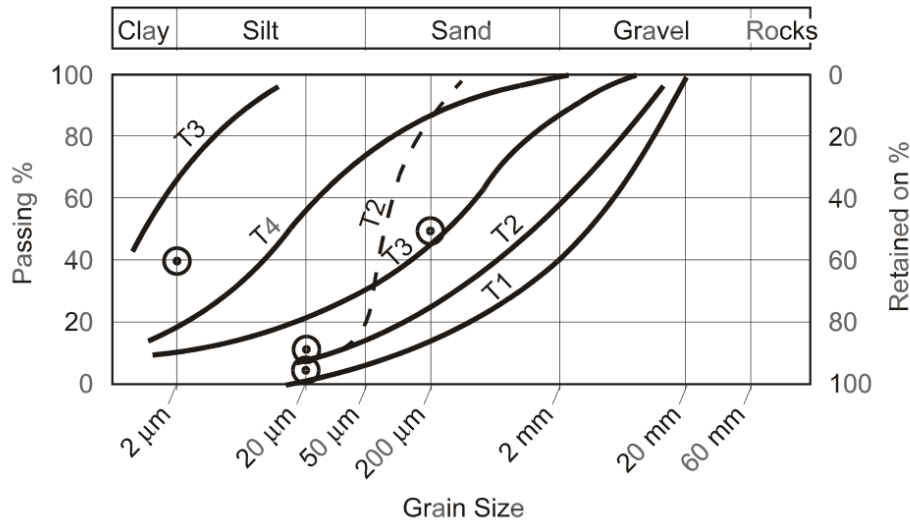


Figure 4.8: Frost susceptibility criteria in Norway (from Hoppe (2000))

The comparison of soils susceptibility and frost heave is presented in Table 4.2.

Table 4.2: Frost-susceptibility of soils (from Slunga and Saarelainen (1989))

Frost Class	Susceptibility	Capillary Rise, m	Fines Factor	Segregation Potential, mm <sup>2</sup> /Kh	Frost Heave Rate, mm/d
NEGLIGIBLE		< 1,0	<2,5	<0,5	<0,5
LOW		1,0-1,5	2,5 - 5,0	0,5 - 1,5	0,5 - 2,0
MEDIUM		1,5-2,0	5,0-10	1,5-3,0	2,0-4,0
STRONG		>2	> 10	>3	>4

The general representation of frost heave can be described by Eq. 4.4 from (Nevzorov, 2000).

$$h_f = h_I + h_{II} = 0,09 (w_{tot} - w_w) \frac{\rho_d}{\rho_w} z + 1,09 \int_0^{t_c} q_{w_f} dt \quad (4.4)$$

Where  $h_I$  – initial heave from water containing in pores;  $h_{II}$  – heave from ice migration;  $\rho_d$  – coefficient of recalculation from mass water content to volumetric;  $z$  – depth of ground freezing;  $q_{w_f}$  – insensitivity of moisture flow to the freezing front.

Frost heave can affect foundations of buildings above tunnel, furthermore, it can initiate faults inside underground constructions.

To reduce the influence of frost heave the ice-wall growth can be reduced after the minimum thickness for structural stability is reached. Also, additional insulation of freeze-tubes defined parts can decrease heave as well as some other methods described in (Jones, 1996):

- dewatering
- raising the viscosity of the pore water by using an additive
- preventing confined freezing
- drilling relief holes to adsorb at least partially the volume expansion.

### 4.3.2 Ground settlements

There are multiple factors affecting settlements formation. The most common cause is thawing of frozen soils, which can occur because of warming of coolant in freeze-tubes, as well as after the abandonment of freezing works.

Soils strength can decrease dramatically, immediately after thawing. The strength will be recovered due to the further consolidation. The thawing of artificially frozen soils around tunnel has a structural feature. It will initially occur under undrained conditions, as drainage will be restricted by the tunnel lining and frozen massive (Figure 4.9).

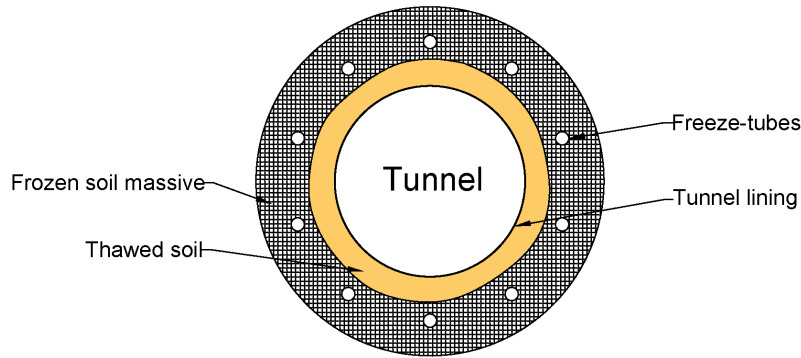


Figure 4.9: Artificially frozen ground thawing around tunnel

Thus, the greatest issues caused by thaw soils weakness are observed in case of frost susceptible grounds freezing from the surface. Settlements can be calculated by Gaussian distribution function, where the shape of settlement trough curve is written by Eq. 4.5 from (Jones, 1996).

$$\frac{s}{s_{max}} = \exp\left(\frac{-y^2}{2i^2}\right) \quad (4.5)$$

Where  $s$  – surface displacement at distance  $y$  from the center line;  $s_{max}$  – displacement at the center line and  $i$  is the parameter defining settlement trough width.

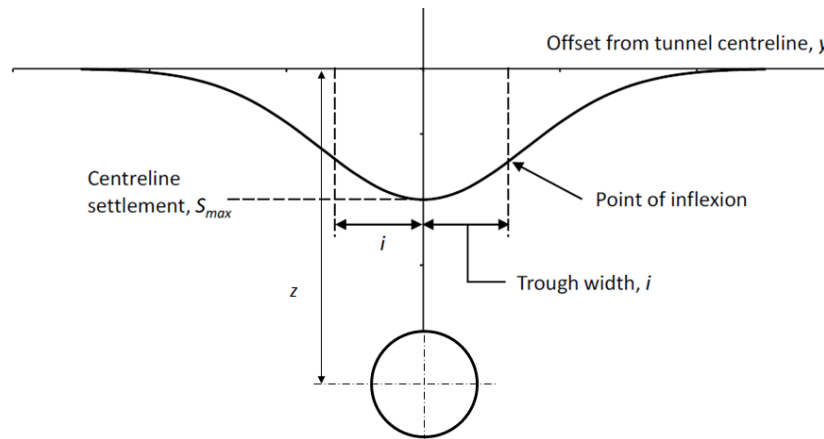


Figure 4.10: Ground settlements (from Hill and Stärk (2015))

### 4.3.3 Ground creep

Frozen soils creep should be considered as it can become significant due to high or long-term load conditions (Berggren, 1983).

Creep is time dependent deformation occurring at constant stress, evaluation of it is based on long time strength. Frozen grounds creep is connected with unfrozen water presence and its movement in soils. Depending on creep-rate variation creep can be divided by several stages. There are three phases – primary for decreasing creep rate during strain-hardening; secondary for constant and tertiary for increasing due to strain-softening (Figure 4.11).

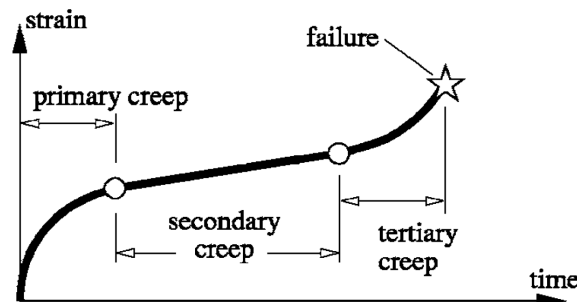


Figure 4.11: Creep performance in frozen soils (from Lackner et al. (2008))

Performed experiments showed that fracture processes occurred during the tertiary phase cause failure of the tested frozen soils samples (Lackner et al., 2008).

In the case of highly stressed ice-walls, when the deformation of ice support system is expected, the thickness of lining should be considered enough to tolerate creep deformation. There are variety of design methods applied in the world practice including initially erected permanent lining with sufficient thickness (USA, UK) or installing of temporary lining and the construction of permanent after soils shrinkage (PRC) (Harris, 1995).

# Chapter 5: Design of Bergåsen tunnel

## 5.1 Tunnel profile

Tunnel cross-section consideration is crucial important for AGF parameters design as well as for the simulation of the tunnel stability.

According to Norwegian standards, road tunnels are divided by categories on the basis of traffic volume expected for 20 years after the tunnel will be opened (Vegvesen, 2010). The designed traffic capacity for Bergåsen tunnel corresponds to category B following NPRA standard for road tunnels (Figure D.1). Thus, tunnel profile T-9,5 has been considered for this category (Vegvesen, 2013a).

Similarly, the geometrical dimensions of the tunnel normal profile can be found from NPRA standard, which are different for each tunnel profile (Figure 5.1). For this class of tunnel the required total width of the normal profile  $B_t$  is 9,5 m, where a roadway width  $B_k$  is equal to 7 m and free height is 4,6 m. The other specific dimensions are shown in Table 5.1.

It should be noted, that all the dimensions are given for a normal profile, which does not include the width of tunnel lining.

The tunnel has semi-circular cross-section. However, its profile is actually formed by 3 arches. One with higher radius for the top of the tunnel, while 2 others are equal and form tunnel sides. Tunnel cross-section parameters are defined in Norwegian standard (Vegvesen, 2010).

Table 5.1: Geometrical specification for T9,5 profile tunnel

	Total bredde	Kjørebane-bredde	Senterhøyde veggradier	Veggradius	Senteravstand veggradier	Senterhøyde hengradius	Hengradius
	Total width	Roadway	Central height of road radius	road radius	Central distance road radius	Central height radius	Height radius
Profile	$B_t$	$B_k$	$Y_v$	$R_v$	$X$	$Y_h$	$R_h$
T9,5	9,50	7,00	1,570	4.790	0,450	1,213	5,212

The theoretical blasting profile area for Bergåsen tunnel is equal to 62,4 m<sup>2</sup> and, in addition to the tunnel profile, includes 0,3 m thick lining, which choice is discussed in chapter 7.

Then, the volume of the material which should be excavated, is equal to  $62,4 \times 20 = 1248 \text{ m}^3$ .

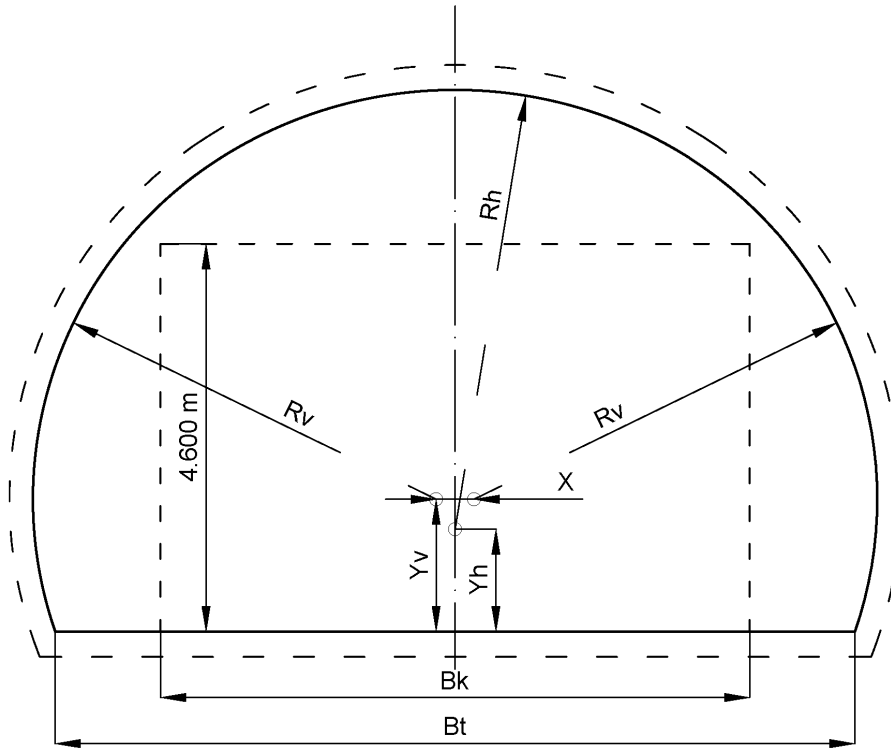


Figure 5.1: Tunnel profile dimensions (after Vegvesen (2010))

## 5.2 Tunnel excavation

Excavation through moraine deposit zone can be carried out only after complete freezing of the designed zone. The whole ice-wall construction should reach the condition of impenetrable structure and the average ice-wall temperature will come to the designed value (Berggren, 2000).

The length of the unsupported frozen construction is represented by equilibrium:

$$L_u P = E \tau \quad (5.1)$$

Where  $L_u$  – unsupported length of ice-wall; the maximum load on the ice-wall  $P = 0,26 \text{ MPa}$ ; designed thickness of the ice-wall  $E_{iw} = 1,2 \text{ m}$ ; shear strength of frozen soil  $\tau = 0,5 \text{ MPa}$  (from (Knutsson, 1981)).

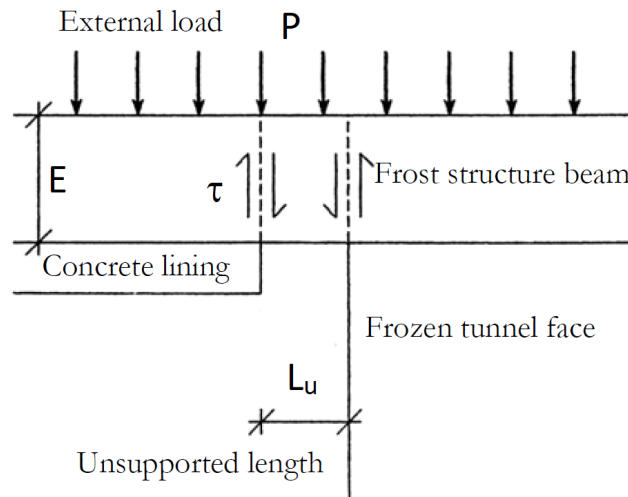


Figure 5.2: Open length of ice-wall, (after Berggren (2000))

Thus, Eq. 5.1 can be modified as:

$$L_u = \frac{E_{iw}\tau}{P} = \frac{1,2 * 0,5}{0,26} = 4,6m \quad (5.2)$$

On the assumption that excavation will be carried out by drill and blast method, the length of each drill and blast round should be approximately 0,5 m shorter then unsupported length. (Figure 5.3). Then, the length of a driving cycle becomes 4,1 m. Thus, there will be 5 cycles in total.

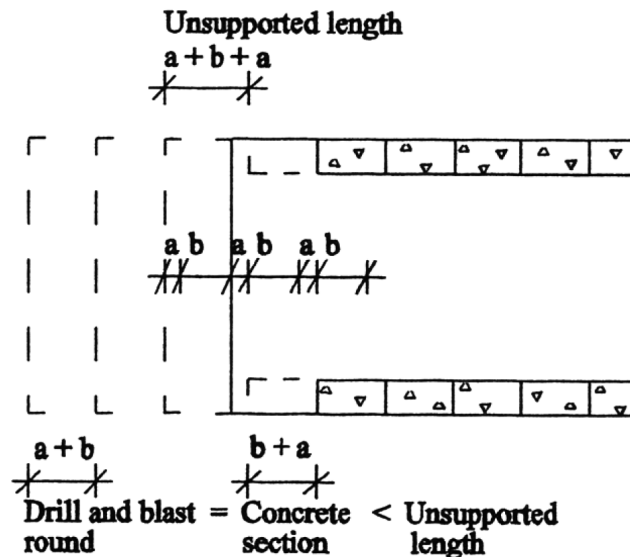


Figure 5.3: Drill and blast rounds, (after Berggren (2000))

The schedule of tunnel excavation described by (Eiksund et al., 2001), is presented below:

- day 1 – Preparation works and blasting (loading of the holes, blasting removing of the soil material, shotcreting );

- day 2 – Drilling for the next round;
- days 3-4 – Concrete works (reinforcement of the bottom slab, casting the slab, preparation for the vault casting);
- day 5 – Reserve time;
- day 6 – Reinforcement and installing of formwork for the tunnel vault;
- day 7 – Casting the vault.

Thus, if the blasting profile of Bergåsen tunnel was equal to Oslofjord, the total time of excavation through the moraine deposit would be equal to 5 weeks. However, considering that theoretical blasting profile of Bergåsen tunnel is approximately two times less than the profile of Oslofjord tunnel, the time for excavation may be shorter.

On the other hand, the soil section of the tunnel can be excavated by a regular excavator with shuffle, hammer or ripper tips, as it was carried out in Joberget tunnel, where moraine deposit was stabilized by pipe umbrella method because of moderate groundwater conditions (Aagaard et al., 2017).

The excavation of 100m long soil part lasted 4 months for the tunnel cross section area  $71 \text{ m}^2$ . Thus, it can be presumed that for Bergåsen tunnel the time duration will be less than 4 weeks without consideration of the time for concrete lining maturity.

The excavation and primary support costed NOK 300 thousand for 100 m at Joberget tunnel. For 20 m it will be approximately NOK 64 thousand in 2018.



# Chapter 6: Design of artificial ground freezing

## 6.1 Theory of ice-wall design

The proper design of artificial ground freezing project is crucial to the successful work performing. Therefore, the proper design consideration should be based on correct structural and thermal analysis of soils affected by freezing. After the justification of the possibility of artificial ground freezing performing, the next basic design criteria are determined:

- Selection of ground freezing approach;
- Coolant characteristics (type, running temperature);
- Number of freeze and observation wells;
- Freeze-tubes characteristics (dimensions, geometry and material);
- Freezing time;
- Required power for the refrigerant plant

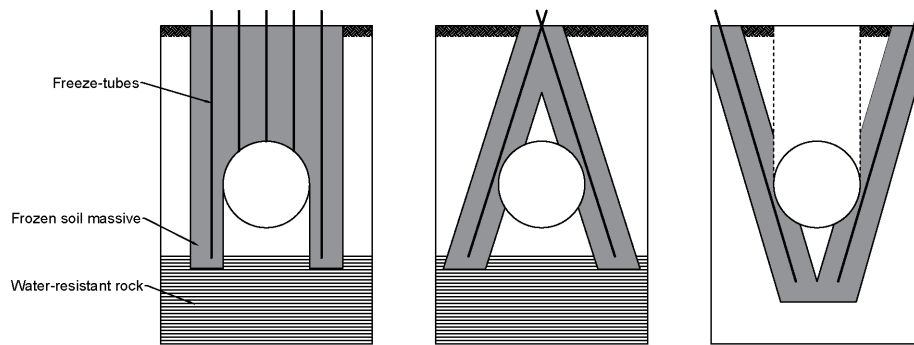
The suitable number of freeze-tubes and refrigerant plant capacity are calculated on the basis of required ice-wall thickness, which in turn depends on ground characteristics discussed in details in chapter 2.

The principles of freeze-tubes positioning, ice-wall thickness and time evaluation methods, costs and project closure are described below.

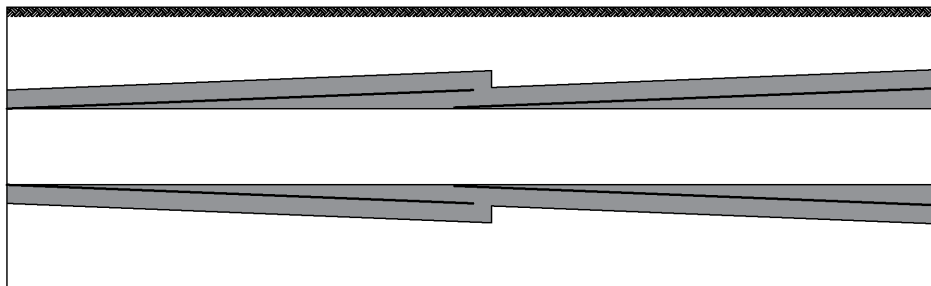
### 6.1.1 Positioning

The placement of freeze-tubes for tunnels excavated under artificial frozen grounds protection can vary due to tunnel configuration and its positioning. For shallow tunnels freezing can be implemented from surface with vertical or angled freeze-tubes (Figure 6.1 a). In the cases when surface drilling is impractical, the option of horizontal installation of freeze-tubes around tunnel can be chosen (Figure 6.1 b). This option is more labour consuming and expensive of combined difficulties, that make it costly in comparison with vertical freezing.

Thus, in world practice it is chosen mostly for tunnels with relatively long freezing required part, when horizontal freeze-tubes positioning is more cost effective than freezing from the surface. Furthermore, the accepted length of horizontal freeze-tubes is significantly shorter than for vertical freezing. Technical literature specifies the maximum length of horizontal freeze-tubes equal to 30-40 m (Harris, 1995). Otherwise, if freezing zone is longer, AGF can be carried out through sequential scheme, as it was described in chapter 3.



a) Vertical fitting of freeze-tubes



b) Horizontal fitting of freeze-tubes

Figure 6.1: Freeze-tubes positioning in tunnels

### 6.1.2 Ice wall thickness

The thickness of frozen ground barrier can be calculated by empirical formulas or by finite element method considering the number of freeze-tubes around tunnel. For general case thermal calculations consider two stages: Stage 1 – the ice-soil columns grow around the separate freeze-tubes; Stage 2 – the separate frozen soil columns form homogeneous continuous wall, which becomes thicker by freeze-tubes work. Furthermore, in case of multi-row location of freeze-tubes the third stage is considered, when walls formed by rows of frozen soil columns form a single wall (Sanger and Sayles, 1979).

Ice wall thickness mainly depends on temperature and time of freezing. In technical

papers the Domke equation is quite common used for the thickness calculation (Eq. 6.1).

$$E_{iw} = R_t \left[ 0,29 \left( \frac{p_0}{\sigma_{cs}} \right) + 2,3 \left( \frac{p_0}{\sigma_{cs}} \right)^2 \right] \quad (6.1)$$

Where  $R_t$  – the tunnel radius, m;  $p_0$  – overburden pressure, MPa;  $\sigma_{cs}$  – uniaxial compressive strength of soils, MPa

However, this formula has significant disadvantages. It does not recognize time related deformation and due to practical experience it is advised to use for depths 100 – 150 m. Besides, there are modified Domke equations developed by Vyalov and Klein, who added angle of internal friction. Then, the new equation taking in an account plastic deformation of the ice-wall, was proposed by Shangdong Mining College (Harris, 1995; Nasonov et al., 1992).

In total, it can be noticed that there are no universal solution to define ice-wall thickness. Thus, the decision to use proper equation should be based on the building conditions.

The number of freeze-tubes depends on the thickness of ice-wall and tunnel diameter. To calculate the number of 1 row freeze-tubes around a circular tunnel, Eq. 6.2 is used from (Trupak, 1974).

$$N = \frac{\pi(D + E_{iw})}{S} \quad (6.2)$$

Where  $D$  – tunnel diameter;  $E_{iw}$  – ice-wall thickness;  $S$  – spacing between freeze-tubes.

### 6.1.3 Time evaluation methods

There are two basic methods for the estimation of time required to freeze the designed volume of soil. The first is based on the separate evaluation of the time for primary and secondary freezing. Initially, time required for ice-columns forming around separate freeze-tubes is evaluated. Then, the time for continuous ice-wall formation is estimated. This method was proposed in (Sanger and Sayles, 1979; Khakimov, 1966). Evaluation of freezing time formulated by Sangers&Sayles is presented in Appendix B.

Another method of freezing time assessment is based on heat transfer between freeze-tubes and surrounding soils (Nasonov et al., 1992).

The method includes refrigeration required to freeze appropriate volume of soil  $Q_f$ , refrigeration to cool soil to the designed temperature of freezing  $Q_c$  and heat absorption capability of freeze-tubes  $Q_t$ , which are measured in kJ.

$$Q_f = q_f V_s \quad (6.3)$$

Where  $V_s$  – soil volume to be frozen, m<sup>3</sup>.

$$V_s = \pi(b^2 - a^2)L \quad (6.4)$$

$L$  – length of freeze-tubes;  $q_f$ –required heat for 1 m<sup>3</sup> soil freezing,kJ/m<sup>3</sup>.

$$q_f = q_1 + q_2 + q_3 + q_4 \quad (6.5)$$

$q_1$  – required heat for 1 m<sup>3</sup> groundwater cooling from it natural temperature  $t_s$  to the freezing point temperature  $t_0$ .

$$q_1 = V_{gw} \rho_{gw} C_{gw} (t_n - t_0) \quad (6.6)$$

$q_2$ –required heat for ice forming.

$$q_2 = V_{gw} \rho_{gw} Q \quad (6.7)$$

$Q$  is a latent heat of ice formation.

$q_3$  – heat to cool ice from ice formation temperature  $t_0$  to the average temperature in the ice-wall zone  $t_f$ .

$$q_3 = V_i \rho_i C_i (t_o - t_f) \quad (6.8)$$

$q_4$  is required heat for dry soil cooling from it natural temperature to the designed freezing temperature.

$$q_4 = V_{ds} \rho_s C_s (t_n - t_f) \quad (6.9)$$

Parameters used in equations 6.3 – 6.9:

- $V_{gw}$  and  $V_{ds}$  are groundwater and dry soil volume in 1 m<sup>3</sup> of soil;
- $\rho_{gw}, \rho_i, \rho_s$  are groundwater, ice and soil density, kg/m<sup>3</sup>;
- $C_{gw}, C_i, C_s$  are specific heat capacity of groundwater, ice and dry soil, kJ/kg°C.

Required heat for the soils in the ice-wall structure cooling,  $Q_c$ ,kJ/h is calculated in Eq. 6.10.

$$Q_c = 2\pi(R_i n + R_e x) L q_c \quad (6.10)$$

Where  $q_c$  is heat infiltration to the 1 m<sup>2</sup> of ice-wall structure,kJ/m<sup>2</sup>h.

Heat absorption capability of freeze-tubes  $Q_t$ ,kJ/h is estimated in Eq. 6.11.

$$Q_t = F q_t \quad (6.11)$$

$F$  here is freeze-tubes surface, m<sup>2</sup>, which is equal to  $\pi 2r_0 NL$ . While  $q_t$  is specific heat flow rate, kJ/hm<sup>2</sup>. For a group of freeze-tubes,  $q_t$  can be determined as:

$$q_t = \frac{2k_f T_f}{2r_0 \ln \left( \frac{S}{\pi 2r_o} + \frac{E}{2S} \right)} \quad (6.12)$$

Eventually, the time of freezing is estimated as:

$$t = \frac{Q_f}{(Q_t - Q_c)24}, \text{ days} \quad (6.13)$$

It should be noted that the method gives the time of freezing only when heat flow between soils and freeze-tubes is stabilized.

Despite the universality of this method, which can be implemented for brine freezing as well as for nitrogen, its main disadvantage is lack of direct relation between frozen ground parameters and heat absorption properties of freeze-tubes. Moreover, specific heat infiltration and heat flow are considered as constants. Thus, the parameters affect the accuracy of the method.

Furthermore, all observed time evaluation methods consider freezing from surface. Despite authors of some literature sources (Harris, 1995) point out that such methods can be used for horizontal ground freezing, these equations should be revised to get proper results.

#### 6.1.4 Costs

Generally, the process of freezing is divided by three phases. The first phase is defined as primary or active freeze period and constitutes the development of the freezing until it reaches the designed thickness. The second phase is called as secondary or passive freeze period and covers the period of underground construction maintenance during it excavation. The final phase corresponds to thaw period after the tunnel lining, when freeze system becomes redundant (Ozdemir, 2006).

Estimating of ground freezing is based on the next items followed by (Braun et al., 1979):

1. Mobilization of all equipment and material;
2. Drilling and installation of freeze-tubes;
3. Installation of surface piping system and refrigeration plant;
4. Installation of instrumentation to monitor the freezing process;
5. Pre-freezing time to form the wall;
6. Insulation of the exposed wall during and/or after excavation;
7. Maintenance of the wall during subsurface construction;
8. Removal of the system and demobilization.

Therefore, the costs of artificial ground freezing project depend significantly on the freezing time. Furthermore, the final design of the project includes risks assessment, which are described in modern technical literature (Harris, 1995).

### 6.1.5 Freezing process completion

After permanent lining of the tunnel part under artificial ground freezing protection, refrigeration plant can be switched off and the process of freeze-tubes recovery or abandonment begins. This period is followed by frozen soils thawing, which can be natural, when thawing is achieved only by heat infiltration from unfrozen soils. In this case natural defrosting velocity is around 0,1-0,15 cm/day depending on thermal properties of unfrozen soils. Moreover, because of uncontrolled soils thawing there is a possibility of unsteady defrosting which can be initialized by groundwater flow.

This process can be intensified by artificial defrosting. The technology considers warm coolant circulation through freeze-tubes after permanent lining of the tunnel. For this option coolant should be heated for 2–3 °C to prevent freeze-tubes wrecking. After defrosting is completed at the sufficient depth around the tunnel providing uniform hydrostatic pressure of soils on the tunnel lining, refrigeration plant is dismantled, coolant is pumped out and freeze-tubes are recovered (Nasonov et al., 1992).

Considering that freeze-tubes recovery can be a complicated process in tunnels, their abandonment can be adopted as well. Then, tubes are merely filled by sand or cement without their recovery (Harris, 1995).

### 6.1.6 Risks

In general, risk assessment can be carried out through risk level estimation which consists of two fundamental parameters – the probability of hazards (particular threat occurs within a given period of time) and Consequence (degree of loss to a given element within the area affected by a hazard) (Shahriar et al., 2008). Thus, the risk level can be expressed in Eq. 6.14.

$$Risk = Probability * Consequence \quad (6.14)$$

The probability of hazard and consequence are categorized in tables 6.1 and 6.2.

Table 6.1: Probability of hazards occurrence (after Shahriar et al. (2008))

Category	Probability	Description
L1	Improbable	Event is extremely unlikely to occur once
L2	Remote	Event is unlikely to occur once
L3	Probable	Event is likely to occur at least once
L4	Expected	Event is likely to occur more than once but infrequently
L5	Frequent	Event is likely to occur frequently

Table 6.2: Consequence of hazards (after Shahriar et al. (2008))

Category	Consequence	Description
C1	Negligible	Event does not cause delay or damage
C2	Moderate	Event causes minor damage and/or delay up to 2 days
C3	Serious	Event causes repairable damage and/or delays up to 1 week
C4	Critical	Event causes significant repairable damage and/or delays between 1 and 2 weeks
C5	Catastrophic	Event causes irreparable damage and/or delays greater than 2 weeks

The total level of risk can be summarized in Table 6.3

Table 6.3: Risk level evaluation (after Shahriar et al. (2008))

Risk level	Index	Description
Low	1-4	Risk is tolerable without any mitigation
Medium	5-9	Risk is moderately tolerable. Mitigation may be needed
High	10-15	Risk is at the border of tolerability. Mitigation should be identified and implemented to reduce risk
Very high	16-25	Risk is intolerable. Mitigation that reduces risk must be implemented

Therefore, the risk assessment can be represented by colourized scheme:

	Consequence					
L5						Probability
L4						
L3						
L2						
L1						
	C1	C2	C3	C4	C5	

Figure 6.2: Risk assessment (after Einarson (2014))

Where:

- ■ – Insignificant risk;
- ■ – Mostly accessible risk, which can be mitigated; when it is required
- ■ – Inaccessible risk, which must be mitigated

Furthermore, it is common to use factor of safety  $F_s$ , which is generally represented as:

$$F_s = \frac{\text{Resistance}(\text{Bearing capacity of structure})}{\text{Specified Load}} \quad (6.15)$$

Thus, if  $F_s > 1$ , then the structure is considered safe.

The risks assessment for the special method should be based on the analysis adverse and beneficial effects of technical uncertainties, programme changes and safety measures on security, time and cost. While the risk analysis of the whole geotechnical project should include considerations of force majeure as flood or earthquakes, supply of materials, finance and taxes, industrial relations and other parameters according to each country standards.

Generally AGF is compared with other special methods and on the basis of combination between risk factor and costs, the most appropriate method is chosen. (Harris, 1995) noted 3 models of risk factor assessment.

1. Model A – based on three clauses: control of ground conditions, groundwater control and safety during excavation and lining. Each aspect is assessed according to the perceived quality of the contractor's presentation of his design, execution and safety proposals.
2. Model B – based on five clauses: installation, strata changes, adverse groundwater, deformation, equipment breakdown.
3. Model C – based on decision tree principle and based on the following points:
  - Identification of special methods to be compared



- Preparation of a list with principal activities of events for each method
- Preparation the list of risks connected with each activity and responses to those risks
- Probability factors distribution which ranges from 0 – maximum adverse effect to 1 – total success
- Application of a decision tree and following evaluation of risk

To evaluate risk AGF application for the current project, the model B will be used. Knowing each value of Probability and Consequence, the Risk factor can be determined by their multiplication. The average risk value is counted as arithmetic mean of Risk factors. Table 6.4 shows the range of hazards, their probability and consequence based on Model B.

Table 6.4: Risk assessment range (after (Harris, 1995))

Method	Hazard	Probability	Consequence
Ground freezing	Installation	0-1,5	0-3,04
	Strata changes	0-1,5	0-3,32
	Adverse groundwater	0-2	0-4,68
	Deformation	0-1,5	0-3,74
	Innaccurate monitoring	0-1	0-3,95
	Equipment breakdown	0-0,5	0-1,355

Principally the following hazards have the most effect on AGF project:

- Rupture of freeze-tubes;
- Changed properties of frozen soil;
- Incorrect groundwater conditions research;
- Damage of surface constructions by ground heave and creep;
- Secondary hazards as inaccurate monitoring and equipment breakdown;

The table with common solutions of hazards mitigation is shown in Appendix C.

## 6.2 Ice-wall design for Bergåsen tunnel

Considering the principle of ice-wall creation and the project data analysis made in chapter 2, the designed ice-wall should cover only that section of tunnel where the highest water inflow is expected. Thus, the bottom of the tunnel remains uncovered by the ice-wall structure. However, a case, when the whole tunnel is excavated in water saturated soil material, is analysed in chapter 7.

For Bergåsen tunnel AGF project, a scheme with the horizontal fitting of freeze-tubes was considered as the optimum option because of relative long section to be frozen, which would demand around 200 vertical freeze-tubes.

### 6.2.1 Ice-wall thickness

As it was discussed above, the most common equation to calculate the thickness of ice-wall is provided by Domke method. However, considering shallow depth of the tunnel in the area exposed to freezing (12-20 m), Lamé-Gadolin method (Eq. 6.16) is more preferable for this case, since it gives more appropriate values for up to 50 m depth (Nasonov et al., 1992).

$$E_{iw} = R_t \sqrt{[\sigma_c] / ([\sigma_c] - 2P)} - 1 \quad (6.16)$$

Where  $R_t$  – tunnel radius, m;  $[\sigma_c]$  – frozen grounds compressive stress. It can be defined as:  $[\sigma_c] = \frac{\sigma_{c(iw)}}{F_s}$ . Where  $\sigma_{c(iw)}$  – frozen soil compressive strength, MPa;  $F_s$  – safety factor.  $P$  is water-saturated soils pressure on the ice wall, MPa.

For the current case  $R_t = 5,21\text{ m}$ ;  $\sigma_{c(iw)} = 3\text{ MPa}$  (from (Martin-Luther-Universität, 2018)).

$$P = p_0 + p_h \quad (6.17)$$

Where  $p_0$  – overburden pressure, MPa  $p_h$  – hydrostatic pressure, MPa.

$$p_0 = \nu_s h t g^2 \left[ \frac{90^\circ - \phi}{2} \right] \quad (6.18)$$

$$p_h = \nu_{gw} H_{gw} \quad (6.19)$$

$\nu_s$  – unit weight of soils;  $h$  – depth of soils above the tunnel, m;  $\phi$  – angle of internal friction of soils.  $\nu_{gw}$  – unit weight of ground water;  $H_{gw}$  – height of water column above the tunnel.

Therefore:

$$E_{iw} = 5,21 \sqrt{\frac{1,5}{1,5 - 2(0,1 + 0,13)}} - 1 \approx 1,1\text{ m} \quad (6.20)$$

Following recommendations for minimum ice-wall depth,  $E_{iw} = 1,2\text{ m}$  (Nasonov et al., 1992).

It should be noted that the value of ice-wall thickness strongly depends on the type of

soil. Considering that moraine deposit is highly heterogeneous material, the real value of designed ice-wall thickness can be different from the estimated above.

In the design practise, freeze-tubes are placed closer to external ice-wall border. The internal spacing is accepted as  $0,6 * E_{iw}$  and external is  $0,4 * E_{iw}$ . Spacing between freeze-tubes on average is  $0,8 - 1,2$  m. Table 6.5 describes how many freeze-tubes will surround the tunnel, if each one spacing will be chosen. As it can be seen from the figure, the number of freeze-tubes varies significantly from 18 freeze-tubes for  $1,2$  m spacing to 28 for  $0,8$  m.

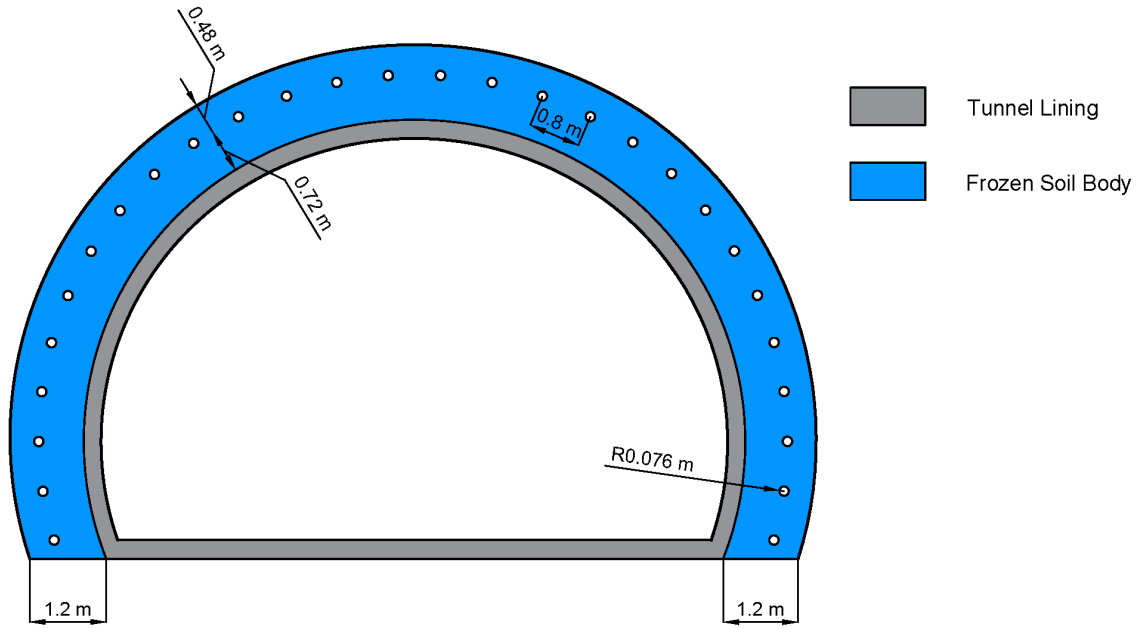


Figure 6.3: Ice-wall scheme

Table 6.5: Variation of wells number by spacing

S	m	0,8	1	1,2
N	[-]	28	22	18

### 6.2.2 Temperature of freezing

Freezing temperature is highly depended on soil natural conditions. Thus, considering that soil temperature is equal to 2,5 °C (Vegvesen, 2010) and seepage velocity in the zone of AGF can reach 12m/day, which was discussed in chapter 2, Eq. 4.2 can be used to find the optimal temperature of freezing. Furthermore, given equation operates with spacing between freeze-tubes.

Knowing the natural soils salinity, the temperature shift can be estimated follow Eq. 4.3.

$$\Delta T = 32,5 \left[ \frac{0,02}{1000 + 0,02} \right] = 0,00065 \quad (6.21)$$

Considering relatively low value of temperature shift, it can be neglected in further calculations. The values of freezing temperature for different spacing and seepage velocity are shown in Table 6.6

Table 6.6: Freezing temperature fluctuation due to seepage velocity and spacing variation

$u_c$	m/day	3	9	12
$T_f$ (for S=0,8 m)	°C	-9	-32	-44
$T_f$ (for S=1 m)	°C	-15	-51	-69
$T_f$ (for S=1,2 m)	°C	-22	-72	-96

Therefore, freezing temperature varies from -9 to -96 °C. Considering the worst case, when groundwater seepage velocity is around 12 m/day and knowing that average temperature of coolant circulated in freeze-tubes is around -40°C, which was discussed in chapter 3, the spacing S=0,8 m gives the most acceptable result.

### 6.2.3 Time of freezing

To calculate active freezing time, both methods described above can be used. However, heat balance gave more appropriate results than Sangers&Sayles method, since their approach depends significantly on natural soil temperature and is more appropriate for ground temperatures close to 20°C (Vakulenko, 2014).

Parameters for freezing time evaluation can be summarized in Table 6.7.

Table 6.7: Input data for freezing time calculation

Parameter	$R_i$	$R_e$	$L$	$E_{iw}$	$S$
Dimension	$m$	$m$	$m$	$m$	$m$
Value	5,21	6,41	20	1,2	0,8

Parameter	$N$	$n$	$t_s$	$t_f$	$t_0$
Dimension	-	-	°C	°C	°C
Value	28	0,4 <sup>a</sup>	2,5 <sup>b</sup>	-16	0

Parameter	$\rho_{gw}$	$\rho_i$	$\rho_s$	$q_f$	$k_f$
Dimension	kg/m <sup>3</sup>	kg/m <sup>3</sup>	kg/m <sup>3</sup>	kJ/m <sup>2</sup> h	W/m*K
Value	1000	900	1680	16 <sup>c</sup>	2

Parameter	$r_0$	$Q$	$C_i$	$C_{gw}$	$C_s$
Dimension	m	kJ/kg	kJ/kg°C	kJ/kg°C	kJ/kg°C
Value	0,076	330 <sup>c</sup>	2,108	4,187	3,515 <sup>d</sup>

<sup>a</sup> from (Johansen, 1975)

<sup>b</sup> from (Vegvesen, 2010)

<sup>c</sup> from (Nasonov et al., 1992)

<sup>d</sup> from (Farouki et al., 1981)

Then the freezing time can be calculated through Equations 6.22 – 6.29.

$$q_1 = 0,16 * 1000 * 4,187 * (2,5 - 0) = 1674,8 \quad (6.22)$$

$$q_2 = 0,16 * 1000 * 330 = 52800 \quad (6.23)$$

$$q_3 = 0,176 * 900 * 2,108(0 - (-16)) = 5342,5 \quad (6.24)$$

$$q_4 = 0,6 * 1680 * 3,515(0 - (-16)) = 65539,5 \quad (6.25)$$

$$q_f = 1674,8 + 52800 + 5342,5 + 65539,5 = 125356,8 \quad (6.26)$$

$$Q_f = 125356,8 * 438,1 = 54914274 \quad (6.27)$$

$$Q_c = 2\pi * (5,21 + 6,41) * 20 * 16 = 23363 \quad (6.28)$$

$$Q_{ft} = \pi * 2 * 0,076 * 25 * 20 * 1062,9 = 279159,5 \quad (6.29)$$

Finally, the time will be equal to:

$$t = \frac{54914274,2}{(279159,5 - 23363,4) * 24} = 9days \quad (6.30)$$

As it was noticed in chapter 6, the calculated time is usually underestimated in ground freezing practice. The proper time calculation depends on the technical parameters of refrigeration power plant.

#### 6.2.4 Approximate costs evaluation

As it was discussed in chapter 6, the evaluation of AGF costs is based on multiple factors. Power consumption of refrigeration plant is one of significant aspects forming the project cost. Thus, the approximate cooling capacity of the refrigeration plant can be estimated with Eq. 6.31.

$$Q_{rp} = 1,1 * Q_{ft} = 307075,5kJ = 853kWh \quad (6.31)$$

In order to reach designed coolant temperature -40 °C, a two-stage refrigeration system is more advantageous, since an one-stage systems are efficient for freezing temperatures up to -20 °C (Repski, 2015)

The evaluation of approximate cost of the project is based on empirical method. Thus, comparison with other similar projects may be indicative of approximate price of AGF project. In general, the volume of  $26,136 \times 20 = 522,72 \text{ m}^3$  should be frozen, with the comparison of project in Oslo city center the cost of freezing will constitute USD 1,11 million or NOK 9 million in 2018. The recent project of a tunnel in Moss commune costed NOK 75 million in 2007 with a length 200m (Berggren, 2007). The temperature in the frozen zone was around -10 °C. As a coolant, ammonium was used. The frozen zone was 3-4 m with 35 freeze-tubes per stage. In total there was 7 stages 40 m each, drilling constituted 50% of the price. Therefore, without drilling the total price was NOK 37,5 million, or NOK 5,4 million for each stage. Considering the inflation, the price will be around NOK 6,8 million for 2018 (Norges Bank, 2018). That constitutes roughly NOK 3,4 million for 20 m.

### 6.2.5 Risk assessment

The evaluation of risk factor for AGF method applying at Bergåsen tunnel is based on the consideration of the highest Probability and Consequence factors noted in Table 6.4. Thus, Table 6.8 shows that "inaccurate monitoring" and "equipment breakdown" have the lowest impact on risk value. "Installation", "Strata change" and "Deformation" hazards have moderate influence, while "Adverse groundwater" is the most significant danger for AGF process. Therefore, the average risk value is almost equal to 5, which responds to medium risk.

Table 6.8: Risk assessment for Bergåsen tunnel ice-wall creation

Method	Hazard	Probability	Consequence	Risk Factor	Risk value (average)
Ground freezing	Installation	1,5	3,04	4,56	4,86
	Strata changes	1,5	3,32	4,98	
	Adverse groundwater	2	4,68	9,36	
	Deformation	1,5	3,74	5,61	
	Innaccurate monitoring	1	3,95	3,95	
	Equipment breakdown	0,5	1,355	0,6775	

# Chapter 7: Modelling of the tunnel stability

The tunnel stability modelling consists of two parts. The first includes the calculation of AGF parameters, such as ice-wall thickness, temperature and time of freezing. Then, the model of tunnel cross-section is analysed in Rocscience software. For modelling, the most extremal tunnel position was set-up, when it is completely excavated in moraine deposit with bottom laying on marble layer. Furthermore, a case of tunnel lying 5 m above designed depth was analysed as well. The case, when the tunnel is completely excavated in marble, is not discussed, since it is not covered by the topic of the thesis.

## 7.1 Rocscience modelling

The numerical analysis of the tunnel stability was carried out in Rocscience RS2 software. The finite element method (FEM) is lied in the base on simulation. That means, a model is divided by continuum elements with designed size and stress-strain properties, which allows to simulate stresses distributions in rocks and soils around an excavation. To analyse 3D tunnel construction case, a 2D approach is commonly used, since it is more time consuming method, which gives more accurate results (Moldovan and Popa, 2012). The sequence of steps applied in RS2 to build a model is shown in Figure 7.1.

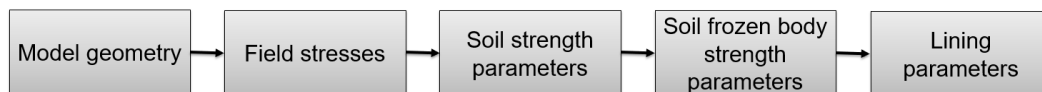


Figure 7.1: Steps of simulation in RS2

### 7.1.1 Principles of modelling

Few simplifications were carried out for the model.

1. a thin soil layer is merged with moraine deposit
2. The analysis of displacements is applied for a rectangular model, since it has been found that the inclination of ground surface gives false stress concentration in the area



of the highest ground surface inclination ( Figure F.1).

Thus, there are 2 layers of soil material – moraine deposit, where tunnel is excavated and marble, which extends to the tunnel bottom (Figure 7.2).

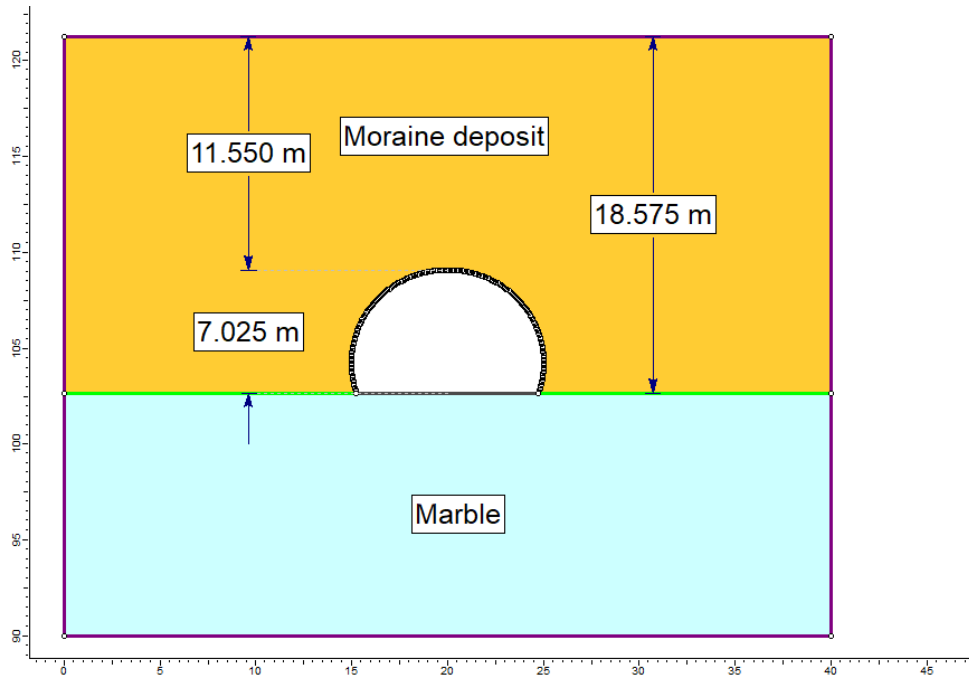


Figure 7.2: Tunnel model

Taking into account that ice-wall is forming before the tunnel's excavation, it is considered that it is excavated in a single stage. Therefore, for model set-up were selected 3 main stages.

- Stage 1 – Initial stresses distribution (unexcavated tunnel)
- Stage 2 – Tunnel is excavated under ice-wall protection (Stresses around tunnel)
- Stage 3 – Tunnel is lined by reinforced concrete lining (stresses around tunnel)

Mesh for the model consists of graded 6 noded triangles with automatic fineness division (Figure 7.3).

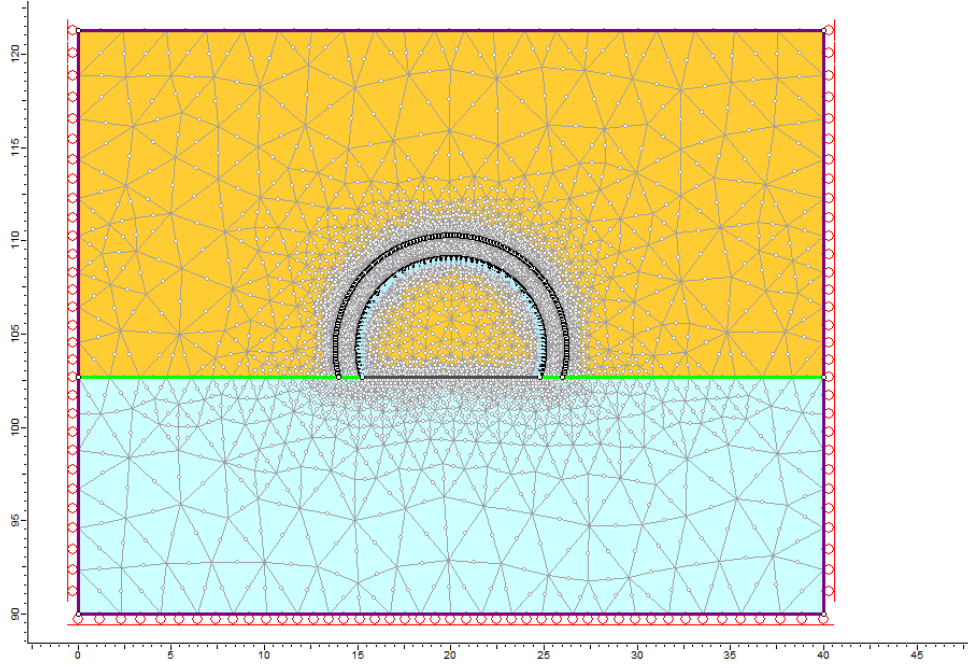


Figure 7.3: Mesh fitting for the tunnel model

### 7.1.2 Field stress parameters

The initial field stresses for the model can be set as constant or depending on gravity. Constant field stresses are wide used for deep excavations, whereas gravity are applied for near surface. Gravity field stress is specified by actual ground surface of the model. For this case the coefficient of earth pressure  $K$  should be determined (Figure 7.4). Considering the common assumption for soils, the coefficient is set up equal to  $K=1$  (Hoek, 1991). Besides, the relationship between horizontal and vertical stresses forming  $K$ , can be expressed through Eq. 7.1.

$$K = \frac{\sigma_H}{\sigma_V} \quad (7.1)$$

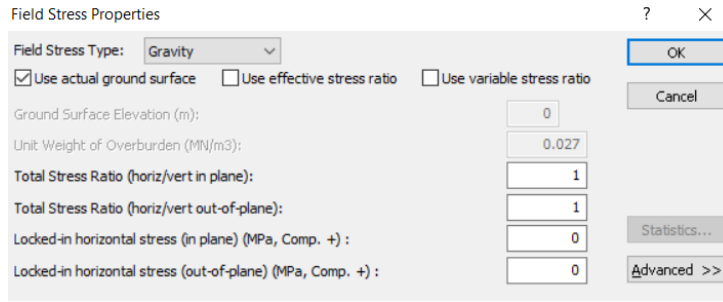
Where:

•

$$\sigma_V = \rho gh \quad (7.2)$$

•

$$\sigma_H = \frac{v_s}{1 - v_s} \sigma_V \quad (7.3)$$



The dialog box titled 'Field Stress Properties' contains the following fields and options:

- Field Stress Type:** Gravity (dropdown menu)
- ☒ Use actual ground surface
- ☐ Use effective stress ratio
- ☐ Use variable stress ratio
- Ground Surface Elevation (m):** 0
- Unit Weight of Overburden (MN/m3):** 0.027
- Total Stress Ratio (horiz/vert in plane):** 1
- Total Stress Ratio (horiz/vert out-of-plane):** 1
- Locked-in horizontal stress (in plane) (MPa, Comp. +):** 0
- Locked-in horizontal stress (out-of-plane) (MPa, Comp. +):** 0
- Buttons:** OK, Cancel, Statistics..., Advanced >>

Figure 7.4: Field stress dialog

### 7.1.3 Strength parameters

Rocscience allows to use different critical strength equations. Generally, the choice of appropriate method depends on type of material. It is commonly accepted to use Hoek-Brown criteria for Rock material and Mohr-Coulomb for soil materials. Hoek-Brown criteria characterises rock mass by elastic brittle plastic behaviour, while Mohr-Coulomb describes soils behaviour by elastic perfectly plastic model ( Figure 7.5).

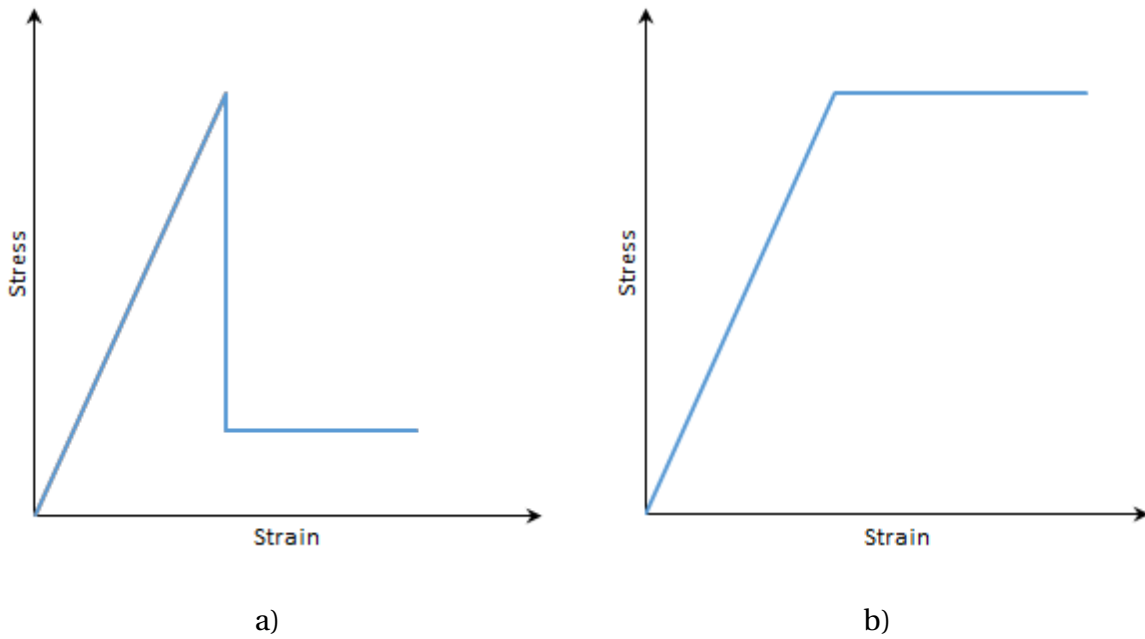


Figure 7.5: Strength criteria (after Saiang et al. (2014))

In RS2 generalized Hoek-Brown and Mohr-Coulomb criteria are used written by equations 7.4 and 7.7:

#### Hoek-Brown

$$\sigma'_1 = \sigma'_3 + \sigma_{ci} \left( m_b \frac{\sigma'_3}{\sigma_{ci}} + s \right)^a \quad (7.4)$$

Where  $\sigma'_1$  and  $\sigma'_3$  are the maximum and minimum effective principal stresses at failure and  $\sigma_{ci}$  is the uniaxial compressive strength of the intact rock.  $m_i$  is a Hoek-Brown constant for the rock mass and  $s$  and  $a$  are constant parameters depending on the rock mass characteristics. The  $m_b$  value and the  $s$  parameter can be calculated in Eq. 7.5 and Eq. 7.6 respectively.

$$m_b = m_i \exp\left(\frac{GSI - 100}{28 - 14D}\right) \quad (7.5)$$

$$s = \exp\left(\frac{GSI - 100}{28 - 14D}\right) \quad (7.6)$$

Where GSI – geological strength index and D – disturbance factor.

### Mohr-Coulomb

$$\tau_f = c + \sigma_n \tan\phi \quad (7.7)$$

Where:

- $\tau_f$  – critical shear stress (shear stress at failure);
- $\sigma_n$  – normal stress;
- $c$  – cohesive strength;
- $\phi$  – friction angle

## 7.1.4 Ground material parameters

### Rock mass

Marble strength behaviour can be described by Hoek-Brown criteria. Thus, all required parameters are shown in Table 7.1. GSI describes the quality of rock mass. Since there was no data about RQD and the Joint condition, the value of GSI is received by the rock mass structure and surface conditions matching. Following information from the project geological reports GSI is considered to be approximately equal to 70 (Figure E.1).

The Hoek-Brown constant  $m_i$  and  $\sigma_{ci}$  can be obtained by laboratory testing, otherwise they are found in Figure E.2 and Figure E.3.

The disturbance factor D describes the condition of excavation affected by blast damage and stress relaxation. The D value varies from 0 to 1 (Figure E.4). For Bergåsen tunnel the D value 0 is assumed, because it is considered that the tunnel will be excavated mechanically with minimal disturbance to the surrounding rock mass.

Table 7.1: Marble strength properties

$\sigma_{c(m)}$	GSI	$m_i$	D	MR	$\nu_m$	$\rho_m$	$\nu_m$	E
MPa	-	-	-	-	-	kg/m <sup>3</sup>	kN/m <sup>3</sup>	GPa
100	70	9	0	800	0,2 <sup>a</sup>	2800 <sup>a</sup>	26,5 <sup>a</sup>	60 <sup>a</sup>

<sup>a</sup> from Geosciences (2013)

### Moraine deposit

The grain size distribution of moraine sediments presented in chapter 2 shows that it is partly divided between moraine clay and gravel. Therefore the strength input data required for Mohr-Coulomb equation were obtained from different sources which describe parameters of moraine soil with similar composition.

Table 7.2: Moraine properties

$\nu_s$	$\rho_s$	$\nu_s$	E	c	$\sigma_t$	$\phi_s$
-	kg/m <sup>3</sup>	kN/m <sup>3</sup>	GPa	MPa	MPa	degree
0,3 <sup>a</sup>	1680 <sup>b</sup>	16,5 <sup>b</sup>	0,05 <sup>c</sup>	0,017 <sup>b</sup>	0 <sup>d</sup>	39 <sup>e</sup>

<sup>a</sup> from Johansson (2009)

<sup>b</sup> from Andersland and Ladanyi (2004)

<sup>c</sup> from Geotechdata.info (2018)

<sup>d</sup> from Melbourne School of Engineering (2018)

<sup>e</sup> from Gella (2017)

### 7.1.5 Ice-wall modelling in Rocscience

It should be noted, that there is no specific criteria for ice-wall modelling in RS2. Therefore, it has been decided to represent ice-wall as an improved soil layer.

Considering, that frozen clayey soils are mainly described by elastic-plastic behaviour (Figure 4.4), the ice-wall was modelled using Mohr Coulomb strength criteria.

Parameters for frozen soil layer are found in technical and scientific literature describing frozen moraine properties.

Table 7.3: Artificially frozen ground parameters

$\nu_{iw}$	$\rho$	$\nu_{iw}$	E	$c_{iw}$	$\sigma_t$	$\phi_{iw}$
	kg/m <sup>3</sup>	KN/m <sup>3</sup>	Gpa	MPa	Mpa	degree
0,3 <sup>a</sup>	1900 <sup>b</sup>	18,6333 <sup>c</sup>	2,8 <sup>c</sup>	0,5 <sup>c</sup>	1 <sup>d</sup>	23,5 <sup>e</sup>

<sup>a</sup> from Johansson (2009)

<sup>b</sup> from Yershov (2004)

<sup>c</sup> from Andersland and Ladanyi (2013)

<sup>d</sup> from Akagawa and Nishisato (2009)

<sup>e</sup> from Johansson (2012)

The AGF layer set-up in RS2 model, is shown in Figure 7.6.

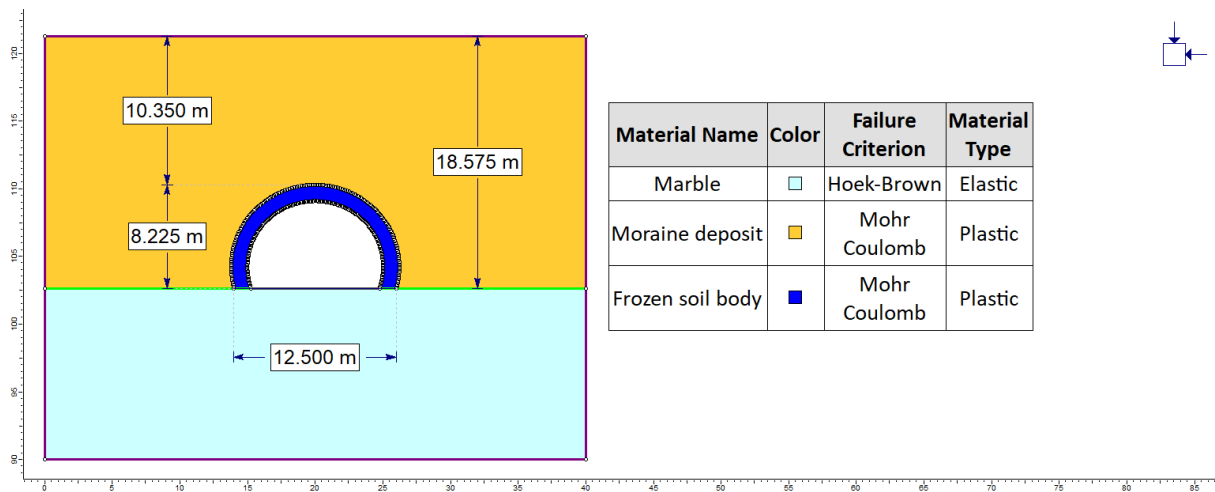


Figure 7.6: Ice-wall model in RS2

### 7.1.6 Groundwater flow modelling

It is possible to perform finite element analysis of groundwater flow in RS2. Thus, knowing the average groundwater level, the theoretical direction and variation of seepage infiltration can be modelled. Consequently, a real ground surface height was applied for this model (Figure 7.7).

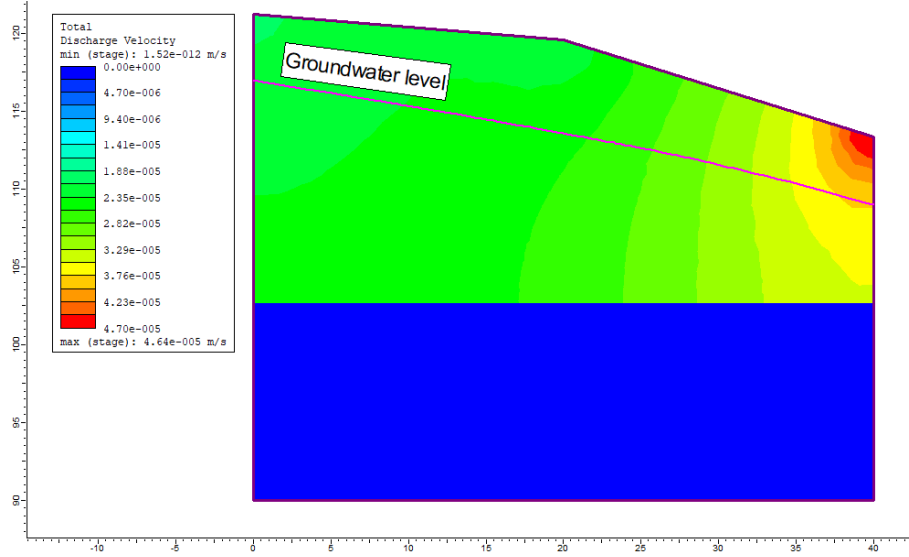


Figure 7.7: Natural groundwater level

When ice-wall layer is applied, it is possible to simulate an area with maximum discharge velocity (Figure 7.8).

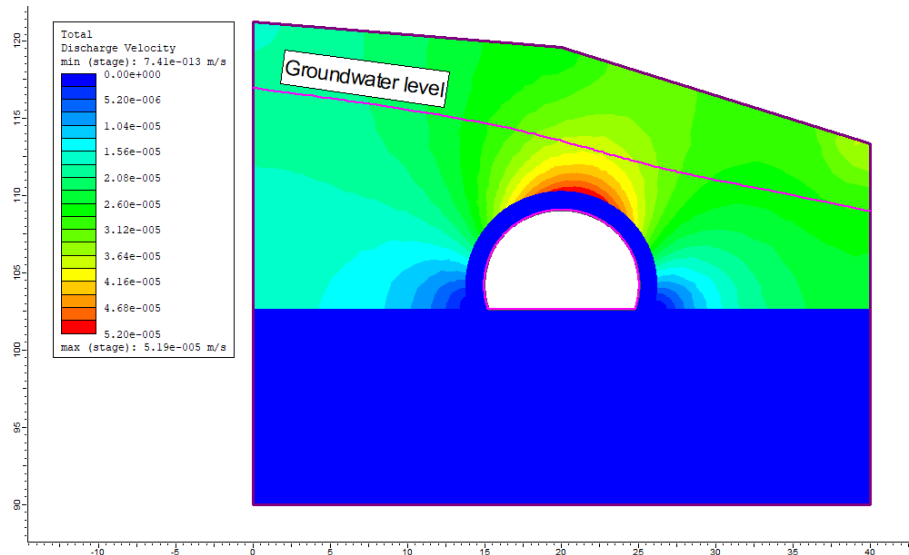


Figure 7.8: Groundwater level variation in case of ice-wall applying

It should be noted, that groundwater is modelled in rectangular models through total head to estimate hydraulic pressure on the tunnel.

### 7.1.7 Support modelling

The estimation of lining properties for the tunnel was not a key point for this paper. Considering the lack of available project papers which would describe designed type of lining, lining properties are based on the analysis of tunneling projects, fulfilled in soils with similar geological conditions. The most detailed information were provided in project described Joberget tunnel. The tunnel was constructed in phyllite rock and intersected an 80 m section of moraine material. Because of low ground water content in soil, it was constructed without using of special methods for water treatment (Langåker, 2014).

Initially, parameters for reinforced concrete lining applied at Joberget tunnel, were considered for the model (Figure 7.9).

**Reinforced Concrete liner**

Name: Reinforced Concrete liner Color:  

Reinforcement ☒ Common Types

Spacing (m):

Section Depth (m):

Area (m<sup>2</sup>):

Moment of Inertia (m<sup>4</sup>):

Young's Modulus (MPa):

Poisson Ratio:

Compressive Strength (MPa):

Tensile Strength (MPa):

Weight (kg/m):

Lattice girder (3-Bar): #115, Bar Size:20,30mm

☐ Stage Concrete Properties

[Define Factors...](#)

Liner Type: Reinforced Concrete

Concrete ☒

Thickness (m):

Young's Modulus (MPa):

Poisson Ratio:

Compressive Strength (MPa):

Tensile Strength (MPa):

Unit Weight (MN/m<sup>3</sup>):

Material Type: ☒ Elastic ☐ Plastic

☐ Include Weight in Analysis

☐ Sliding Gap

Strain at Locking:  %

Beam Element Formulation: Timoshenko

Shape: Lattice girder

Type: 3-Bar

Designation (Metric)

#50, Bar Size:18,26mm
#50, Bar Size:20,30mm
#70, Bar Size:18,26mm
#70, Bar Size:20,30mm
#70, Bar Size:26,34mm
#95, Bar Size:18,26mm
#95, Bar Size:20,30mm
#95, Bar Size:26,34mm
#115, Bar Size:18,26mm
#115, Bar Size:20,30mm
#115, Bar Size:26,34mm
#130, Bar Size:18,26mm
#130, Bar Size:20,30mm
#130, Bar Size:26,34mm

☐ Imperial ☒ Metric

Section Depth (mm):

Area (mm<sup>2</sup>):

Moment of Inertia (10e6mm<sup>4</sup>):

Weight (kg/m):

a)
b)

Figure 7.9: Lining properties

Then, the the tunnel displacements protected by this lining was compared with lining with thinner concrete layer (0,3 m), which is minimal allowed thickness of concrete due to Norwegian standard (Vegvesen, 2015). The results of comparison are discussed later in the chapter.



## 7.2 Tunnel displacements

In total three models characterized displacements at stages of tunnel excavation were composed:

- Unlined tunnel;
- Tunnel under ice-wall protection;
- Tunnel under reinforced concrete lining protection

The total displacement values generated by modelling are described by Eq. 7.8, where  $D_X$  and  $D_Y$  define horizontal and vertical displacements respectively.

$$D_t = \sqrt{D_X^2 + D_Y^2} \quad (7.8)$$

### 7.2.1 Unlined tunnel

This case is considered to demonstrate inevitable collapse of the tunnel without lining (Figure 7.10). The result of the modelling shows unrealistic displacements which reach 40m with the main zone of displacement located in the tunnel roof. It should be noted, that the model compilation was not finished because of number of iterations exceeding. Thus, the current case proves extreme susceptibility of unlined tunnel to failure.

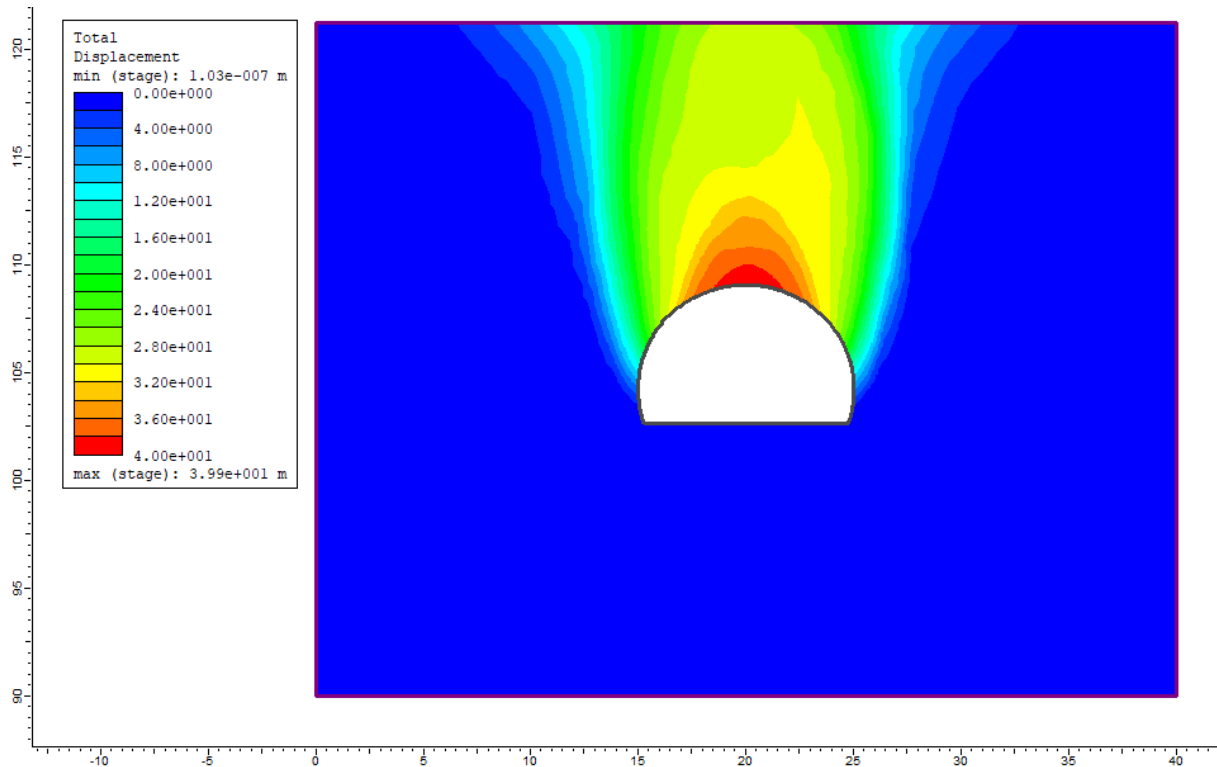
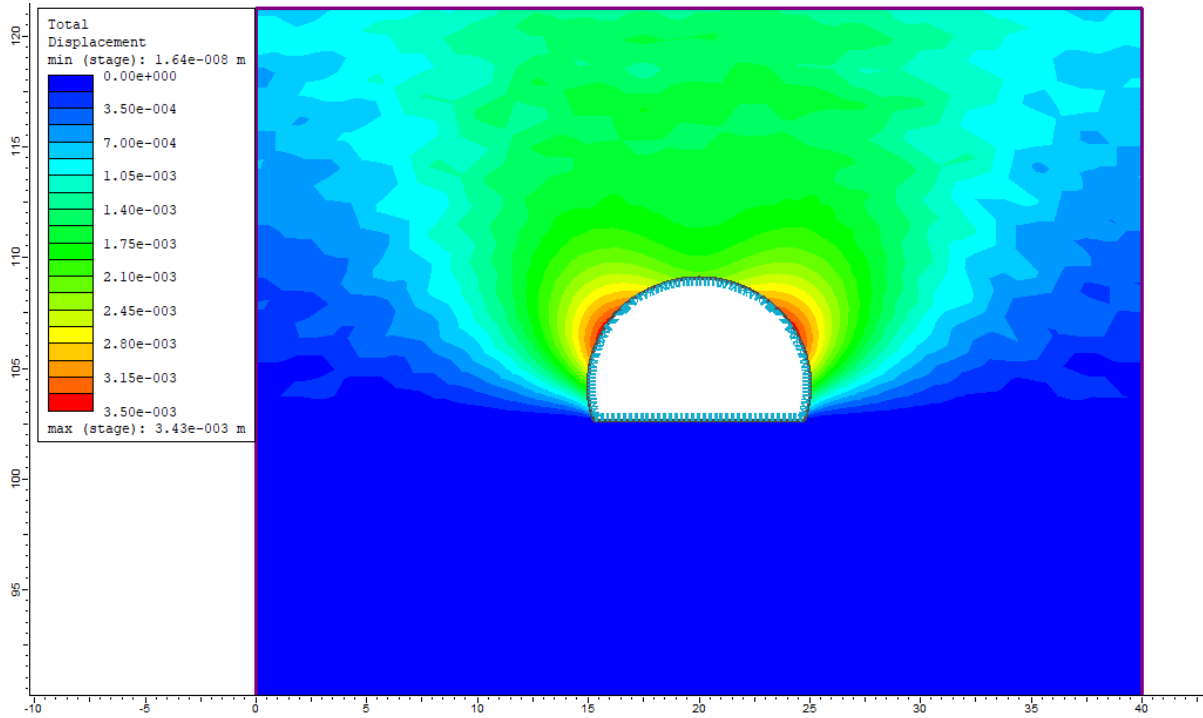


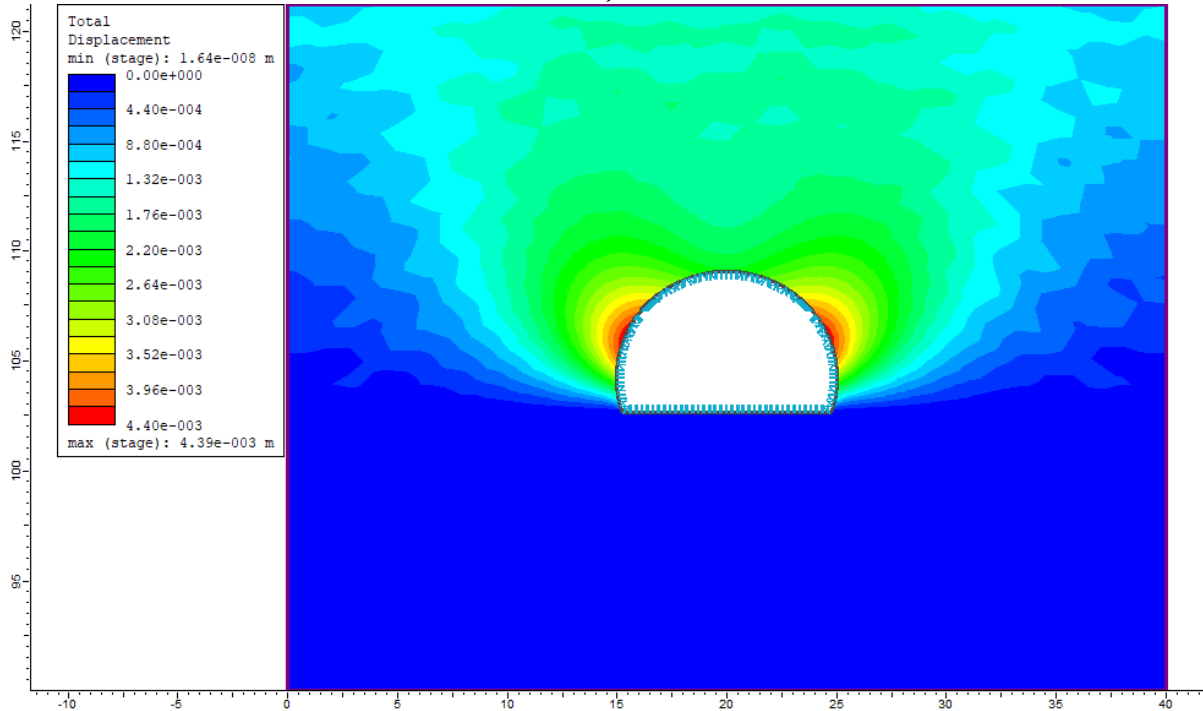
Figure 7.10: Deformations occurred in the unlined tunnel

## 7.2.2 Lined tunnel

As it has been discussed above, two types of lining were compared. Figure 7.11 a) shows displacements at the tunnel with the using of lining similar to the one used for Joberget tunnel modelling. Then, the lining properties were modified and the thickness of concrete were decreased to 30 cm (Figure 7.11 b).



a)



b)

Figure 7.11: Deformations occurred in the tunnel with lining

As it can be seen in Figure 7.11, displacements with thinner reinforced concrete lining are slightly higher than in the case a) and reach 4,39 mm. However, they are still quite low and still can be considered as safe for the tunnel construction, which is proved by support capacity diagrams (Appendix H).

### 7.2.3 Ice-wall protection

When ice-wall has been created from artificially frozen ground around the tunnel, it can carry in-situ stresses on the tunnel. The accepted 1,2 m thick ice-wall is integrated in the model. Figure 7.12 shows that the created ice-wall dissipate deformations which are accumulated almost in the same points as for the lined tunnel case. The maximum values of displacements do not exceed 3,1 mm which is 1,3 mm lower than in the tunnel with lining

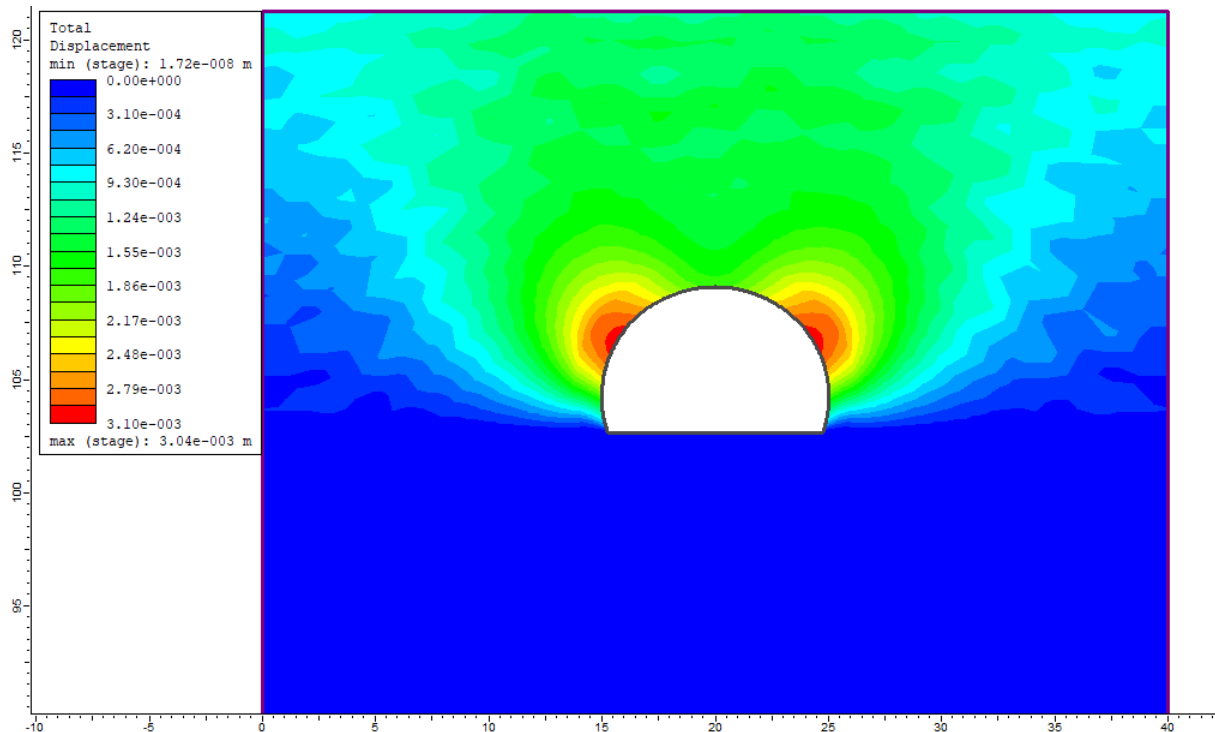


Figure 7.12: Deformations occurred in the tunnel with artificial frozen ground layer

## 7.3 Tunnel excavation in soil

Considering the discussion in chapter 2, the area with moraine sediments can spread few meters below the tunnel. Therefore, the case of tunnel excavation in water-saturated material should be analysed as well (Figure 7.13).

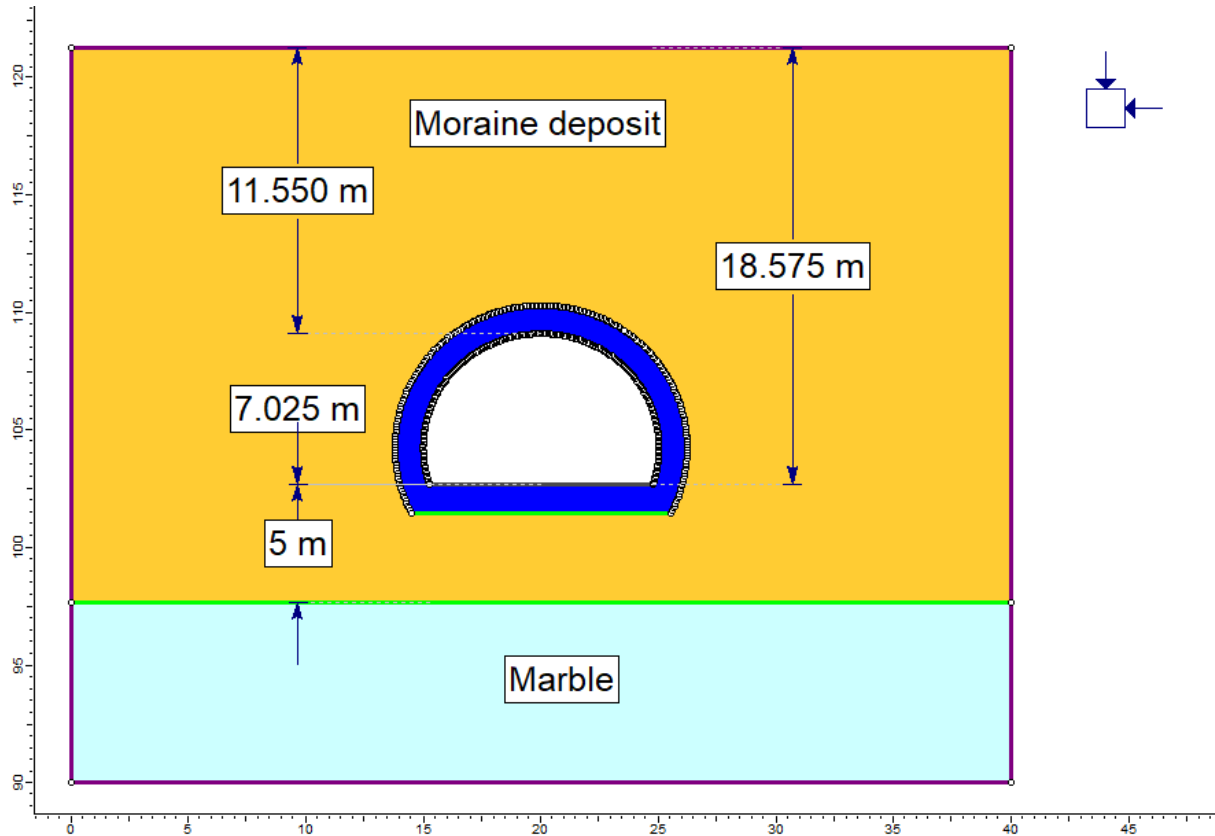


Figure 7.13: Location of shifted tunnel

The soil layer is shifted 5 m down to the current tunnel route location. In this case ice-wall should cover the whole tunnel to prevent water inflow. Thus, AGF layer will be expanded and 14 additional freeze-tubes should be placed below the tunnel bottom.

### 7.3.1 Displacements

The distribution of displacements is different than for the tunnel with the bottom lying on the marble basement. As it can be seen in Figures 7.14 and 7.15, the highest displacements are concentrated in the tunnel bottom and reach 2,41 and 3,17 cm respectively. In general, the total displacement distribution of the excavated tunnel in soil, is approximately 10 times higher than for the case of tunnel lying on marble basement. The tunnel cross-section can be changed to more stable shape with inverted roof, which was discussed in details by (Bollingmo et al., 2010).

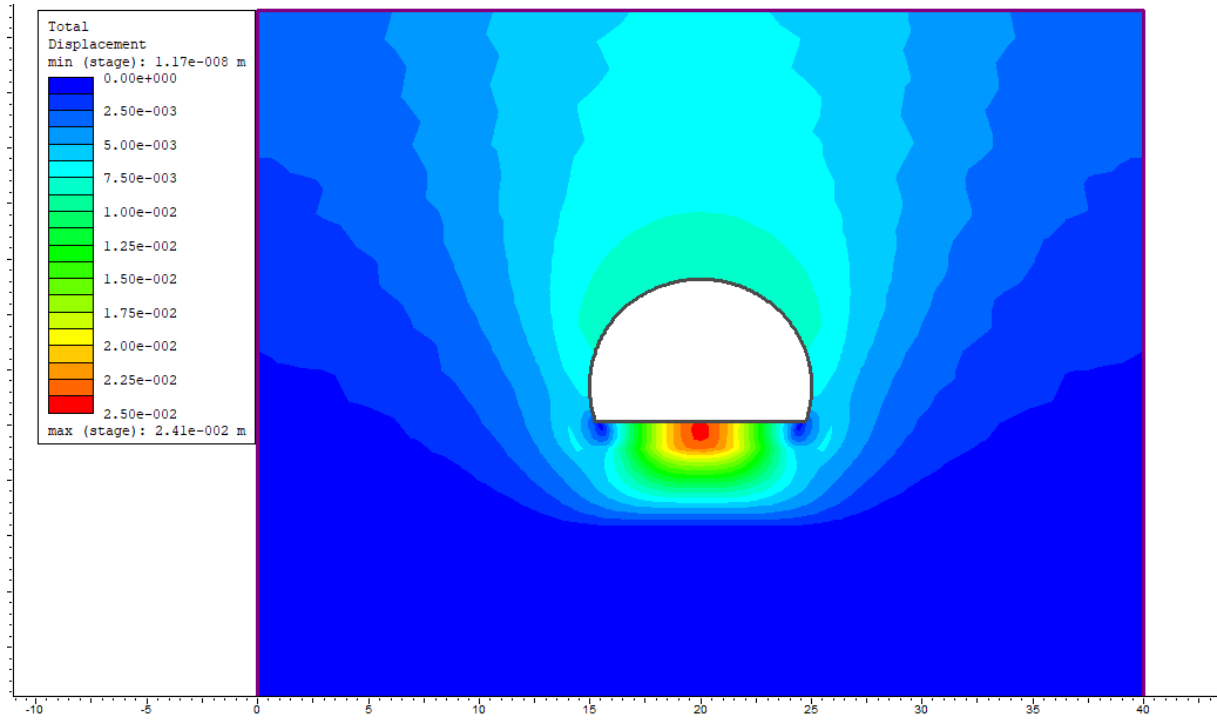


Figure 7.14: Deformations occurred in the shifted tunnel with ice-wall layer

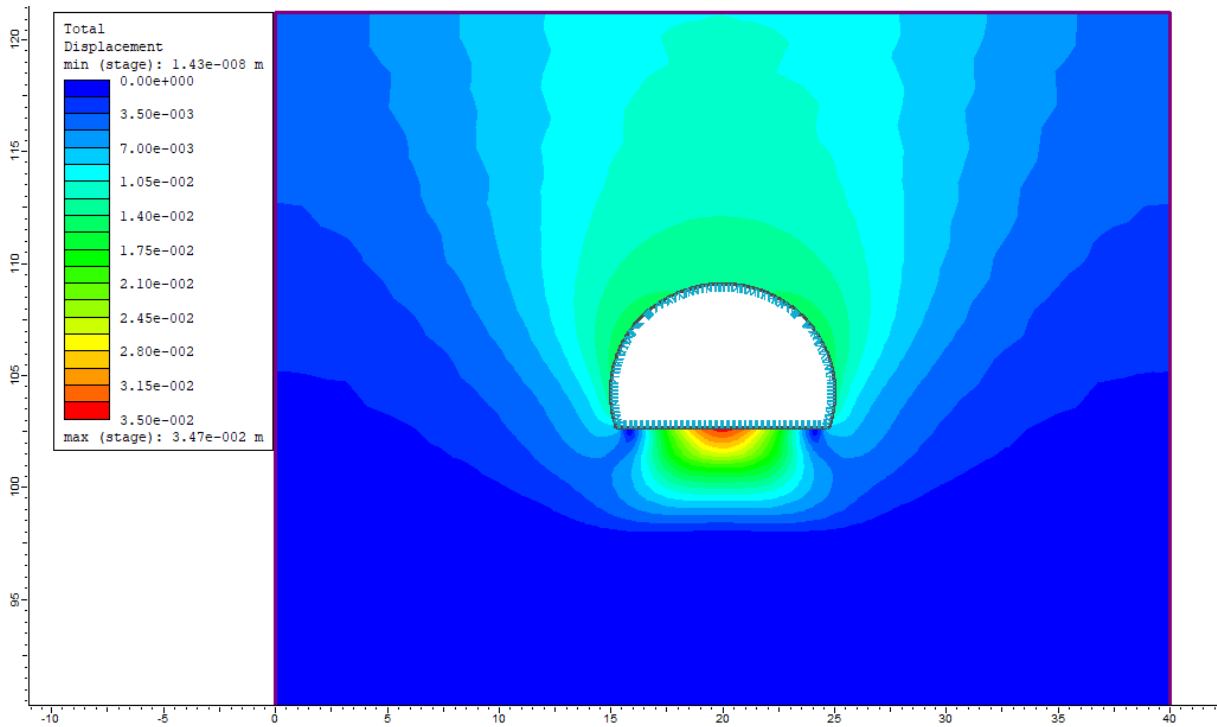


Figure 7.15: Deformations occurred in the shifted tunnel with lining

### 7.3.2 Groundwater conditions

Figure 7.16 shows theoretical groundwater level variation and total discharge velocity for the case of the tunnel excavation in water-saturated material. The highest groundwater impact is observed in the adjacent areas to the ice-wall bottom and roof, where it reaches  $7 * 10^{-5}$  and  $5 * 10^{-5}$  m/s.

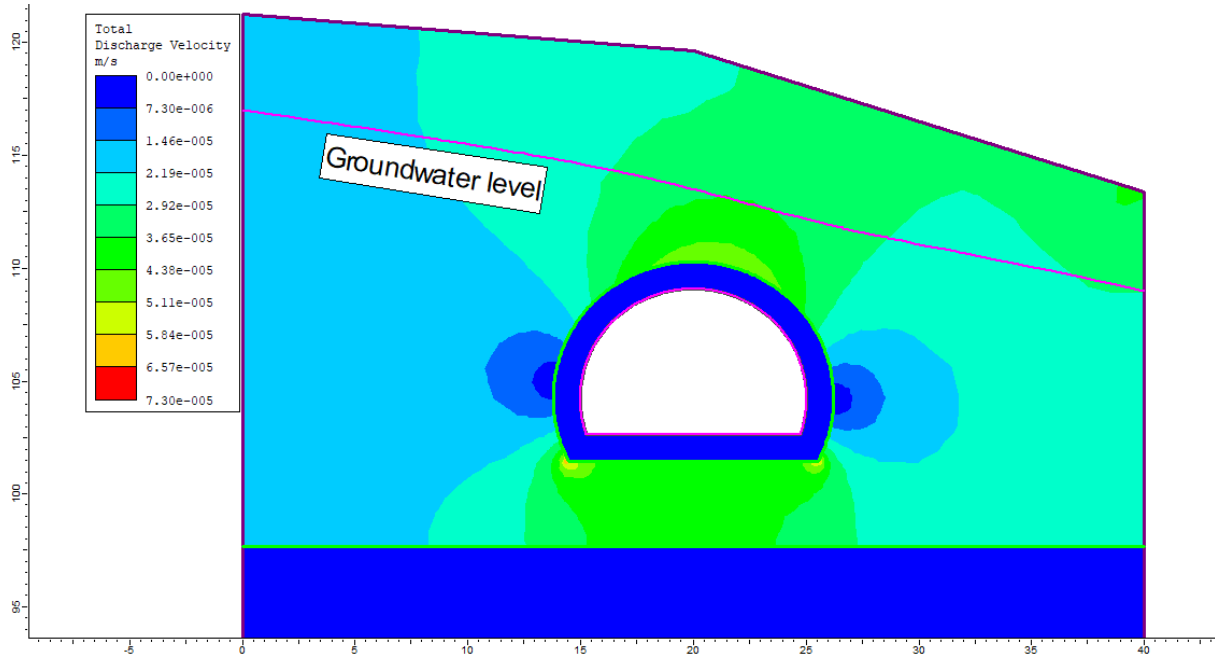


Figure 7.16: Groundwater level variation, when ice-wall is applied for the shifted tunnel

## 7.4 Moraine parameters effects

To figure out which parameters have larger impact on displacements, there was conducted an analysis with variation of soil properties, such as friction angle  $\phi$ , cohesion  $c$  and Young modulus  $E$ . For the analysis the designed values of the parameters were modified by 10 and 20% as it is shown in Table 7.4.

Table 7.4: Moraine parameters variation

		Moraine					Frozen soil body				
		-20%	-10%	Designed	+10%	+20%	-20%	-10%	Designed	+10%	+20%
$\phi$	deg	31,2	35,1	39	42,9	46,8	18,8	21,15	23,5	25,85	28,2
$c$	MPa	0,0136	0,0153	0,017	0,0187	0,0204	0,4	0,45	0,5	0,55	0,6
$E$	MPa	40	45	50	55	60	2240	2520	2800	3080	3360

The analysis was conducted for both cases – for ice wall and lining protection respectively. The displacements were measured in two points – Point 1 on the edge of tunnel and Point 2 on the edge of ice-wall zone, as it is shown in Figure 7.17. Graphs in Figure 7.18 show distribution of displacements with the variation of each parameter.

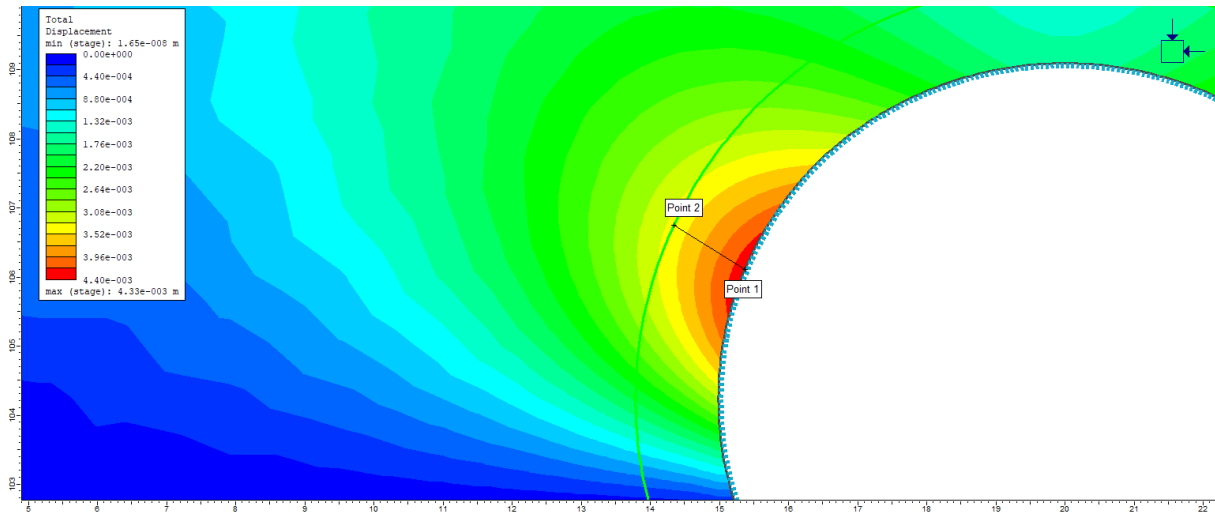
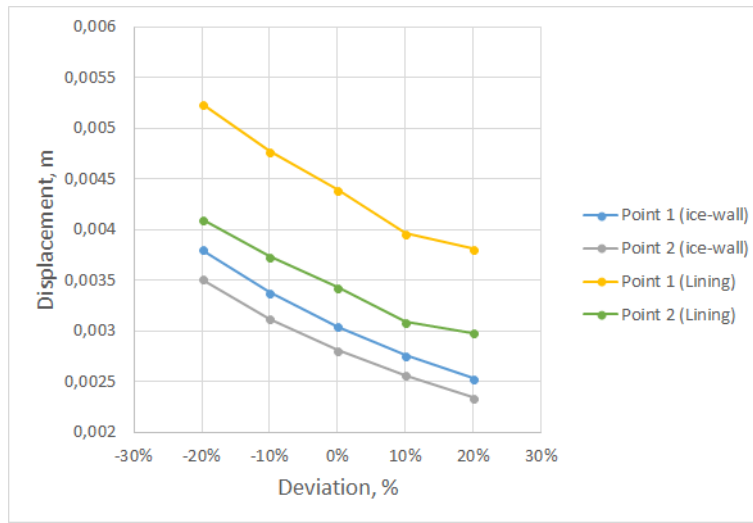


Figure 7.17: Points indication for displacements analysis

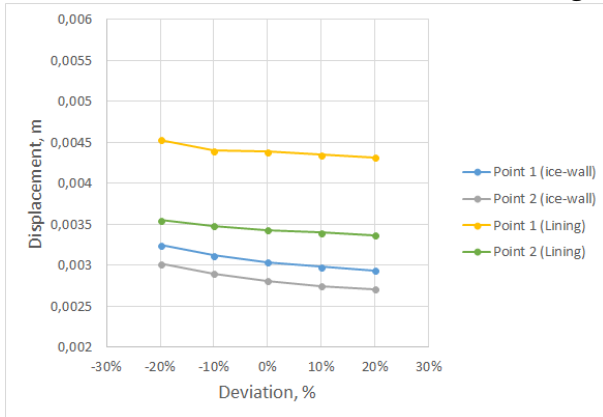
As it is seen from Figure 7.18, the displacements at ice-wall stage are lower than at permanent lining stage in both points. The stiffness of soil material represented by Young's modulus has the highest impact on tunnel stability as it is shown in Figure 7.18 a). The displacements caused by its variation raise 1,4 times for lining and 1,5 times for ice-wall.

The strength parameters  $\phi$  and  $c$  have less impact (Figure 7.18 b) and c). Friction angle variation causes rise by 1,1 times for ice-wall and 1,05 for lining.

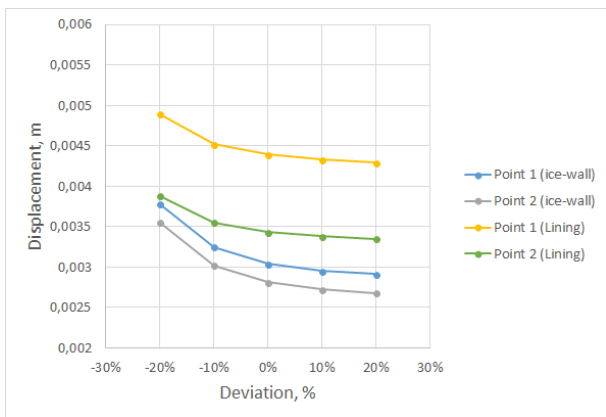
Cohesion has much higher impact on ice-wall than on lining. For the rate of variation from designed value to +20% the displacements raise by 1,05 times for ice-wall and 1,02 times for lining. However, with the further decreasing of  $c$  value, the displacement rate shows trend to sharp increase. Thus, The raise of displacements constitutes 1,25 times for ice-wall and 1,12 times for lining.



a) Young's modulus  $E$



b) Friction angle  $\phi$



c) Cohesion  $c$

Figure 7.18: Displacements due to parameters variation



# Chapter 8: Discussion

The discussion of the thesis can be divided by several sections represented each stage of the work. Thus, the main results of geology and hydrology analysis, AGF design considerations, tunneling design and modeling of tunnel stability are presented in the chapter.

## 8.1 Geology and hydrology

Based on the projects papers, the content of moraine deposit and type of bedrock was analyzed. Thus, the analysis of grain size distribution showed that the moraine deposit consist of mixed grave and clay. However, due to data restriction, the distribution analysis was performed for 5-10 m depth. Furthermore, there was an uncertainty about rock material below the tunnel. The last project documents described it as marble, while old considered granite (A). Thus, marble was counted as a rock material for modeling. The communication with Statens Vegvesen representatives revealed that the bottom of weak zone represents mainly by crushed rock with high water appearance which was not investigated.

The designed natural ground temperature is equal to 2,5 C, which is based on Norwegian standard (Vegvesen, 2010). However, during communication with Statens Vegvesen representatives it turned out, that real natural temperature can be higher than designed. Nonetheless, it has been decided to keep the designed temperature, since there was no research about real ground temperature.

Groundwater analysis was based on the same data as grain size distribution. Therefore, estimated coefficients of seepage velocity are applied for the depths of boreholes. The value 12m/day was chosen for AGF design considerations and modeling of groundwater flow in RS2 as the maximum seepage velocity based on calculations. However, this value is theoretical and possibly does not represent the real conditions.

## 8.2 Tunnel design

The tunnel cross-section was designed following information from Statens Vegvesen documentation.

Considering that there was no information about type of lining for weak zone, it was considered as reinforced concrete analyzed in Rocscience RS2, initially with parameters, applied

at Joberget tunnel with 70 cm thick concrete layer. Then a thinner layer of concrete equal to 30 cm was analyzed, which satisfied the Statens Vegvesen standard requirements.

### 8.3 Design of ice-wall parameters

The design of ice-wall has high flexibility. Depending on groundwater movement, its thickness, number of freeze-tubes and temperature of freezing can be modified for more acceptable option.

The analysis of seepage velocity impact on the temperature of freezing showed that the variation between 3 and 12 m/day reflects dramatical drop of temperature at 35 °C with 0,8 m spacing between freeze-tubes and at 74 °C for spacing equal to 1,2 m.

Therefore the designed parameters of AGF are:

- Spacing between freeze-tubes  $S = 0,8$  m;
- Number of freeze-tubes  $N = 28$ ;
- Freezing temperature  $T_f = -40$  °C;
- Ice-wall thickness  $E_{iw} = 1,2$  m;
- Active freezing time  $t = 9$  days

The estimated time of freezing can be considered as approximate value because of inaccuracy of data and simplifications applied during its calculation. As it was discussed in 6, the real time of freezing is generally longer than estimated.

Considering highly heterogeneous content of moraine deposit an ice-wall can be applied only for a tunnel side which is affected by water infiltration, as it was described in chapter 3

Furthermore, the risks and costs of AGF method were evaluated. Following approach offered by Harris (1995), the maximum risk level of the method amounted to 4,86, which can be considered as a medium risk. The costs comparison with other projects applied in Norway gave a number of NOK 3,4 million for the freezing of 20 meters.

### 8.4 Modeling of the tunnel stability

The stability analysis of the tunnel was performed to get areas of maximum displacements and covered next points:

- Unlined tunnel;
- Tunnel under ice-wall protection;
- Tunnel under permanent reinforced concrete lining

Thus, the model of unlined tunnel showed unrealistic scenario, when displacement exceed the height of the tunnel and likely lead to the tunnel collapse.

Ice wall was modeled as a soil layer with parameters responding to frozen moraine deposit. The model presented a case of excavated tunnel under the protection of ice-wall, showed that displacements were distributed mainly on the sides of the tunnel and did not exceed 3,04 mm. Thus, the designed ice-wall can be counted sufficient to bear ground stresses and prevent water inflow in the tunnel.

The results of the tunnel stability modeling covered by 0,7 m thick reinforced concrete lining gave 3,43 mm displacements. While, in case of 0,3 m thick reinforced concrete lining applying the displacements reached 4,4 mm. It should be noticed that the distribution of displacements for a case of tunnel covered by permanent lining is similar to the case of ice-wall applying.

In case when the whole tunnel was excavate in moraine soil layer, the results of modeling showed that the maximum displacements concentrated below the tunnel bottom. Therefore, different type of the tunnel shape (with inverted arch) should be designed.

The influence of moraine deposit strength parameters variation was researched as well. The results indicated the highest impact of Young's modulus. Besides, the low soil cohesion results in dramatic raise of displacements in ice-wall, which almost become equal to displacements at the permanent lining stage.

It should be stated that the models had significant simplifications. Because of unrealistic in-situ stresses distribution in the model with real ground surface cross-section it was decided to set-up the rectangular model. Furthermore, considering that heterogeneous soil layer is complicated to model, generally 2 materials were used - soil, containing moraine deposit and rock represented by marble.

## Chapter 9: Conclusions

The detailed investigation of different finished projects applied in Norway and other Scandinavian countries used AGF for water saturated soils stabilization can be concluded with a statement that the AGF method is accepted to use in geological conditions similar to Bergåsen tunnel case.

Comprehensive analysis of available project data, standards information and results of previously completed studies about soils properties in natural and frozen condition allowed to design an ice-wall, sufficient to carry overburden and hydrostatic pressure on the tunnel. That was proved by stability analysis made in Rocscience RS2 software. Therefore, the research made in the thesis, allows to state that the designed ice-wall can be an option for Bergåsen tunnel stabilizing at the section of moraine layer.

Additionally, the case of the whole tunnel excavation in moraine was considered, for which the ice-wall was modified to cover the whole tunnel. It was determined, that deformations are much higher in this case and distributed differently, what can cause displacements of the tunnel.

The impact of moraine deposit strength parameters on the tunnel stability was analyzed as well. It was found that Young's modulus variation has the highest effect on deformations rate. Moreover, low cohesion decreases significantly the strength of ice-wall.

### 9.1 Further work recommendations

To obtain more relevant design parameters of ice-wall and evaluate the tunnel stability, the further geological and hydrological research of moraine deposit should be applied. The properties of moraine natural condition should be tested as well as its frozen state during different temperatures below 0 °C. Furthermore, the effects of ground creep, frost heave and the influence of the process of concrete casting on the ice-wall should be analyzed. Then, ground settlements can be researched as well.

# References

- Aagaard, B., Gylland, A. S., Schubert, P., and Løne, B. (2017). The Joberg tunnel. successful tunnelling in moraine. In *Proceedings of the World Tunnel Congress 2017 – Surface challenges – Underground solutions*. Bergen, Norway., pages 1–10.
- Akagawa, S. and Nishisato, K. (2009). Tensile strength of frozen soil in the temperature range of the frozen fringe. *Cold Regions Science and Technology*, 57(1):13–22.
- Andersland, O. B. and Ladanyi, B. (2004). *Frozen ground engineering*. John Wiley & Sons.
- Andersland, O. B. and Ladanyi, B. (2013). *An introduction to frozen ground engineering*. Springer Science & Business Media.
- Andreassen, F. (1999). Oslofjordtunnelen – Erfaringer fra frysing og driving gjennom frysesonen. In *Proceedings from the Norwegian conference on rock blasting, rock mechanics and geotechnical engineering*. NJF.
- Backer, L. and Blindheim, O. (1999). The Oslofjord subsea road tunnel. crossing of a weakness zone under high water pressure by freezing. *Challenges for the 21st Century*, Alten et al.(eds), pages 309–316.
- Barry, C. R., Schwartz, C., and Boudreau, R. (2005). Geotechnical aspects of pavements. Report No. FHWA NHI-05-037. National Highway Institute, Federal Highway Administration, Washington, DC.
- Berggren, A. (1983). Engineering creep models for frozen soil behavior. *Dr. of Engineering Thesis, Norwegian Institute of Technology*.
- Berggren, A. (2000). The Oslofjord subsea tunnel, a case record. In *Proceedings of the International Symposium on Ground Freezing and Frost Action in Soils*. Louvain-La-Neuve, Belgium: AA Balkema, pages 267–272.
- Berggren, A.-L. (2007). Grunnfrysing for tunnel under Moss sentrum. [https://www.moss.kommune.no/\\_f/i978c0a0e-b313-4e77-a5f9-21beaf276f0b/referanse\\_3\\_geofrost\\_iup-00-a-01582\\_00\\_001.pdf](https://www.moss.kommune.no/_f/i978c0a0e-b313-4e77-a5f9-21beaf276f0b/referanse_3_geofrost_iup-00-a-01582_00_001.pdf). Accessed: 2018-02-08.
- Bollingmo, P., Gammelsæter, B., Skjeggcdal, T., and Ravlo, A. (2010). Rock support in norwegian tunnelling. NORWEGIAN TUNNELLING SOCIETY. Publication no 19.

- Bond, A. and Harris, A. (2008). *Decoding eurocode 7*. CRC Press.
- Braun, B., Shuster, J., and Burnham, E. (1979). Ground freezing for support of open excavations. *Engineering Geology*, 13(1-4):429–453.
- Bronfenbrener, L. and Bronfenbrener, R. (2010). Modeling frost heave in freezing soils. *Cold Regions Science and Technology*, 61(1):43–64.
- Chamberlain, E. (1979). Ground freezing: Proceedings of the first international symposium on ground freezing, Bochum, 1978. edited by hans l. jessberger (reprinted from engineering geology, vol. 13, no. 1–4), developments in geotechnical engineering vol. 26, elsevier, amsterdam, 1979, viii+ 550 pp., dfl. 160.00. Elsevier.
- Eiksund, G., Berggren, A., and Svano, G. (2001). Stabilisation of a glacifluvial zone in the oslofjord subsea tunnel with ground freezing. In *PROCEEDINGS OF THE INTERNATIONAL CONFERENCE ON SOIL MECHANICS AND GEOTECHNICAL ENGINEERING*, volume 3, pages 1731–1736. AA BALKEMA PUBLISHERS.
- Einarson, M. (2014). Eidangertunnelen: Valg av drivemetode ved forsering av kritisk sone. Master's thesis, Institutt for bygg, anlegg og transport.
- Farouki, O., Research, C. R., and (U.S.), E. L. (1981). *Thermal Properties of Soils*. CRREL monograph. U.S. Army Corps of Engineers, Cold Regions Research and Engineering Laboratory.
- Gella, K. P. (2017). Geotechnical and geological characterization of a quick clay site at flotten, Trondheim. Master's thesis, NTNU.
- Geosciences, T. (2013). Some useful numbers on the engineering properties of materials (geologic and otherwise). <http://www.jsg.utexas.edu/tyzhu/files/Some-Useful-Numbers.pdf>. Accessed: 2018-02-08.
- Geotechdata.info (2018). Soil young's modulus. <http://geotechdata.info/parameter/soil-elastic-young-modulus.html>. Accessed: 2018-02-08.
- Hansen, A., Garshol, K., Blomberg, R., and Grøv, E. (2017). The principles of norwegian tunnelling. NORWEGIAN TUNNELLING SOCIETY. Publication no 26.
- Harris, J. S. (1995). *Ground freezing in practice*. Thomas Telford.
- Hill, N. and Stärk, A. (2015). Volume loss and long term settlement at Kempton court, Whitechapel. In *Crossrail Project: Infrastructure design and construction*, pages 347–385. ICE Publishing.
- Hoek, E. (1991). Support for very weak rock associated with faults and shear zones. *Roc-science.com*.

- Hoek, E. (2007). Rock mass properties. *Practical rock engineering*. Available at [www.rock-science.com/learning/hoek-s-corner](http://www.rock-science.com/learning/hoek-s-corner).
- Hoek, E., Carter, T., Diederichs, M., et al. (2013). Quantification of the geological strength index chart. In *47th US rock mechanics/geomechanics symposium*. American Rock Mechanics Association.
- Hoppe, E. J. (2000). Frost action considerations in roadway construction. *Virginia Transportation Research Council*, VA.
- Hu, X.-d., Wang, J.-t., and Yu, R.-z. (2013). Uniaxial compressive and splitting tensile tests of artificially frozen soils in tunnel construction of Hong Kong. *Journal of Shanghai Jiaotong University (Science)*, 18(6):688–692.
- Ignatova, O. and Svertilov, A. (2013). Implementation of gost 25100-2011" soils. classification". *Soil Mechanics & Foundation Engineering*, 50(3).
- Johansen, Ø. (1975). Varmeledningsevne av jordarter.
- Johansson, M. (2012). Ground freezing of weathered rock in the Mölleback zone at the Hallandsås project: Calculations for optimal freezing design.
- Johansson, T. (2009). *Artificial Ground Freezing in Clayey Soils: Laboratory and Field Studies of Deformations During Thawing at the Bothnia Line*. PhD thesis, KTH.
- Jones, R. (1996). Observation and control of movements in works constructed by ground freezing. In *Int. Symposium on Geotechnical Aspects of Underground Construction in Soft Ground*, pages 379–384.
- Jøsang, T. (1980). Ground freezing techniques used for tunneling in Oslo city centre. In *2nd Int Symp on Ground Freezing, Norway, Trondheim*, pages 969–979.
- Karlsrud, K. and Andresen, L. (2008). Design and performance of deep excavations in soft clays.
- Khakimov, K. R. (1966). Artificial freezing of soils-theory and practice.
- Knutsson, S. (1981). The shear strength of frozen soils. In *International conference on soil mechanics and foundation engineering: 15/06/1981-19/06/1981*, pages 731–732. Balkema Publishers, AA/Taylor & Francis The Netherlands.
- Lackner, R., Pichler, C., and Kloiber, A. (2008). Artificial ground freezing of fully saturated soil: viscoelastic behavior. *Journal of engineering mechanics*, 134(1):1–11.
- Langåker, M. Ø. (2014). Joberget tunnel-analysis of stability and support design for tunneling in soil. Master's thesis, NTNU.

- Martin-Luther-Universität (2018). 3 results: Plasticity, compaction, and unconfined compressive strength (qu). <https://sundoc.bibliothek.uni-halle.de/diss-online/06/06H107/t4.pdf>. Accessed: 2018-02-08.
- Melbourne School of Engineering (2018). 8. strength of soils and rocks. [https://people.eng.unimelb.edu.au/stsy/geomechanics\\_text/Ch8\\_Strength.pdf](https://people.eng.unimelb.edu.au/stsy/geomechanics_text/Ch8_Strength.pdf). Accessed: 2018-02-08.
- Moldovan, A. R. and Popa, A. (2012). Finite element modelling for tunneling excavation. *Civil Engineering & Architecture*, 55(1):98–113.
- Nasonov, I., Fedyukin, V., Shuplik, M., and Resin, V. (1992). Tehnologiya stroitelstva podzemnykh sooruzheniy. specialnye sposoby stroitelstva [the technology of underground construction. special methods of excavation]. *High Education*. [in Russian].
- Nevzorov, A. L. (2000). *Fundamenty na sezonnopromerzaiushchikh gruntakh [Foundations on seasonal freezing soils]*. ASV Publishing House. [In Russian].
- Ngi.no (2018). Bedrock N250. <http://geo.ngu.no/kart/kartkatalog/>. Accessed: 2018-02-08.
- Norges Bank (2018). Price calculator. <https://www.norges-bank.no/en/Statistics/Price-calculator-/>. Accessed: 2018-02-08.
- Ozdemir, L. (2006). *North American tunneling 2006: proceedings of the North American tunneling 2006 conference, 10-15 June 2006, Chicago, USA*. Taylor & Francis.
- Repski, A. (2015). Artificial ground freezing refrigeration plant optimization. Master's thesis, University of Saskatchewan.
- Saiang, D., Gywnn, X., and Marshall, N. (2014). Hoek-Brown vs. Mohr-Coulomb—results from a three-dimensional open-pit/underground interaction model. In *Bergmekanikdagene 2014*.
- Sanger, F. and Sayles, F. (1979). Thermal and rheological computations for artificially frozen ground construction. *Engineering geology*, 13(1-4):311–337.
- Schubert, T. (2013). Experiences from the TBM drive through the Hallandåsen in Sweden. *Fjellsprengningsteknikk, Bergmekanikk, Geoteknikk, Oslo*, pages 3.1–3.22.
- Selmer-Olsen, R. (1976). Ingeniørgeologi del 1, generell geologi, 2. utg., 281 pp. *Tapir, Trondheim*.
- Shahriar, K., Sharifzadeh, M., and Hamidi, J. K. (2008). Geotechnical risk assessment based approach for rock tbm selection in difficult ground conditions. *Tunnelling and Underground Space Technology*, 23(3):318–325.



- Slunga, E. and Saarelainen, S. (1989). Determination of frost-susceptibility of soil. In *12th International Conference on Soil Mechanics and Foundation Engineering, Rio de Janeiro*.
- Sturk, R. and Stille, B. (2008). Advanced ground freezing at the Hallandsås project, Sweden. *Geomechanics and Tunnelling*, 1(5):512–517.
- Svintickaya, L. (1997). Vlianie himicheskogo sostava soley na prochnost' merzlyh zasolennyh gruntov [affect of salts chemical content on frozen saline soils strength]. *Ph D thesis, Moscow State University*. [in Russian].
- Trupak, N. (1974). Zamorazhivanie gruntov v stroitelstve [freezing of soils in construction]. *Nedra, M.* [in Russian].
- Vakulenko, I. (2014). Analysis of time evaluation methods of ice walls formation in the course of construction of underground facilities with the use of artificial freezing of rock formations. Diploma thesis, MISIS. [in Russian].
- Vakulenko, I. (2017). Ground freezing as stabilizing measure during tunnelling. NTNU. Report.
- Vakulenko, I. and Nikolaev, P. (2015). Analysis and outlook for development of artificial freezing of rocks in underground construction. *MINING INFORMATIONAL AND ANALYTICAL BULLETIN (SCIENTIFIC AND TECHNICAL JOURNAL)*, (3):338–346.
- Vegvesen, S. (2010). Håndbok 021: Vegtunneler. *Vegdirektoratet, Oslo*.
- Vegvesen, S. (2013a). E6 brattåsen-Lien REGULERINGSPÅN Plan-ID 1825 2013 01. *Vegdirektoratet, Editor*.
- Vegvesen, S. (2013b). Geologi. E6 TUNNEL VED TROFORS I GRANE KOMMUNE. INGENIØR-GEOLOGISK RAPPORT TIL REGULERINGSPÅN. *Vegdirektoratet, Editor*. Ressursavdelingen Nr. 2010231837-66.
- Vegvesen, S. (2013c). Geoteknikk E6-01/02. N-TR/SMALVATNET-BÅFJELLMO NORD-MOSJØEN PARSELL: BRATTÅSEN-LIEN, PROFIL 0-7475. *Vegdirektoratet, Editor*. Ressursavdelingen Nr. 2010231837-66.
- Vegvesen, S. (2015). Prosesskode 1. Standard beskrivelse for vegkontrakter. *Vegdirektoratet, Editor*.
- Vegvesen, S. (2016). Håndbok N500 Vegtunneler. *Vegdirektoratet, Editor*.
- Vegvesen, S. (2018). Hydrologi, Ev. 06 Bergåstunnelen, Svenningdal - Valryggen, hydrogeologisk rapport. *Vegdirektoratet, Editor*. Ressursavdelingen, 50725-HYDR-2.

Vuorela, M. and Eronen, T. (1982). The driving of metro tunnels at Helsinki with the aid of ground freezing. In *Developments in Geotechnical Engineering*, volume 28, pages 377–384. Elsevier.

Yershov, E. D. (2004). *General geocryology*. Cambridge university press.

# Appendix A: Drawings of the project

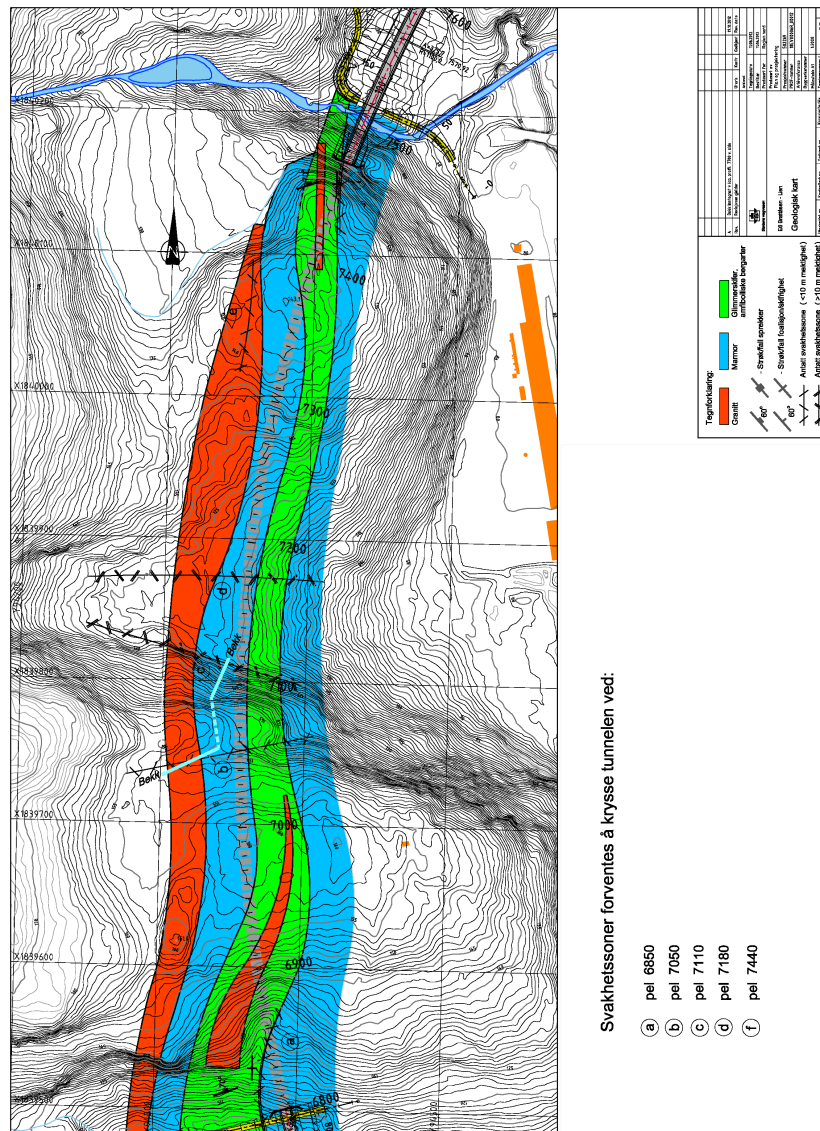


Figure A.1: Bedrock geology (from Vegvesen (2013b))

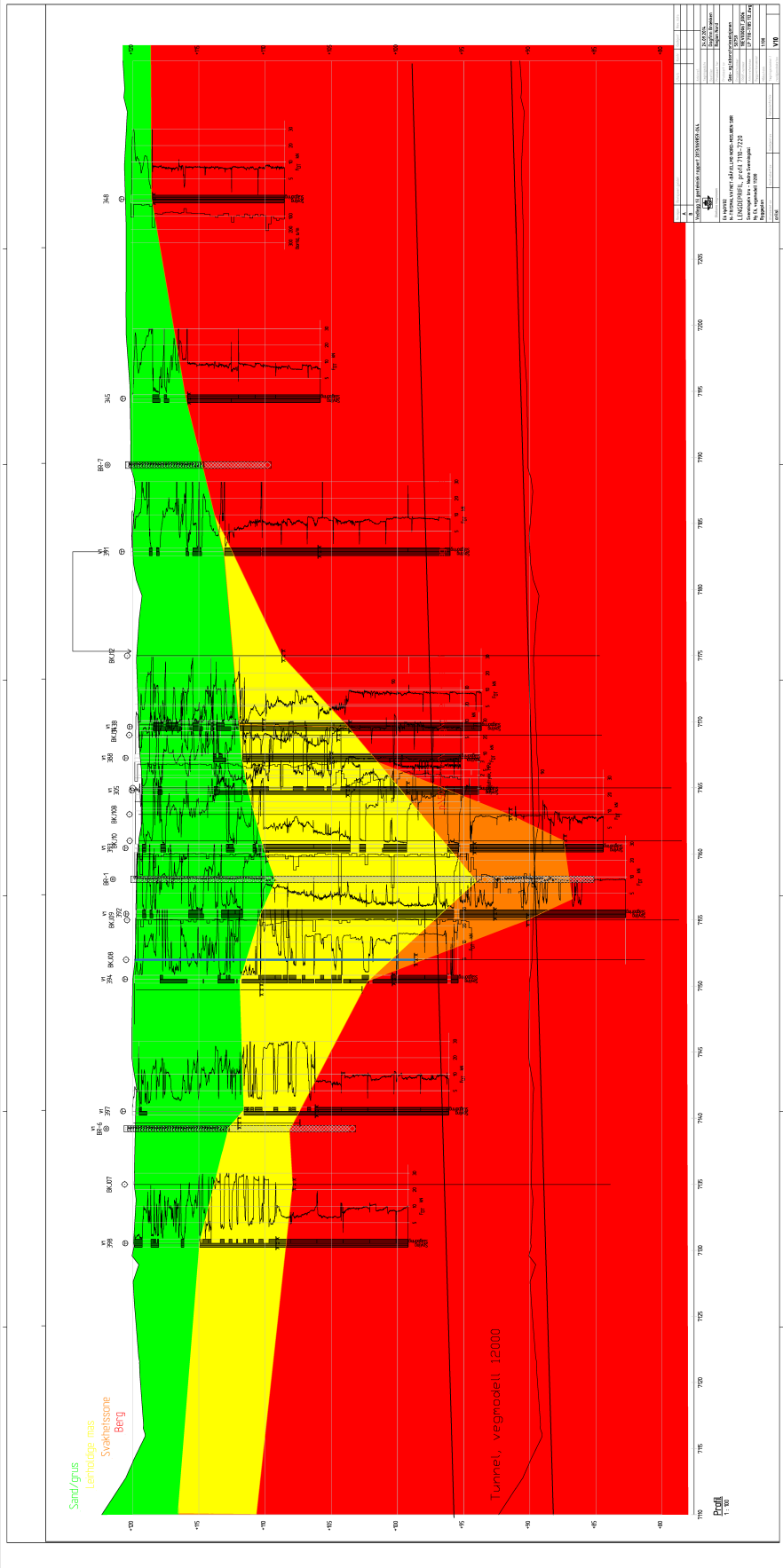


Figure A.2: Soil section (from Vegvesen (2018))

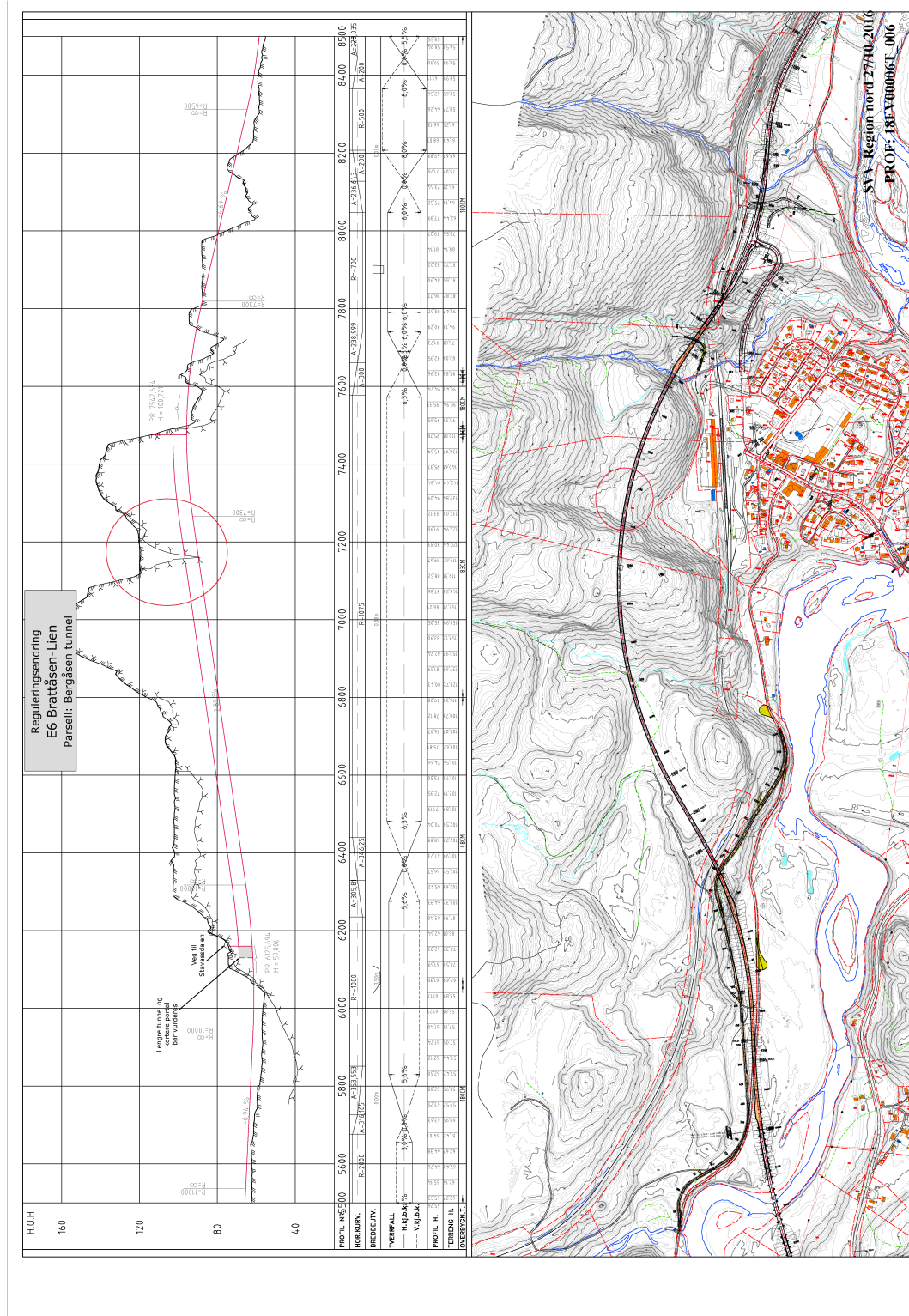


Figure A.3: Bedrock geology (from Vegvesen (2013b))

## Appendix B: Time evaluation (Sangers&Sayles)

Sanger and Sayles implemented separate equations for stage I (Eq. B.1) and for stage II, where freezing of external(Eq. B.2) and internal(Eq. B.3) contours are considered (Sanger and Sayles, 1979). These evaluations describe above mentioned primary freezing when ice-columns grow around separate freeze-tubes and then form a homogeneous ice-wall.

$$t_I = \frac{R^2 L_1}{4K_1 \nu_s} \left[ 2 \ln \left( \frac{R}{r_0} \right) - 1 + \frac{C_1 \nu_s}{L_1} \right] \quad (B.1)$$

Where

- $K_1$ –thermal conductivity of the frozen soil;
- $L_1 = L + \frac{a_r^2 - 1}{2 \ln a_r} C_2 \nu_0$ ;
- $L$  – the volumetric latent heat of fusion of the soil water;
- ratio  $a_r$  is the factor which defines the radius of temperature influence of the freeze-tube;
- $C_1$  and  $C_2$  the volumetric specific heat capacity for frozen and unfrozen soils respectively;
- $R$  – the radius to the interface between the frozen and unfrozen soil;
- $r_0$  – the radius of the freeze-tube;
- $\nu_s$  – the difference between the temperature at the surface of the freeze-tube and the freezing point of water;
- $\nu_0$  – the difference between the original temperature of the ground and the freezing point of water.

$$t_{IIe} = \frac{1}{2K_1 \nu_s} L_{IIe} \left[ b^2 \ln \left( \frac{b}{R_p + \delta} \right) - \frac{b^2 - (R_p + \delta)^2}{2} \right] + \frac{C_1}{2K_1} \left[ \frac{b^2 - (R_p + \delta)^2}{2} \right] \quad (B.2)$$

$$t_{IIi} = \frac{1}{2K_1 \nu_s} L_{IIi} \left[ (R_p - \delta)^2 \ln \left( \frac{R_p - \delta}{a} \right) - \frac{(R_p - \delta)^2 - a^2}{2} \right] + \frac{C_1}{2K_1} \left[ \frac{(R_p - \delta)^2 - a^2}{2} \right] \quad (B.3)$$

Where

- $a$  – internal radius and  $b$  is the external radius of the freeze wall;
- $L_{II} = L + 2,5(2,0)C_2\nu_0 + 0,5C_1\nu_s$  – parameters computed by field observations;
- $R_p$  – radius of the freeze-tubes circle;
- $S$  – tube spacing (Fig. B.1).

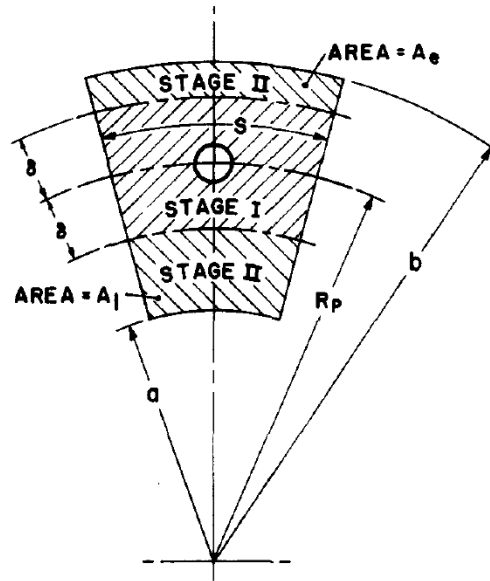


Figure B.1: 2 stages of ice-wall freezing; ( $\delta = 0,393S$ ) (from Sanger and Sayles (1979))

The authors noted that in practical experience, single freeze-tubes ring is acceptable for wall thickness up to 3 m, while for 7 m two rows are needed. three rows were set for 9m ice-wall.

## Appendix C: Risk assessment table

Table C.1: Risks mitigation for artificial groun freezing method (from Harris (1995))

Element at risk	Possible hazard	Risk mitigation
Installation		
converging FTs	Damage to neighbouring FT; thicker ice-wall	Monitoring control/redrill or install extra FT
diverging FTs	Longer PFP. 'window' in ice-wall; flooding/soil influx	Monitoring control/redrill or install extra FT
broken FT	Loss of brine to strata; depressed freezing point	Monitoring control/install salvage FT
Strata changes		
strata more clayey	Longer PFP	More comprehensive geotechnical appraisal
strata more granular	Shorter PFP	
large voids above WT	Chilled air contributes nothing	
large voids below WT	Ice is weaker than frozen ground	
poor cut-off stratum	Flooding of excavation	
Adverse groundwater		
fluctuating WL	Longer PFP; less effective	More comprehensive geotechnical appraisal, monitoring control
reduced WL	Low mc yields weaker frozen strength	Increase the mc by irrigation
multiple aquifers	Interconnection via drill-holes	Seal annuli
flowing water	Longer PFP; load may exceed plant capacity	Reduce flow-rate by filling voids or stopping pumping
saline soil/water	Depressed freezing point; longer PFP	Dilute by irrigation
Deformation		
ground heave	Distress to neighboring property	Monitoring control
creep deformation	Damage to FTs and/or to structural lining	
Other hazards		
Inaccurate monitoring	Misinterpretation	More frequent calibration checks, education
Equipment breakdown	Longer PFP; (eventual) loss of ice-wall support	Maintenance, provide backup



## Appendix D: Road tunnels standards

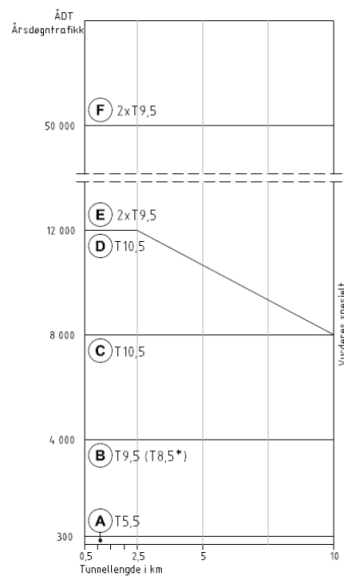


Figure D.1: Tunnel categories classification (from Vegvesen (2010))

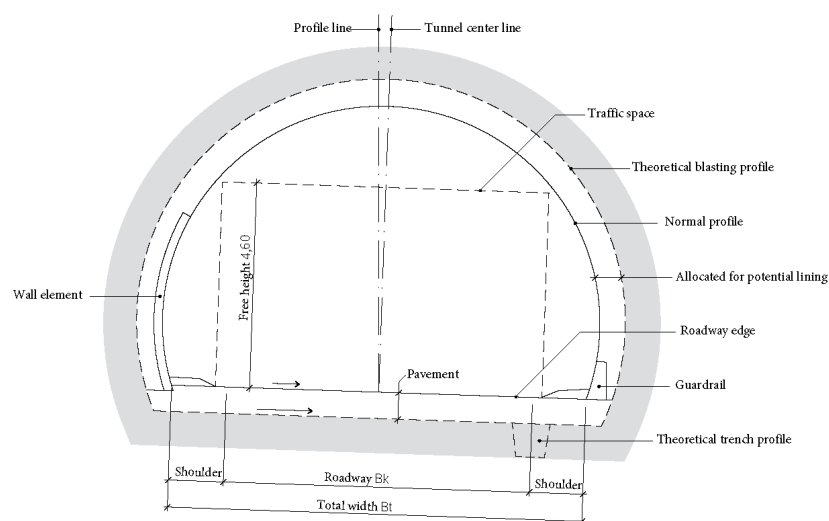


Figure D.2: Tunnel cross-section elements (from Vegvesen (2016))

## Appendix E: Hoek-Brown criteria

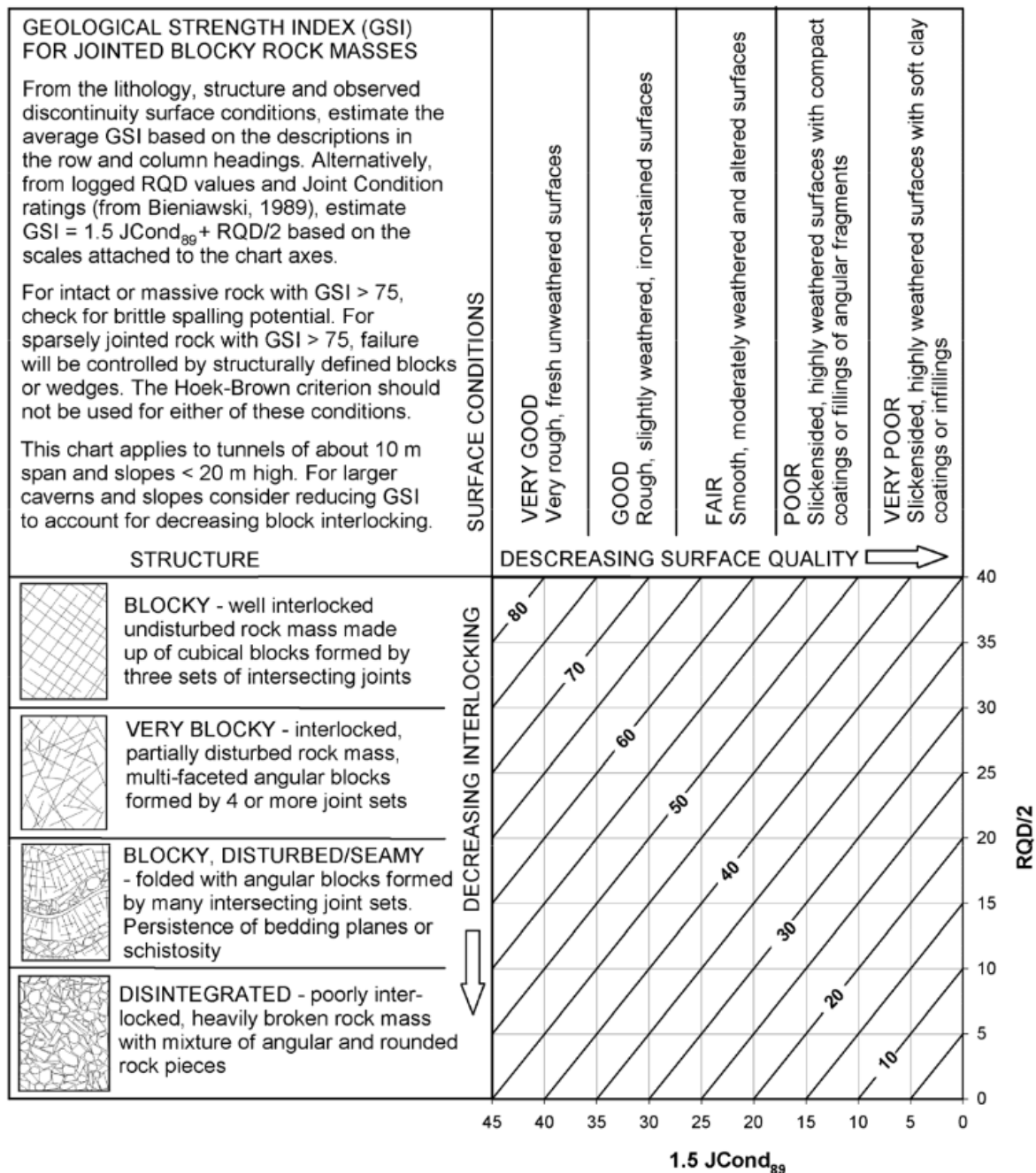


Figure E.1: Quantification of GSI (from Hoek et al. (2013))

Rock type	Class	Group	Texture			
			Coarse	Medium	Fine	Very fine
SEDIMENTARY	Clastic		Conglomerates* (21 ± 3)	Sandstones 17 ± 4	Siltstones 7 ± 2	Claystones 4 ± 2
			Breccias (19 ± 5)		Greywackes (18 ± 3)	Shales (6 ± 2) Marls (7 ± 2)
	Non-Clastic	Carbonates	Crystalline Limestone (12 ± 3)	Sparitic Limestones (10 ± 2)	Micritic Limestones (9 ± 2)	Dolomites (9 ± 3)
		Evaporites		Gypsum 8 ± 2	Anhydrite 12 ± 2	
		Organic				Chalk 7 ± 2
METAMORPHIC	Non Foliated		Marble 9 ± 3	Hornfels (19 ± 4) Metasandstone (19 ± 3)	Quartzites 20 ± 3	
	Slightly foliated		Migmatite (29 ± 3)	Amphibolites 26 ± 6		
	Foliated**		Gneiss 28 ± 5	Schists 12 ± 3	Phyllites (7 ± 3)	Slates 7 ± 4
IGNEOUS	Plutonic	Light	Granite 32 ± 3 Granodiorite (29 ± 3)	Diorite 25 ± 5		
		Dark	Gabbro 27 ± 3 Norite 20 ± 5	Dolerite (16 ± 5)		
	Hypabyssal		Porphyries (20 ± 5)		Diabase (15 ± 5)	Peridotite (25 ± 5)
	Volcanic	Lava		Rhyolite (25 ± 5) Andesite 25 ± 5	Dacite (25 ± 3) Basalt (25 ± 5)	Obsidian (19 ± 3)
		Pyroclastic	Agglomerate (19 ± 3)	Breccia (19 ± 5)	Tuff (13 ± 5)	

Figure E.2: Values of the constant  $m_i$  for intact rock (from Hoek et al. (2013))

Grade*	Term	Uniaxial Comp. Strength (MPa)	Point Load Index (MPa)	Field estimate of strength	Examples
R6	Extremely Strong	> 250	>10	Specimen can only be chipped with a geological hammer	Fresh basalt, chert, diabase, gneiss, granite, quartzite
R5	Very strong	100 - 250	4 - 10	Specimen requires many blows of a geological hammer to fracture it	Amphibolite, sandstone, basalt, gabbro, gneiss, granodiorite, limestone, marble, rhyolite, tuff
R4	Strong	50 - 100	2 - 4	Specimen requires more than one blow of a geological hammer to fracture it	Limestone, marble, phyllite, sandstone, schist, shale
R3	Medium strong	25 - 50	1 - 2	Cannot be scraped or peeled with a pocket knife, specimen can be fractured with a single blow from a geological hammer	Claystone, coal, concrete, schist, shale, siltstone
R2	Weak	5 - 25	**	Can be peeled with a pocket knife with difficulty, shallow indentation made by firm blow with point of a geological hammer	Chalk, rocksalt, potash
R1	Very weak	1 - 5	**	Crumbles under firm blows with point of a geological hammer, can be peeled by a pocket knife	Highly weathered or altered rock
R0	Extremely weak	0.25 - 1	**	Indented by thumbnail	Stiff fault gouge

Figure E.3: Field estimates of uniaxial compressive strength (from Hoek (2007))






Appearance of rock mass	Description of rock mass	Suggested value of D
	Excellent quality controlled blasting or excavation by Tunnel Boring Machine results in minimal disturbance to the confined rock mass surrounding a tunnel.	D = 0
	Mechanical or hand excavation in poor quality rock masses (no blasting) results in minimal disturbance to the surrounding rock mass.  Where squeezing problems result in significant floor heave, disturbance can be severe unless a temporary invert, as shown in the photograph, is placed.	D = 0  D = 0.5 No invert
	Very poor quality blasting in a hard rock tunnel results in severe local damage, extending 2 or 3 m, in the surrounding rock mass.	D = 0.8
	Small scale blasting in civil engineering slopes results in modest rock mass damage, particularly if controlled blasting is used as shown on the left hand side of the photograph. However, stress relief results in some disturbance.	D = 0.7 Good blasting  D = 1.0 Poor blasting
	Very large open pit mine slopes suffer significant disturbance due to heavy production blasting and also due to stress relief from overburden removal.  In some softer rocks excavation can be carried out by ripping and dozing and the degree of damage to the slopes is less.	D = 1.0 Production blasting  D = 0.7 Mechanical excavation

Figure E.4: Disturbance factor D (from Hoek (2007))

## Appendix F: Model with natural ground level set-up

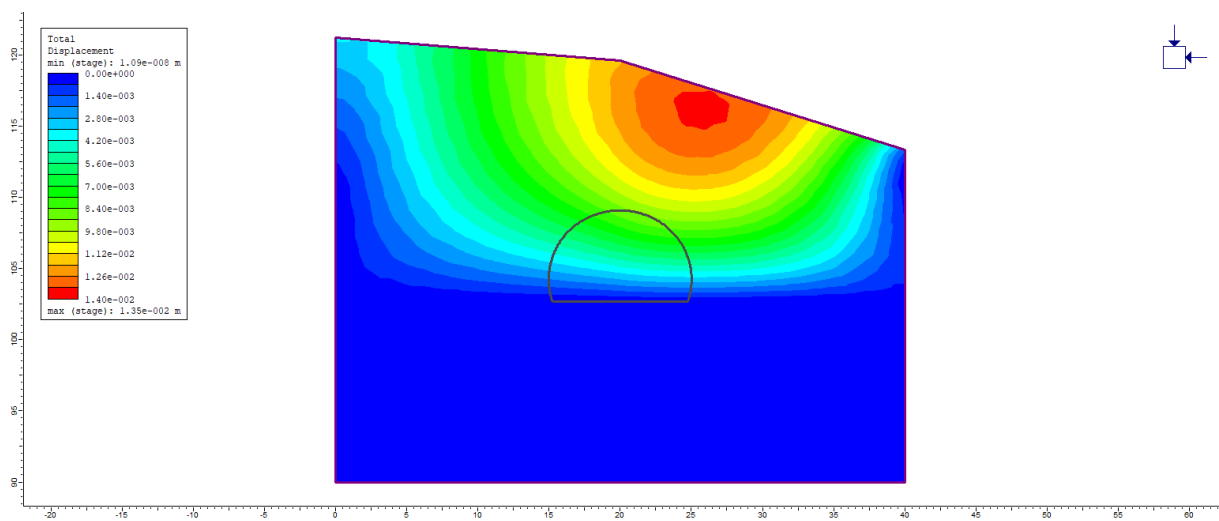


Figure F.1: Displacements distribution in soil layer before tunnel excavation

## Appendix G: K-value estimation

1. Vertical stress:  $\sigma_V = \rho gh = \gamma h = 19 * 18,575 = 352,925 kN/m^2$

- unit weight of dry soil  $\gamma = 19 kN/m^3$  from (Karlsrud and Andresen (2008));
- Tunnel depth  $h=18,575$  m.

2. Horizontal stress:  $\sigma_H = \frac{\nu}{1-\nu} \sigma_V = \frac{0,3}{1-0,3} 352,925 = 151,254 kN/m^2$

- Poisson ratio  $\nu = 0,3$

3.  $K = \frac{\sigma_H}{\sigma_V} = \frac{151,254}{352,925} = 0,429$

The graph below demonstrates maximum displacements at  $K=0,43$  and  $K=0,25$  in comparison with designed value  $K=1$ .

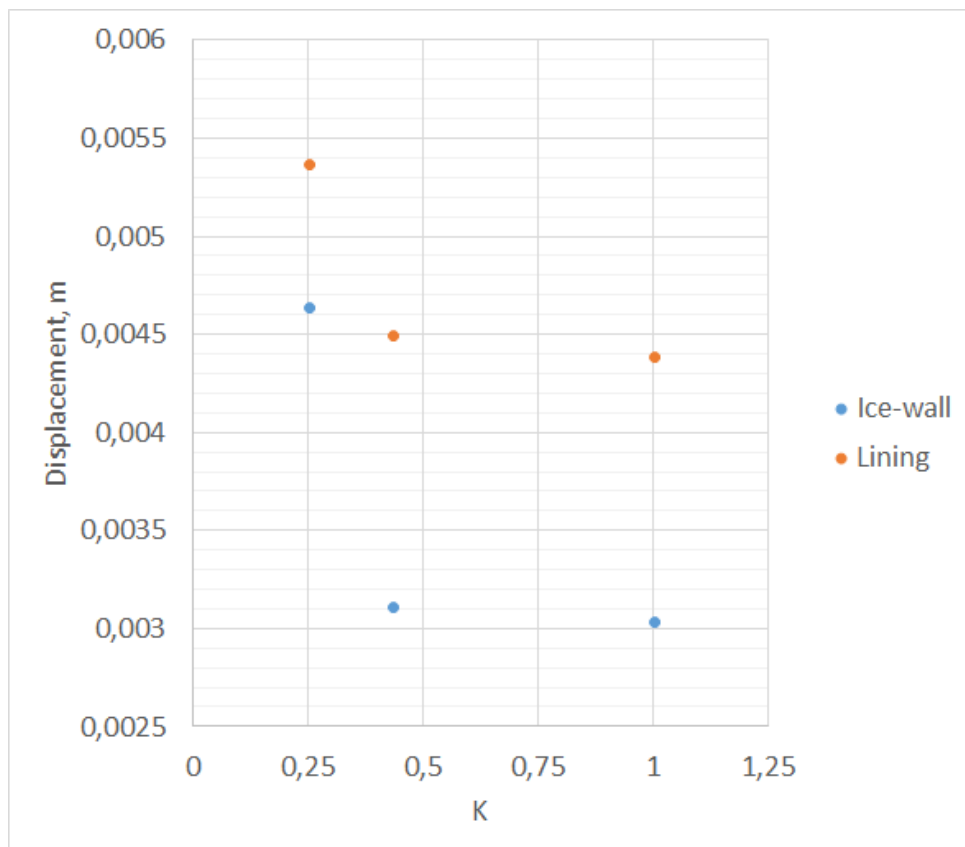


Figure G.1: K values impact on displacement distribution

## Appendix H: Safety factor of reinforced concrete lining

The safety factor for 30 cm thick concrete and reinforcement with 15 cm spacing between rebars are shown below.

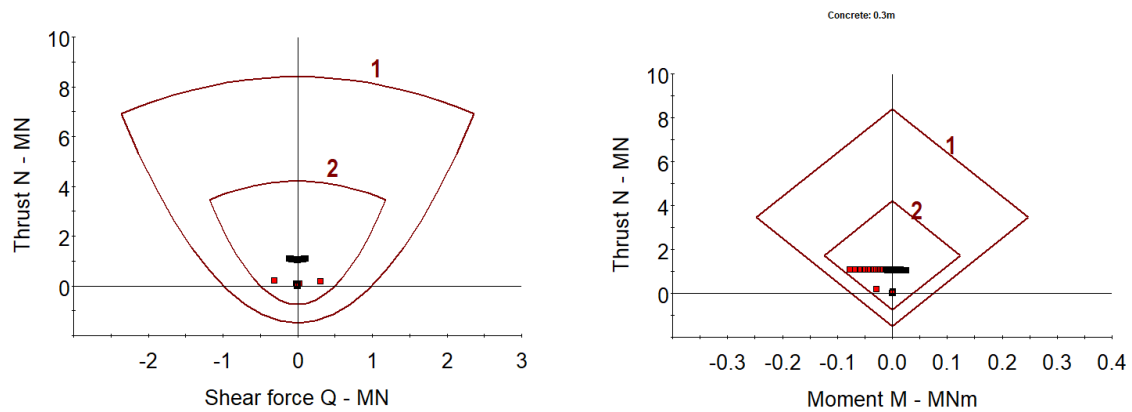


Figure H.1: Safety factor for 0,3 m thick concrete layer

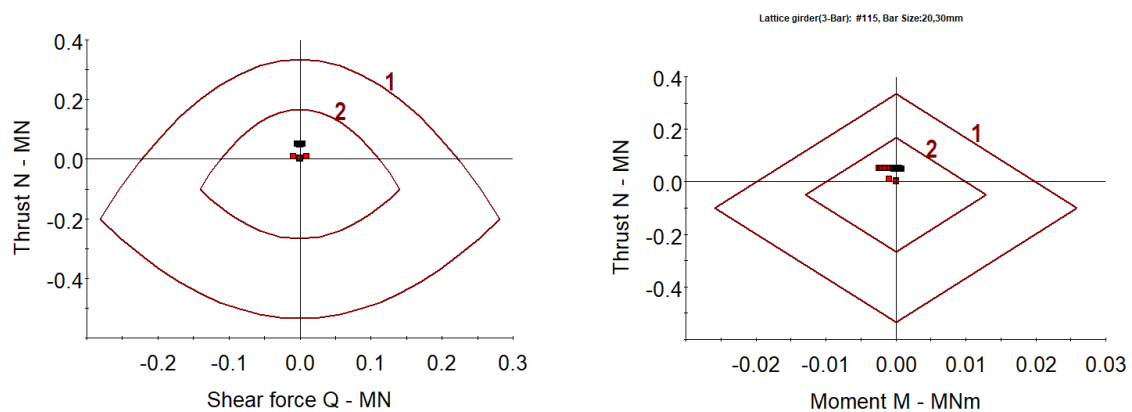


Figure H.2: Safety factor for reinforcement framework

The designed parameters for both concrete lining and reinforcement satisfy the condition of safety factor, since all the nodes of the lining surrounding the tunnel exceed  $FS=1$ .